



RETURNING MATERIALS:  
Place in book drop to  
remove this checkout from  
your record. FINES will  
be charged if book is  
returned after the date  
stamped below.

--	--	--

VOLTAGE STABILITY AND SECURITY  
FOR ELECTRIC POWER SYSTEMS

By  
Louis Parlai Shu

A THESIS

Submitted to  
Michigan State University  
in partial fulfillment of the requirements  
for the degree of

DOCTOR OF PHILOSOPHY

Department of Electrical Engineering

1984

## ABSTRACT

### VOLTAGE STABILITY AND SECURITY FOR ELECTRIC POWER SYSTEMS

By

Louis Parlai Shu

This thesis presents a new approach to voltage stability problems in electric power systems. The study develops (a) the theory that explains the different types and causes of voltage stability and (b) the computer based methods for detecting when a power system will experience voltage stability problems.

The rapid growth of the interconnections between different electric utilities in recent years has brought on very serious and frequent voltage stability problems. Voltages can collapse in certain regions and/or large sustained voltage oscillations have been experienced. The lack of theoretical explanation of these stability problems is due to their being a rather recent phenomenon and that they are described by very large scale models that involve thousands of nonlinear equations.

The voltage stability problem is shown here as a lack of sufficient reactive power support within specific stiffly interconnected groups of buses. Attempting to supply reactive power across the weak transmission boundaries causes voltage collapse. Weak boundaries

are theoretically shown to be a cause of a loss of voltage controllability and a loss of reactive load observability that ultimately can lead to voltage stability or voltage collapse problems. Voltage problems can result from insufficient transmission capacity, heavy current loads on transmission lines in these weak boundaries. Shunt capacitance for long transmission lines or for voltage control was shown to be another cause for this loss of voltage controllability, observability, and stability.

Methods for determining and ranking weak boundaries were tested on a 30 bus New England system. The buses in the stiffly connected groups were shown to act as an equivalent bus for loadflow simulations of multiple line outage or loss of generation contingencies. The buses in weak boundaries were also shown to experience large voltage variations for these contingencies.

Increasing reactive flows across weak transmission boundaries or providing capacitive reactive power for a stiffly connected group requiring reactive support were both shown to further weaken the weak transmission boundary and lead to voltage collapse. These computational results thus confirm the theoretical results on the causes of voltage stability and security problems on power systems.



To my mother Jane  
and my wife Arlene



## ACKNOWLEDGMENTS

I wish to gratefully acknowledge my indebtedness to my major advisor, Professor R.A. Schlueter, for his invaluable assistance in the planning and preparation of this dissertation. I can never repay the tremendous amount of time he devoted to my research, especially on those weekends and holidays.

Also, I thank the other members of my committee, Dr. M.A. Shanblatt, Dr. H.K. Khalil, and Dr. David Yen, for their suggestions to improve the quality of this thesis.

Special acknowledgment is made of the contribution of Dr. G.L. Park and Dr. R.O. Barr, for reviewing my original research proposal.

I thank the system engineers of Consumers Power Company. In particular, I wish to thank Mr. P.A. Rusche, P.E., Executive Engineer, for constant reviewing of my research, Mr. R.H. Roades for coaching me on the data preparation, simulation, and analysis, and Mr. J.E. Sekerke and Mr. C.A. Bunnell for their help in programming.

Mrs. Carol A. Cole improved the overall style and presentation of the manuscript. She also conscientiously typed the manuscript and its revisions in minimum time.

I wish to express my deep appreciation to my wife, Arlene W. Chun, for her constant encouragement and helpful suggestions in the preparation of this thesis. Without her encouragement and consent,

this thesis would not have been completed simultaneously with my third masters degree.

My mother fostered my ambition to become a fighter pilot and love for my engineering profession.



## TABLE OF CONTENTS

LIST OF TABLES . . . . .	vii
LIST OF FIGURES . . . . .	ix
CHAPTER	
1. INTRODUCTION . . . . .	1
1.1. The Objective of This Thesis . . . . .	1
1.2. The Natural Structure of Voltage Problems in Large Scale Power Systems . . . . .	3
1.3. State of the Art . . . . .	6
1.4. An Overview of the Thesis . . . . .	10
2. METHODS FOR THE DETERMINATION OF WEAK TRANSMISSION BOUNDARIES . . . . .	14
2.1. Introduction . . . . .	14
2.2. The Linearized Loadflow Models and Stiffly Connected Buses . . . . .	16
2.3. Detection of SSC Group in P - $\theta$ Loadflow Model .	20
2.4. Detection of SSC Group in Q - V Loadflow Model .	26
2.5. Detection of SSC Group in A.C. Loadflow Model .	32
2.6. The Limited Sources and Weak Boundaries . . . . .	40
3. DETERMINATION OF WEAK TRANSMISSION BOUNDARIES FOR THE 30 BUS NEW ENGLAND SYSTEM . . . . .	44
3.1. Introduction . . . . .	44
3.2. Weak Phase Transmission Boundaries . . . . .	53
3.3. Weak Voltage Transmission Boundaries . . . . .	64
3.4. Weak Current Transmission Boundaries . . . . .	71

## CHAPTER

4. CONDITIONS FOR VOLTAGE CONTROLLABILITY, OBSERVABILITY, AND STABILITY . . . . .	76
4.1. Introduction . . . . .	76
4.2. The Model Development . . . . .	77
4.3. The Controllability and Observability Equations and the Sensitivity Matrices Under Light Load Conditions . . . . .	91
4.4. The Theorems for Local and Global Voltage Stability . . . . .	107
4.5. Theorems Integrating the Weak Boundaries and Sensitivity Analysis . . . . .	121
5. VOLTAGE STABILITY AND SECURITY EVALUATION ON THE 30 BUS NEW ENGLAND SYSTEM . . . . .	140
5.1. Introduction . . . . .	140
5.2. The Systematic Impacts of the Weak Boundary to the Voltage Stability . . . . .	142
5.3. Local and Global Effects of Capacitance on Voltage Stability . . . . .	146
5.4. The Effects of Shunt Capacitor on the Control- lability and Observability of the Steady State Voltage Problem . . . . .	157
6. CONCLUSIONS AND RECOMMENDATIONS FOR FUTURE RESEARCH .	181
6.1. Review . . . . .	181
6.2. Recommendations for Future Research . . . . .	185
APPENDIX 1. BASE CASE LOADFLOW DATA IN COMMON FORMAT . . . .	187
BIBLIOGRAPHY . . . . .	189

# LIST OF TABLES

## TABLE

5.1. Summary of results for Case 1 . . . . .	145
5.2. Summary of results for Case 2 . . . . .	148
5.3. New groups obtained from the weak boundary identifications based on voltage measure . . . . .	149
5.4. Summary of results for Case 3 . . . . .	150
5.5. Summary of results for Case 4 . . . . .	151
5.6. Summary of results for Case 5 . . . . .	152
5.7. Summary of results for case 6 . . . . .	154
5.8a. Sensitivity matrix $S_{Q_{GE}}$ for Case 3 . . . . .	158
5.8b. Eigenvalues and eigenvectors of $S_{Q_{LV}}$ for Case 3 . . .	158
5.8c. Sensitivity matrix $S_{Q_{LV}}$ for Case 3 . . . . .	160
5.8d. Eigenvalues and eigenvectors of $S_{Q_{LV}}$ for Case 3 . . .	161
5.9a. Sensitivity matrix $S_{Q_{GE}}$ for Case 4 . . . . .	163
5.9b. Eigenvalues and eigenvectors of $S_{Q_{GE}}$ for Case 4 . . .	163
5.9c. Sensitivity matrix $S_{Q_{LV}}$ for Case 4 . . . . .	164
5.9d. Eigenvalues and eigenvectors of $S_{Q_{LV}}$ for Case 4 . . .	165
5.10a. Sensitivity matrix $S_{Q_{GE}}$ for Case 5 . . . . .	168
5.10b. Eigenvalues and eigenvectors of $S_{Q_{GE}}$ for Case 5 . . .	168
5.10c. Sensitivity matrix $S_{Q_{LV}}$ for Case 5 . . . . .	170
5.10d. Eigenvalues and eigenvectors of $S_{Q_{LV}}$ for Case 5 . . .	171
5.11a. Sensitivity matrix $S_{Q_{GE}}$ for Case 6 . . . . .	173



11  
12  
13  
14

## TABLE

5.11b. Eigenvalues and eigenvectors of $S_{QGE}$ for Case 6 . . .	173
5.11c. Sensitivity matrix $S_{QLV}$ for Case 6 . . . . .	175
5.11d. Eigenvalues and eigenvectors of $S_{QLV}$ for Case 6 . . .	176

10.

11.

12.

13.

14.

15.

16.

17.

18.

19.

20.

21.

22.

## LIST OF FIGURES

### FIGURE

1.1.	A hybrid electromechanical analog model . . . . .	5
3.1.	The original 30 bus New England system . . . . .	48
3.2.	The weak boundaries for a 3-group partition based on real power disturbance and phase rms coherency measure . . . . .	55
3.3.	The weak boundaries for a 4-group partition based on real power disturbance and phase rms coherency measure . . . . .	56
3.4.	The weak boundaries for a 6-group partition based on real power disturbance and phase rms coherency measure . . . . .	57
3.5.	The weak boundaries for a 3-group partition based on complex power disturbance and phase rms coherency measure . . . . .	61
3.6.	The weak boundaries for a 4-group partition based on real power disturbance and phase rms coherency measure . . . . .	62
3.7.	The weak boundaries for a 5-group partition based on real power disturbance and phase rms coherency measure . . . . .	63
3.8.	The weak boundaries for a 3-group partition based on real power disturbance and voltage rms coherency measure . . . . .	65
3.9.	The weak boundaries for a 4-group partition based on real power disturbance and voltage rms coherency measure . . . . .	66
3.10.	The weak boundaries for a 6-group partition based on real power disturbance and voltage rms coherency measure . . . . .	67

100

101

102

103

104

105

106

107

108

## FIGURE

3.11.	The weak boundaries for a 5-group partition based on reactive power disturbance and voltage rms coherency measure . . . . .	70
3.12.	The weak boundaries for a 6-group partition based on reactive power disturbance and voltage rms coherency measure . . . . .	72
3.13.	The weak boundaries for a 5-group partition based on reactive power disturbance and voltage rms coherency measure when all generator buses are regulated . . . .	73
3.14.	The weak boundaries for a 3-group partition based on the current coherency measure for both real and complex power disturbances . . . . .	74
4.1.	The Jacobian matrix of five-bus system in polar form .	96
4.2.	The partitioned Jacobian matrix of a three-SSC-group network . . . . .	123
4.3.	The equivalent sensitivity matrix $\bar{S}_{Q_L V}$ . . . . .	137
5.1.	The four group partition based on reactive power disturbance and voltage rms coherency measure after generators 6 and 10 are removed . . . . .	144

## CHAPTER 1

### INTRODUCTION

#### 1.1. The Objective of This Thesis

The purpose of this chapter is to give an orientation of the voltage problems and define the objectives of the thesis. There are two kinds of voltage problems: (a) voltage collapse, and (b) voltage oscillations. The consequences of these voltage problems are the following: the voltage collapse will cause the blackouts and economic loss to the utilities and customers. The voltage oscillations will cause the maintenance problem and eventually lead to the stability problems of the whole power system. Voltage collapse and voltage oscillations can also cause the inability to transfer real power from the location of generation to the location of the customers. Today those transfers are widespread practice and are essential to the economic and reliable operation of power systems.

Back in the 1950's and 1960's utilities began to interconnect their networks. Initially, they were reluctant to admit that they had voltage problems. As they relied on those interconnections more, these voltage problems became more frequent and severe. It is only recently that utilities have been willing to admit the severity of the voltage problems.

100

101

102

103

104

105

106

107

108

109

110

111

112

113

114

115

116

117

118

119

120

121

122

123

124

125



The following areas have experienced voltage problems and have had to limit transfers of power: Florida, Pennsylvania/Maryland/New Jersey power pool, Ontario, and California.

Some common characteristics of the power systems in the above geographical areas are:

- (1) they all heavily import power from other utilities; and
- (2) the generation stations which supply the power to those areas are located at far away remote sites.

There are many other utilities that have recently reported problems and have indicated the severity of the problems. Although it is understood how severe the problems are, very little research has been performed to date, and the causes and solutions are not well understood. The study of the causes and solution of these voltage problems has been established as the number one priority for research as established by the transmission planning group within a recent EPRI sponsored meeting organized to establish priorities for research in power system operation and planning. One may ask why these interconnections cause problems and what are the causes. This thesis indicates that:

- (1) the weak boundary;
- (2) the insufficient local reactive supply to maintain voltage;
- (3) the installation of capacitors for reactive supply rather than generators; and
- (4) the capacitance associated with long transmission lines in weak transmission boundaries

THE 1971

THE 1971

THE 1971

THE 1971

THE 1971

THE 1971

THE 1971

THE 1971

THE 1971

THE 1971

THE 1971

THE 1971

THE 1971

THE 1971

THE 1971

THE 1971

THE 1971

THE 1971

THE 1971

THE 1971

THE 1971

THE 1971

THE 1971

THE 1971

THE 1971

THE 1971

are some of the causes of the voltage stability problems. This thesis will establish theoretically as well as experimentally that the above four network conditions will cause voltage problems.

The objectives of this research are defined as follows:

- (1) to define the structural causes for weak transmission boundaries;
- (2) to develop methods for identifying locations of weak transmission boundaries;
- (3) to categorize the causes of voltage stability problems as due to:
  - (a) inadequate resources
  - (b) loss of voltage controllability
  - (c) loss of reactive observability
- (4) to determine the necessary conditions that insure voltage stability will not occur for the above categories; and
- (5) to determine conditions that will cause loss of voltage stability for the above categories.

## **1.2. The Natural Structure of Voltage Problems in Large Scale Power Systems**

A typical interconnected power network can be visualized by a **hybrid** electromechanical analog model as shown in Figure 1.1. This **model** highlights the structure of several stiffly interconnected **groups**. The nodes with support of capacitor banks represent the **sources** of reactive power. The big and small masses represent the **reactive** loads of different sizes. The heavy duty springs represent

1000

1000

1000

1000

1000

1000

1000

1000

1000

1000

1000

1000

1000

1000

1000

1000

1000

1000

1000

1000

1000

1000

1000

1000

1000

1000

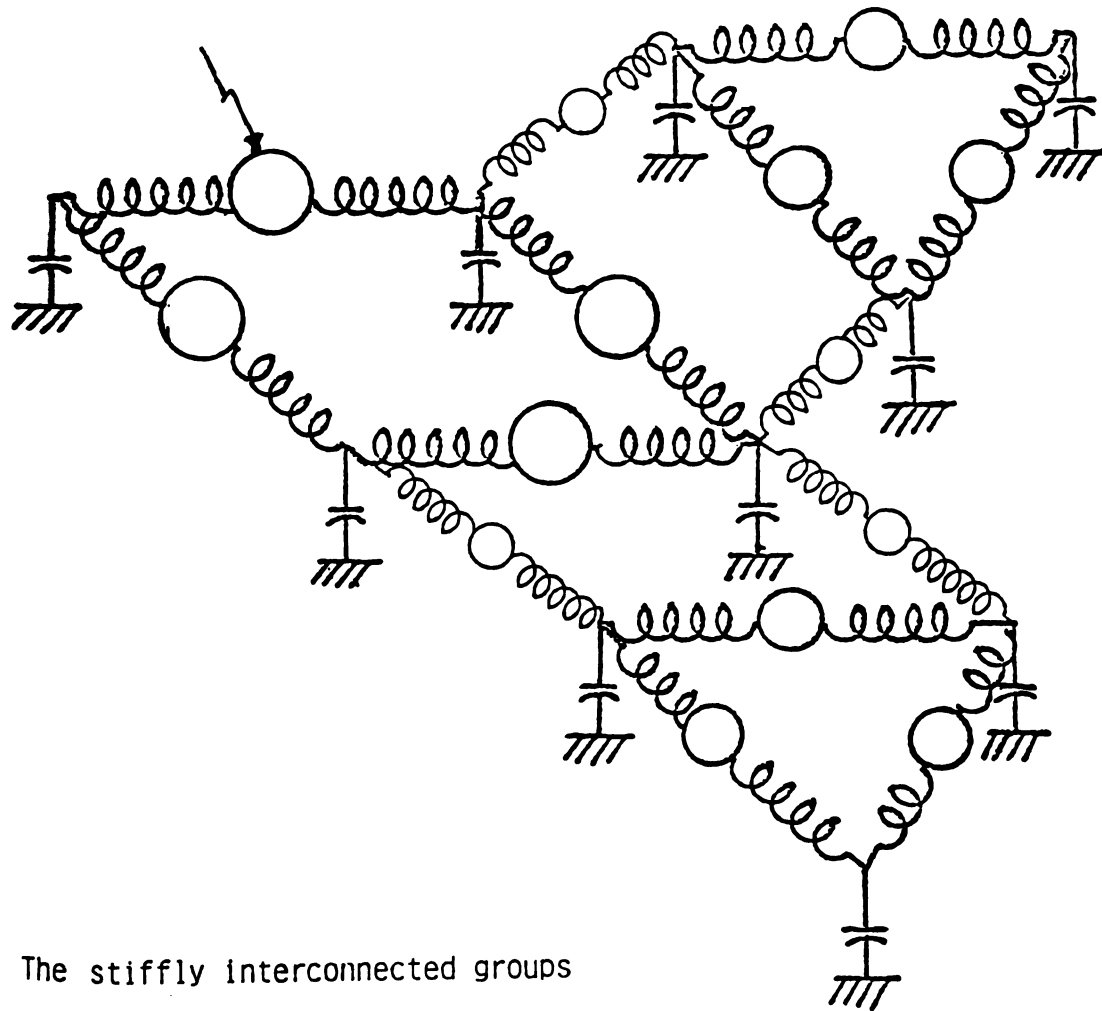
the stiff transmission lines with large power carrying capability. The light springs are those weak tie-lines interconnecting different utilities. The light springs that surround each stiffly connected group can also be regarded as a weak boundary for that particular group of buses.

Imagine that one of the masses was suddenly hit by a hammer, which is an analog to a sudden impulse of load to this group. The stiffly connected group of buses will oscillate together as one bus, and this oscillation is analogous to the oscillation of the phase angles or voltage magnitudes of the voltages at buses. Another situation that might occur is when someone connects an additional mass at a load bus (the mass pointed to by the arrow in Figure 1.1). Suppose the originally designed supports (reactive sources) are not strong enough to sustain the additional load. Then the whole group will sag. The analog in a power system is the decrease of voltage magnitudes at each bus of this group. This electromechanical model is used to indicate and provide insight into the voltage problems. The electromechanical analog is not a one-to-one mapping of our theory but will be referred to in order to help provide understanding.

Figure 1.1 has shown the structural nature of a typical interconnected network. Based on these concepts this thesis will develop a set of reasonable assumptions, models, theorems, and operating constraints for each bus as well as for each strongly interconnected group of buses in a power system transmission network related to voltage stability and security.

2164

2165  
2166  
2167



The stiffly interconnected groups

and their boundaries.

**Figure 1.1.** A hybrid electromechanical analog model.

11

12

13

14

15

16

17

18

19

20

21

22

23

24

25

26

27

28

29

30

31



### 1.3. State of the Art

The stability of power systems has generally been associated with real power such as steady state stability for real power flows across transmission elements, transient stability for large contingencies such as faults, and eigenvalue determined steady state (dynamic) stability [4]. The relationship between steady state stability, eigenvalue based steady state stability, and steady state security has been developed based on the work of Venikov [4] on eigenvalue based steady state stability, recent research on power system dynamic equivalents [2,3], and the recent EPRI 1999-1 project entitled "Methods of Analysis of Generators Governor Response and System Security" [1]. A similar set of analyses on stability and security methods does not at present exist for voltage stability and security but is the subject of this thesis. The analysis and computational methods for assessing steady state disturbance and eigenvalue based phase stability and security are now discussed. The relatively poorly developed state of the art of present analysis and computational methods for steady state disturbance and eigenvalue based voltage stability and security will then be discussed.

Venikov [4] developed a method for analyzing voltage stability by determining eigenvalues of the linearized transient stability model

[

1-11-11

1-11-11

1

1

1-11-11

1

1-11-11

1-11-11

1-11-11

1-11-11

1-11-11

1-11-11

$$\begin{bmatrix} \underline{\Delta \dot{\delta}} \\ \underline{\Delta \dot{\omega}} \end{bmatrix} = \begin{bmatrix} \underline{0} & \underline{I} \\ \underline{M}^{-1} \underline{T} & \underline{0} \end{bmatrix} \begin{bmatrix} \underline{\Delta \delta} \\ \underline{\Delta \omega} \end{bmatrix} + \begin{bmatrix} \underline{0} & \underline{0} \\ -\underline{M}^{-1} & -\underline{M}^{-1} \underline{L} \end{bmatrix} \begin{bmatrix} \underline{\Delta PM} \\ \underline{\Delta PL} \end{bmatrix}$$

$\underline{I}$  -  $n \times n$  identity matrix

$\underline{T}$  -  $n \times n$  Jacobian of the network reduced to internal generator buses

$$\underline{M} = \text{diag} \left\{ -\frac{H_1}{\pi f_s}, -\frac{H_2}{\pi f_s}, \dots, -\frac{H_n}{\pi f_s} \right\}$$

$f_s$  nominal system frequency

It was shown that the determinant of the matrix  $\underline{A}$

$$\underline{A} = \begin{bmatrix} \underline{0} & \underline{I} \\ \underline{M}^{-1} \underline{T} & \underline{0} \end{bmatrix}$$

has the same sign as the determinant of the Jacobian of the determinant of  $\underline{T}$  since

$$\det \underline{T}(S_k) = \sum_{j=1}^n \frac{H_j}{\pi f_s} \det \underline{A} = \sum_{j=1}^n \frac{H_j}{\pi f_s} \sum_{i=1}^{2n} \lambda_{iA}$$

where  $\lambda_{iA}$  are eigenvalues of matrix  $\underline{A}$ .

The changes in sign of  $\underline{T}(S_k)$  for operation condition  $S_k$  is used to check the eigenvalue based steady state stability for

•••••

30

١٥٢

des c

225 601

337

930

000 000

“*Yes, I am*”

၁၁၂

20

22

1992

1

1999

1999

•••••

10

20

10

•

2

•

6:

10

...

different operating conditions  $S_k$ . If the small positive eigenvalues of  $\underline{T}$  go negative a loss of eigenvalue based phase stability results. The small eigenvalues of  $\underline{T}$  correspond to the small imaginary eigenvalues of  $\underline{A}$  (from this investigator's work [2,3] on the theoretical basis for dynamic equivalents based on the model (i)), which always describe the oscillations of stiffly connected generator groups against one another. Thus, the loss of eigenvalue based steady state phase stability occurs across these weak transmission boundaries when for some reason the small positive eigenvalues of  $\underline{T}$  go to zero and then negative, causing the associated eigenvalues of  $\underline{A}$  with small imaginary parts to go to zero and then become positive and real. Positive real eigenvalues for  $\underline{A}$  will obviously indicate an eigenvalue based loss of steady state stability.

The recent work under RP 1999, "Methods of Analysis of Generators Governor Response and System Security," showed that a loss of stability can occur across these weak boundaries between stiffly connected generator groups for loss of generation contingencies. The lost generation for a loss of generation contingency is picked up by every generator in proportion to its inertia and thus these real power flows focus back to the generator bus where the loss of generation contingency occurred. These real power flows all cross the weak boundary of this stiffly connected generator group that experiences the loss of generation contingency causing the already weak boundary to experience thermal insecurity or loss of steady state stability problems. Thus these weak boundaries connecting

stiffly connected generator groups have been shown through this analysis to be associated with both eigenvalue based and loss of generator disturbance based steady state stability problems.

This RP 1999 project also developed algorithms and computer programs for:

- (1) identifying stiffly connected generator groups and the associated weak transmission boundaries;
- (2) determining and ranking (according to vulnerability to stability or security problems) the network elements that belong to the weak boundary surrounding each stiffly connected generator group;
- (3) a security assessment methodology that includes:
  - (a) a contingency measure that can accurately detect single, double, or triple loss of generation or line outage contingencies that experience thermal or steady state stability limit violations on one or more network elements;
  - (b) a network element measure that can detect whether a network element experiences one or more thermal overload or steady state stability limit violations over the set of single, double, and triple contingencies evaluated; and
  - (c) a system security index that measures all the relative thermal or stability limit violations over each contingency and network element combination times the probability of occurrence of the contingency and times the relative weighting of the network element's importance to security for the base case operating conditions.

1000

1000

1000

1000

1000

1000

1000

1000

1000

1000

1000

1000

1000

1000

1000

1000

1000

1000

1000

1000

1000

1000

1000

1000

1000

The existing steady state voltage stability methods [5-8] address the eigenvalue based steady state stability problem. Sensitivity matrices relating operating or dependent variables such as load bus voltage to control variables such as terminal voltage  $E$  on generators, turns ratios on off nominal tap changing transformer, and susceptance of capacitors have been developed [5-8]. The papers [5,6] showed that the sensitivity matrices, which are products of an inverse matrix times another matrix, will have positive elements as long as the matrix being inverted is approximately an  $M$  matrix and thus has strictly positive eigenvalues. The sensitivity matrices will then also have strictly positive entries. The paper [8] did not attempt to analyze the structure of the sensitivity matrix relating operating and control variables as in [5,6]. The loss of stability was inferred if a significant percentage of the elements in this sensitivity matrix change sign as the operating conditions change. Such changes in sign obviously reflect changes in the sign of eigenvalues of the matrix that is inverted. Thus both methods assess eigenvalue based steady state voltage stability.

#### 1.4. An Overview of the Thesis

In order to achieve the objectives defined in section 1.1, two parallel approaches will be used to explain the causes of the voltage problems. Since the nature of the structure dictates the behavior and response of the network, both approaches concentrate on the structural causes of these voltage problems. The first approach



is the identification of weak boundaries. The second approach is the sensitivity analysis.

Chapter 2 will develop the weak boundary identification procedure based on a linearized loadflow model. In a power network each source bus has its own upper and lower limits for reactive power generation. On the other hand, the reactive power at each load bus is specified. If the reactive requirement at a source bus exceeds the limit the reactive power injection will be fixed at that limit. The source bus is then considered as a load bus, because it can no longer match the demands of the load reflected to it or adjust for disturbances. If one increases the reactive power requirement at load buses in a group until it exceeds the capability of all the source buses in a group, all source buses in that group will be converted to load buses. This will cause that group of buses to lose the voltage control. This problem is due to the fact that the increased reactive load is only reflected to reactive sources in its own group, and because the weak boundary isolates one group from the other groups. If reactive load continues to increase and there are no sources in that group, sources in other groups will attempt to supply the reactive power but in so doing cause the voltage to collapse. Once that specific group of buses loses voltage control, its neighboring groups will not be able to use that part of the network to transfer real power. Voltage collapse in the group can also cause voltage problems for the whole system.

Chapter 2 defines what is meant by a stiffly connected group in terms of voltage phase and/or voltage magnitude. A method is then proposed for determining the stiffly connected groups and is then shown theoretically to detect such groups. Finally, the above discussion of how these weak transmission boundaries can cause voltage collapse due to insufficient reactive reserve within each group is discussed. Chapter 3 then presents computational results on the New England system that determines the stiffly connected groups and indicates how the weak boundaries surrounding these groups are affected by load level, line outages, capacitors, and local reactive reserve.

In the second approach, the sensitivity analysis, the same linearized loadflow model will be used but for a different purpose. In order to determine the controllability of voltage magnitudes at the load buses and the observability of changes in reactive power load at the source buses, two algebraic equations will be developed in the sensitivity analysis. These two algebraic equations will be called the controllability equation and the observability equation, respectively. Based on these two equations it can be shown that the lack of controllability will induce stability problems and the lack of observability will induce stability problems.

Chapter 4 will discuss the theoretical part of the sensitivity approach, which includes the mathematical model, a set of theorems derived based on these two equations. These results indicate that a loss of voltage controllability or observability can occur due to

weak boundaries, thus combining the results of the weak boundary and sensitivity approaches. It is also shown that the capacitive reactive sources at any bus or stiffly interconnected group are constrained by the stiffness of the elements connecting the bus or connecting this group to the rest of the system, respectively. Chapter 5 will discuss the experimental results of the sensitivity analysis. In both Chapter 3 and Chapter 5 the 30 bus New England system will be used. Chapter 6 provides an overview of the theorems and results of the thesis and their application to the power industry. A brief discussion of future research is also included in Chapter 6.

11.

12.

13.

14.

15.

16.

17.

18.

19.

20.

21.

22.

23.

24.

25.

26.

27.

28.

29.

## CHAPTER 2

### METHODS FOR THE DETERMINATION OF WEAK TRANSMISSION BOUNDARIES

#### 2.1. Introduction

The linearized load flow model developed in this chapter will be utilized in this research to study interrelationship of sources and loads. This load flow model will be used to first define what is meant by a stiffly connected group and a weak transmission boundary. The basic concept of a stiffly interconnected group is similar in nature to the concept based on the electromechanical analog depicted in Figure 1.1. As pointed out in the previous chapter, these weak boundaries decouple the stiffly-connected groups and prevent the real power from being transferred from one group to another. Although the existence of weak transmission boundaries is well understood, there is no method for determining the location of these weak boundaries. Under normal operating conditions an experienced operator may be able to tell where these weak boundaries are in his area. However, for the larger regional interconnected networks that are more complicated and for the case where abnormal operating conditions caused by multiple line outage or loss of generation contingencies, operator experience may not be sufficient to locate these weak boundaries. Systems planners also need methods to determine the

location of weak transmission boundaries and their relative level of insecurity to ensure the security and reliability of the system. Therefore the concept of strict synchronizing coherency for both voltage and phase, and a set of measures will be developed for locating and ranking of the insecurity of weak boundaries. The measures will then be proven to detect strict synchronizing and thus the location of weak boundaries. Finally, the decoupling of stiffly connected groups of buses that characterize the weak transmission boundaries will be justified as the cause of voltage problems, because (a) the voltage changes at buses due to all line outage or loss of reactive source contingencies are used in the algorithms developed to detect the location and rank the insecurity of weak boundaries; (b) the weak boundaries decouple the buses in different stiffly interconnected groups and thus prevent the requirement for reactive supply to cross such boundaries and the reactive supply to cross the weak boundaries; and (c) the local reactive reserve within each stiffly interconnected group may not be sufficient to handle the reactive load change which cannot be met by sources in other groups due to the weak boundaries.

The sensitivity analysis in Section 4 will develop the necessary conditions for loss of voltage stability due to loss of controllability and loss of observability. The existence of weak transmission boundaries will then be shown to cause the loss of controllability and observability induced stability problems.

## 2.2. The Linearized Loadflow Models and Stiffly Connected Buses

The following three linearized loadflow models will be discussed in this chapter:

1) A.C. loadflow model:

$$\begin{bmatrix} \Delta P \\ \Delta Q \end{bmatrix} = \begin{bmatrix} \partial P / \partial \theta & \partial P / \partial V \\ \partial Q / \partial \theta & \partial Q / \partial V \end{bmatrix} \begin{bmatrix} \Delta \theta \\ \Delta V \end{bmatrix} \quad (2.1)$$

2) Real power and phase angle (P -  $\theta$ ) loadflow model:

$$[\Delta P] = [\partial P / \partial \theta][\Delta \theta] \quad (2.2)$$

3) Reactive power and voltage magnitude (Q - V) loadflow model:

$$[\Delta Q] = [\partial Q / \partial V][\Delta V] \quad (2.3)$$

where

P is the vector of real power injections or residuals at the buses

Q is the vector of reactive power injections or residuals at the buses

$\theta$  is the vector of voltage phase angles at the buses

V is the vector of voltage magnitude at the buses

In general, at any bus i we have

$$P_i = \sum_{j=1}^n V_i V_j Y_{ij} \cos (\theta_i - \theta_j - \gamma_{ij}) \quad (2.4)$$

$$Q_i = \sum_{j=1}^n V_i V_j Y_{ij} \sin (\theta_i - \theta_j - \gamma_{ij}) \quad (2.5)$$

$$\partial P_i / \partial \theta_i = - \sum_{j=1, j \neq i}^n V_i V_j Y_{ij} \sin (\theta_i - \theta_j - \gamma_{ij}) \quad (2.6)$$

$$\partial P_i / \partial \theta_j = V_i V_j Y_{ij} \sin (\theta_i - \theta_j - \gamma_{ij}) \quad (2.7)$$

$$\partial Q_i / \partial \theta_i = \sum_{j=1, j \neq i}^n V_i V_j Y_{ij} \cos (\theta_i - \theta_j - \gamma_{ij}) \quad (2.8)$$

$$\partial Q_i / \partial \theta_j = -V_i V_j Y_{ij} \cos (\theta_i - \theta_j - \gamma_{ij}) \quad (2.9)$$

$$\partial P_i / \partial V_i = \sum_{j=1}^n V_j Y_{ij} \cos (\theta_i - \theta_j - \gamma_{ij}) + V_i Y_{ii} \cos (-\gamma_{ii}) \quad (2.10)$$

$$\partial P_i / \partial V_j = V_i Y_{ij} \cos (\theta_i - \theta_j - \gamma_{ij}) \quad (2.11)$$

$$\partial Q_i / \partial V_i = \sum_{j=1}^n V_j Y_{ij} \sin (\theta_i - \theta_j - \gamma_{ij}) + V_i Y_{ii} \sin (-\gamma_{ii}) \quad (2.12)$$

$$\partial Q_i / \partial V_j = V_i Y_{ij} \sin (\theta_i - \theta_j - \gamma_{ij}) \quad (2.13)$$

where



P and Q are the real and reactive power injections,  
respectively

i,j are the index of buses

$Y_{ij}$  is the magnitude of the admittance between buses i  
and j

$\gamma_{ij}$  is the phase angle of the admittance between buses i  
and j

Since it is assumed that there is no power dissipation in the network the Jacobian matrices are singular, therefore the inverse matrix of each of the Jacobians does not exist unless we take one of the buses as reference. Without loss of generality let the buses in the network be indexed from 0 to N, with bus 0 as the reference bus, and define the reduced Jacobian matrix as

$$\begin{bmatrix} \Delta \tilde{P} \\ \Delta \tilde{Q} \end{bmatrix} = \begin{bmatrix} \partial \tilde{P} / \partial \tilde{\theta} & \partial \tilde{P} / \partial \tilde{V} \\ \partial \tilde{Q} / \partial \tilde{\theta} & \partial \tilde{Q} / \partial \tilde{V} \end{bmatrix} \begin{bmatrix} \Delta \tilde{\theta} \\ \Delta \tilde{V} \end{bmatrix}$$

$$J_{\tilde{\theta}} = \begin{bmatrix} \partial \tilde{P}_s / \partial \tilde{\theta}_s & \partial \tilde{P}_s / \partial \tilde{\theta}_c \\ \partial \tilde{P}_c / \partial \tilde{\theta}_s & \partial \tilde{P}_c / \partial \tilde{\theta}_c \end{bmatrix}$$

where

$J_{\tilde{\theta}}$  is the phase Jacobian matrix

$\tilde{P}$  is the vector of real power injections or residuals at the buses except the reference bus

$\tilde{Q}$  is the vector of reactive power injections or residuals at the buses except the reference bus

the

the

the

the

the

the

the

the

the

the

the

the

the

the

the

the

the

the

the

$\tilde{\theta}$  is the vector of differences of voltage phase angle at the buses with respect to the phase angle of the reference bus

$\tilde{V}$  is the normalized vector of voltage magnitudes at the buses with respect to the voltage magnitude of the reference bus

Note that from now on we will drop the symbol "~" for the referenced power model and the term Jacobian matrix will replace the term reduced Jacobian matrix in this thesis.

Definition: Strict Synchronizing Coherent Group (SSC)

A group of buses are called strict synchronizing coherent if the voltage angles and relative voltage magnitudes of each pair of buses in the group respond identically for any disturbance.

This definition of strict synchronizing coherency can be applied to the nonlinear model and to all three of the linearized loadflow models. It will now be shown that a sufficient condition for SSC to hold is that there be  $n - 1$  elements with infinite admittance that form a tree and connect all  $n$  buses in the SSC group. It is intuitively clear that this sufficient condition will cause SSC to hold in the nonlinear model since all  $n$  buses are shorted together and thus form a single equivalent bus. This sufficient condition for strict synchronizing coherency is now proven to hold in each of the linearized loadflow models and is then proven to be detected by an appropriate coherency measure. The proofs are developed for the  $P - \theta$ ,  $Q - V$ , and AC loadflow models, respectively. It can be proved that the  $n - 1$  admittances connecting the  $n$  buses in a group to form a tree will cause phase, voltage, and both voltage and phase angles for buses in the same SSC group to respond identically for appropriate

disturbance. Then a phase coherency measure and a composite voltage/phase coherence measure can be established to detect this SSC property.

### 2.3. Detection of SSC Group in P - $\theta$ Loadflow Model

The P -  $\theta$  loadflow model is now broken into a study group and a test group and the group is then assumed to be connected by  $n - 1$  infinite admittance elements forming a tree. This group of  $n$  buses is then proven to be an SSC group. Now let

$S$  be the index set of the study group, and  $S = \{ 1, 2, \dots, m \}$

$C$  be the index set of the coherency test group, and  
 $C = \{ m + 1, m + 2, \dots, m + n \}$

and the real power/phase angle Jacobian becomes

$$\begin{bmatrix} \Delta P_S \\ \Delta P_C \end{bmatrix} = \begin{bmatrix} \partial P_S / \partial \theta_S & \partial P_S / \partial \theta_C \\ \partial P_C / \partial \theta_S & \partial P_C / \partial \theta_C \end{bmatrix} \begin{bmatrix} \Delta \theta_S \\ \Delta \theta_C \end{bmatrix} \quad (2.14)$$

where

$$J_\theta = \begin{bmatrix} \partial P_S / \partial \theta_S & \partial P_S / \partial \theta_C \\ \partial P_C / \partial \theta_S & \partial P_C / \partial \theta_C \end{bmatrix} \quad (2.15)$$

is the phase Jacobian matrix. The sufficient condition for SSC requires that there are at least  $n - 1$  interconnections such that  $Y_{ij} \rightarrow \infty$  that connect all  $n$  buses in the test group. Therefore sub-matrix  $[\partial P_C / \partial \theta_C]$  has the following properties:

- 1) It is a symmetric matrix.
- 2) It has at least  $2(n - 1)$  infinitely large off-diagonal elements.
- 3) All the  $n$  diagonal elements are also infinitely large and thus can be expressed as

$$[\partial P_c / \partial \theta_c]^{-1} = 1/\mu[H] \quad \text{for } \mu > 0 \text{ and } \mu \rightarrow 0 \quad (2.16)$$

where the  $H_{ij}$  is the element of  $H$  at the  $i^{\text{th}}$  row and  $j^{\text{th}}$  column.

Then

$$\begin{aligned} H_{ij} &= 0 \text{ if no connection between buses } i \text{ and } j \\ &= \mu \epsilon_{ij} \text{ if it is not an infinitely stiff connection} \\ &= \epsilon_{ij} \text{ if it is an infinitely stiff connection} \end{aligned}$$

where  $\epsilon_{ij}$ 's are non-zero real numbers in the same order of magnitude.

**Property 2.1:** If there is a set of  $n - 1$  infinite admittances connecting all  $n$  buses forming a tree in the  $n$  bus test group, then

$$(i) \quad [\partial P_c / \partial \theta_c]^{-1} \rightarrow [0] \quad (2.17)$$

$$(ii) \quad \Delta \theta_c \rightarrow 0$$

for any disturbance  $\Delta P$  and this test group is a strict synchronizing coherent group.

**Proof (i):**

Since SSC holds in the  $P - \theta$  model, it can be shown that this condition causes

$$\begin{aligned}
[\partial P_C / \partial \theta_C]^{-1} &= \{1/\mu[H]\}^{-1} \\
&= \mu\{[H]\}^{-1}
\end{aligned}
\tag{2.18}$$

where  $\mu > 0$  and  $\mu \rightarrow 0$  implies

$$[\partial P_C / \partial \theta_C]^{-1} \rightarrow [0]$$

Proof (ii):

Given that  $[\partial P_S / \partial \theta_S]$  and  $[\partial P_C / \partial \theta_C]$  are nonsingular square matrices, and the corresponding partitioned Jacobian inverse is

$$J_{\theta}^{-1} = \begin{bmatrix} K_{11} & K_{12} \\ K_{21} & K_{22} \end{bmatrix} \tag{2.19}$$

such that

$$\begin{aligned}
K_{11} &= \{[\partial P_S / \partial \theta_S] - [\partial P_S / \partial \theta_C][\partial P_C / \partial \theta_C]^{-1}[\partial P_C / \partial \theta_S]\}^{-1} \\
K_{12} &= -K_{11}[\partial P_S / \partial \theta_C][\partial P_C / \partial \theta_C]^{-1} \\
K_{21} &= -[\partial P_C / \partial \theta_C]^{-1}[\partial P_C / \partial \theta_S]K_{11} \\
K_{22} &= [\partial P_C / \partial \theta_C]^{-1} - [\partial P_C / \partial \theta_C]^{-1}[\partial P_C / \partial \theta_S]K_{12}
\end{aligned}
\tag{2.20}$$

Now if  $[\partial P_C / \partial \theta_C]^{-1} \rightarrow 0$ , then

$$K_{12} \rightarrow [0]$$

$$K_{21} \rightarrow [0] \quad (2.21)$$

$$K_{22} \rightarrow [0]$$

Solving for  $\begin{bmatrix} \Delta\theta_s \\ \Delta\theta_c \end{bmatrix}$  in (2.14) and substituting (2.20), it is clear that

$$\begin{bmatrix} \Delta\theta_s \\ \Delta\theta_c \end{bmatrix} = J_{\theta}^{-1} \begin{bmatrix} \Delta P_s \\ \Delta P_c \end{bmatrix} = \begin{bmatrix} K_{11} & 0 \\ 0 & 0 \end{bmatrix} \begin{bmatrix} \Delta P_s \\ \Delta P_c \end{bmatrix} \quad (2.22)$$

Therefore  $\Delta\theta_c \rightarrow 0$  for any  $\Delta P_s$  and  $\Delta P_c$  and thus the test group is SSC.

Having shown that the SSC sufficient condition holds in the linearized P -  $\theta$  loadflow model, a measure

$$C_{\theta}(k,1) = E\left\{[\Delta\theta_k - \Delta\theta_i]^2\right\}^{1/2}$$

$$E\{\Delta P\} = E\left\{\begin{bmatrix} \Delta P_s \\ \Delta P_c \end{bmatrix}\right\} = 0 \quad (2.23)$$

$$E\{\Delta P \Delta P^t\} = R_{\theta} \quad (2.24)$$

is proposed and is then shown to detect the SSC property.

Before proceeding, the coherency measure is written as

$$C_{\theta}(k,1) = \{e_{k1}^t S_{\theta} e_{k1}\}^{\frac{1}{2}} \quad (2.25)$$

where the  $j^{\text{th}}$  element of the vector  $e_{k1}$  is defined as

$$\{e_{k1}\}_j = \begin{cases} 1 & \text{if } j = k \\ -1 & \text{if } j = 1 \\ 0 & \text{otherwise} \end{cases} \quad (2.26)$$

with  $k,1 = 1, 2, \dots, m + n$

$$S_{\theta} = E\{\Delta\theta\Delta\theta^t\} \quad (2.27)$$

**Property 2.2:** The coherency measure satisfies  $C_{\theta}(k,1) \leq \epsilon$  for any small  $\epsilon > 0$  if bus  $k,1$  belong to the coherent group i.e.,  
 $k,1 = m + 1, m + 2, \dots, N$

**Proof:**

Since

$$J_{\theta}^{-1} = \begin{bmatrix} K_{11} & K_{12} \\ K_{21} & K_{22} \end{bmatrix}$$

which is partitioned into the study and SSC group respectively, then

$$\Delta\theta\Delta\theta^t = \begin{bmatrix} K_{11} & K_{12} \\ K_{21} & K_{22} \end{bmatrix} \begin{bmatrix} \Delta P_s \\ \Delta P_c \end{bmatrix} [\Delta P_s^t \quad \Delta P_c^t] \begin{bmatrix} K_{11} & K_{12} \\ K_{21} & K_{22} \end{bmatrix}^t \quad (2.28)$$



but from property 2.2 we have

$$K_{12} \rightarrow [0]$$

$$K_{21} \rightarrow [0] \quad (2.29)$$

$$K_{22} \rightarrow [0]$$

so that

$$\Delta\theta\Delta\theta^t \rightarrow \begin{bmatrix} K_{11}\Delta P_s \Delta P_s^t K_{11}^t & 0 \\ 0 & 0 \end{bmatrix} \quad (2.30)$$

In order to detect the SSC group we can artificially create a set of loss-of-generation contingencies such that  $E\{\Delta P\Delta P^t\}$  has all elements on the principle diagonal nonzero. Therefore, the coherency measure between each pair of buses becomes

$$\begin{aligned} C_\theta(k,1) &= \{e_{k1}^t S_\theta e_{k1}\}^{\frac{1}{2}} \\ &= \{e_{k1}^t E\{\Delta\theta\Delta\theta^t\} e_{k1}\}^{\frac{1}{2}} \\ &\rightarrow \left\{ e_{k1}^t E \left\{ \begin{bmatrix} K_{11}\Delta P_s \Delta P_s^t K_{11}^t & 0 \\ 0 & 0 \end{bmatrix} e_{k1} \right\} \right\}^{1/2} \end{aligned} \quad (2.31)$$

Hence  $C_\theta(k,1) \rightarrow 0$  if both buses  $k$  and  $1$  belong to the SSC coherent group ( $k,1 = m + 1, m + 2, \dots, N$ ).

#### 2.4. Detection of SSC Group in Q - V Loadflow Model

The Q - V loadflow model is now broken into a study group and a test group, and the group is then assumed to be connected by  $n - 1$  infinite admittance elements forming a tree. This group of  $n$  buses is then proven to be an SSC group. Now let

$$\begin{bmatrix} \Delta Q_s \\ \Delta Q_c \end{bmatrix} = \begin{bmatrix} \partial Q_s / \partial V_s & \partial Q_s / \partial V_c \\ \partial Q_c / \partial V_s & \partial Q_c / \partial V_c \end{bmatrix} \begin{bmatrix} \Delta V_s \\ \Delta V_c \end{bmatrix} \quad (2.32)$$

Define

$$J_v = \begin{bmatrix} \partial Q_s / \partial V_s & \partial Q_s / \partial V_c \\ \partial Q_c / \partial V_s & \partial Q_c / \partial V_c \end{bmatrix} \quad (2.33)$$

If buses  $i$  and  $j$  belong to the SSC group, then

$$\partial Q_i / \partial V_j = V_i Y_{ij} \sin(-\gamma_{ij}) \quad (2.34)$$

and the submatrix  $[\partial Q_c / \partial V_c]$  has the following properties:

- 1) It is an asymmetric\* matrix.
- 2) It has at least  $2(n - 1)$  infinitely large-off diagonal elements.
- 3) All the  $n$  diagonal elements are also infinitely large.

Let

---

\*It can be structurally symmetric with all symmetric elements.

$$[\partial Q_c / \partial V_c] = 1/\mu[H] \quad (2.35)$$

$\mu > 0$  and  $\mu \rightarrow 0$

$H_{ij}$  be the element of  $k$  at the  $i^{\text{th}}$  row and  $j^{\text{th}}$  column

$H_{ij} = 0$  if no connection between buses  $i$  and  $j$

$= \mu \epsilon_{ij}$  if it is not infinitely stiff connection

$= \epsilon_{ij}$  if it is an infinitely stiff connection

where  $\epsilon_{ij}$ 's are non-zero real numbers in the same order of magnitude.

Property 2.3: If there is an  $n - 1$  admittance connecting all  $n$  buses forming a tree in the  $n$  bus test group, then

$$\begin{aligned} \text{(i)} \quad & [\partial Q_c / \partial V_c]^{-1} \rightarrow [0] \\ \text{(ii)} \quad & \Delta V_c \rightarrow [0] \end{aligned} \quad (2.36)$$

for any disturbance  $\Delta Q$  and this test group is a strict synchronizing coherent group.

Proof (i):

Since SSC holds in the  $Q - V$  model, it can be shown that

$$\begin{aligned} [\partial Q_c / \partial V_c]^{-1} &= \{1/\mu[H]\}^{-1} \\ &= \mu\{[H]\}^{-1} \end{aligned} \quad (2.37)$$

where  $\mu > 0$  and  $\mu \rightarrow 0$  implies

$$[\partial Q_c / \partial V_c]^{-1} \rightarrow [0]$$

**Proof (ii):**

Assume that  $[\partial Q_s / \partial V_s]$  and  $[\partial Q_c / \partial V_c]$  are nonsingular square matrices, and the corresponding partitioned Jacobian inverse is

$$J_V^{-1} = \begin{bmatrix} K_{11} & K_{12} \\ K_{21} & K_{22} \end{bmatrix} \quad (2.38)$$

such that

$$\begin{aligned} K_{11} &= \{[\partial Q_s / \partial V_s] - [\partial Q_s / \partial V_c][\partial Q_c / \partial V_c]^{-1}[\partial Q_c / \partial V_s]\}^{-1} \\ K_{12} &= -K_{11}[\partial Q_s / \partial V_c][\partial Q_c / \partial V_c]^{-1} \\ K_{21} &= -[\partial Q_c / \partial V_c]^{-1}[\partial Q_c / \partial V_s]K_{11} \\ K_{22} &= [\partial Q_c / \partial V_c]^{-1} - [\partial Q_c / \partial V_c]^{-1}[\partial Q_c / \partial V_s]K_{12} \end{aligned} \quad (2.39)$$

Note that if  $[\partial Q_c / \partial V_c]^{-1} \rightarrow 0$ , then

$$K_{12} \rightarrow [0]$$

$$K_{21} \rightarrow [0]$$

$$K_{22} \rightarrow [0]$$

Solving for  $\begin{bmatrix} \Delta V_s \\ \Delta V_c \end{bmatrix}$  in (2.32) and substituting (2.39), we get

$$\begin{bmatrix} \Delta V_s \\ \Delta V_c \end{bmatrix} = J_v^{-1} \begin{bmatrix} \Delta Q_s \\ \Delta Q_c \end{bmatrix} = \begin{bmatrix} K_{11} & 0 \\ 0 & 0 \end{bmatrix} \begin{bmatrix} \Delta Q_s \\ \Delta Q_c \end{bmatrix}$$

Therefore  $\Delta V_c \rightarrow [0]$  for any  $\Delta Q_s$  and  $\Delta Q_c$  and thus the test group is SSC.

Having shown that the SSC sufficient condition holds in the linearized Q - V loadflow model, a measure

$$C_v(k,1) = E [\Delta V_k/V_k - \Delta V_1/V_1]^2 \quad \frac{1}{2}$$

$$E\{\Delta Q\} = E \begin{bmatrix} \Delta Q_s \\ \Delta Q_c \end{bmatrix} = 0$$

$$E\{\Delta Q \Delta Q^t\} = R_v$$

is proposed and is then shown to detect the SSC property. Define a diagonal matrix

$$[\lambda] = \begin{bmatrix} \lambda_s & 0 \\ 0 & \lambda_c \end{bmatrix}$$

where the  $i^{\text{th}}$  element on the principle diagonal of  $[\lambda]$  is  $1/V_i$  with  $i = 1, 2, \dots, m + n$ ,  $e_{k1}$  as defined in (2.26), and define the matrix

$$\begin{aligned} S_V &= E\{\Delta \bar{V} \Delta \bar{V}^t\} \\ &= E\{[\lambda][\Delta V \Delta V^t][\lambda]\} \end{aligned} \quad (2.40)$$

where  $\Delta \bar{V}_k = \Delta V_k / V_k$ , then the coherency measure has the following form:

$$C_V(k,1) = \{e_{k1}^t S_V e_{k1}\}^{\frac{1}{2}} \quad (2.41)$$

Property 2.4: The coherency measure satisfies  $C_V(k,1) \leq \epsilon$  for any small  $\epsilon > 0$  if bus  $k,1$  belong to the coherent group,  $k,1 = m + 1, m + 2, \dots, m + n$ .

**Proof:**

Since

$$J_V^{-1} = \begin{bmatrix} K_{11} & K_{12} \\ K_{21} & K_{22} \end{bmatrix},$$

which is partitioned into the study and SSC group, respectively, then

$$\Delta V \Delta V^t = \begin{bmatrix} K_{11} & K_{12} \\ K_{21} & K_{22} \end{bmatrix} \begin{bmatrix} \Delta Q_s \\ \Delta Q_c \end{bmatrix} [\Delta Q_s^t \quad \Delta Q_c^t] \begin{bmatrix} K_{11} & K_{12} \\ K_{21} & K_{22} \end{bmatrix}^t$$

$$\Delta \bar{V} \Delta \bar{V}^t = [\lambda] [\Delta V \Delta V^t] [\lambda]$$

$$= [\lambda] \begin{bmatrix} K_{11} & K_{12} \\ K_{21} & K_{22} \end{bmatrix} \begin{bmatrix} \Delta Q_s \\ \Delta Q_c \end{bmatrix} [\Delta Q_s^t \quad \Delta Q_c^t] \begin{bmatrix} K_{11} & K_{12} \\ K_{21} & K_{22} \end{bmatrix}^t [\lambda] \quad (2.42)$$

But from property 2.3, matrices  $K_{12}$ ,  $K_{21}$ , and  $K_{22}$  satisfy

$$K_{12} \rightarrow [0]$$

$$K_{21} \rightarrow [0]$$

$$K_{22} \rightarrow [0]$$

so that

$$\Delta \bar{V} \Delta \bar{V}^t \rightarrow [\lambda] \begin{bmatrix} K_{11} \Delta Q_s \Delta Q_s^t K_{11}^t & 0 \\ 0 & 0 \end{bmatrix} [\lambda]$$

$$\Delta \bar{V} \Delta \bar{V}^t \rightarrow \begin{bmatrix} \lambda_s K_{11} \Delta Q_s \Delta Q_s^t K_{11}^t \lambda_s & 0 \\ 0 & 0 \end{bmatrix} \quad (2.43)$$

2016

2017

2018

2019

2020

2021

2022

2023

2024



In order to detect the SSC group in the Q - V model, we can artificially create a set of loss-of-generation (reactive power) contingencies such that  $E\{\Delta Q \Delta Q^t\}$  has all elements on the principle diagonal non-zero. Therefore, the coherency between each pair of buses in the system becomes

$$\begin{aligned}
 C_V(k,1) &= \{e_{k1}^t S_V e_{k1}\}^{\frac{1}{2}} \\
 &= \{e_{k1}^t E\{\Delta \bar{V} \Delta \bar{V}^t\} e_{k1}\}^{\frac{1}{2}} \\
 &\rightarrow \left\{ e_{k1}^t E \begin{pmatrix} \lambda_s K_{11} \Delta Q_s \Delta Q_s^t K_{11}^t \lambda_s & 0 \\ 0 & 0 \end{pmatrix} e_{k1} \right\}^{\frac{1}{2}} \\
 C_V(k,1) &\rightarrow \left\{ e_{k1}^t \begin{pmatrix} \{\lambda_s K_{11} E\{\Delta Q_s \Delta Q_s^t K_{11}^t \lambda_s\}\} & 0 \\ 0 & 0 \end{pmatrix} e_{k1} \right\}^{\frac{1}{2}} \quad (2.44)
 \end{aligned}$$

Hence  $C_V(k,1) \rightarrow 0$  if both buses  $k$  and  $1$  belong to the SSC group.

## 2.5. Detection of SSC Group in A.C. Loadflow Model

The A.C. loadflow model is now broken into a study group and a test group and the group is then assumed to be connected by  $n - 1$  infinite admittance elements forming a tree. This group of  $n$  buses is then proven to be an SSC group.

$$\begin{bmatrix} \Delta P_S \\ \Delta Q_S \\ \Delta P_C \\ \Delta Q_C \end{bmatrix} = \begin{bmatrix} \partial P_S / \partial \theta_S & \partial P_S / \partial V_S & \partial P_S / \partial \theta_C & \partial P_S / \partial V_C \\ \partial Q_S / \partial \theta_S & \partial Q_S / \partial V_S & \partial Q_S / \partial \theta_C & \partial Q_S / \partial V_C \\ \partial P_C / \partial \theta_S & \partial P_C / \partial V_S & \partial P_C / \partial \theta_C & \partial P_C / \partial V_C \\ \partial Q_C / \partial \theta_S & \partial Q_C / \partial V_S & \partial Q_C / \partial \theta_C & \partial Q_C / \partial V_C \end{bmatrix} \begin{bmatrix} \Delta \theta_S \\ \Delta V_S \\ \Delta \theta_C \\ \Delta V_C \end{bmatrix} \quad (2.45)$$

where

$$J \triangleq \begin{bmatrix} \partial P_S / \partial \theta_S & \partial P_S / \partial V_S & \partial P_S / \partial \theta_C & \partial P_S / \partial V_C \\ \partial Q_S / \partial \theta_S & \partial Q_S / \partial V_S & \partial Q_S / \partial \theta_C & \partial Q_S / \partial V_C \\ \partial P_C / \partial \theta_S & \partial P_C / \partial V_S & \partial P_C / \partial \theta_C & \partial P_C / \partial V_C \\ \partial Q_C / \partial \theta_S & \partial Q_C / \partial V_S & \partial Q_C / \partial \theta_C & \partial Q_C / \partial V_C \end{bmatrix}$$

$$= \begin{bmatrix} J_{11} & J_{12} \\ J_{21} & J_{22} \end{bmatrix} \quad (2.46)$$

and the submatrix

$$J_{22} = \begin{bmatrix} \partial P_C / \partial \theta_C & \partial P_C / \partial V_C \\ \partial Q_C / \partial \theta_C & \partial Q_C / \partial V_C \end{bmatrix}$$

has the following properties:

- 1) It is an asymmetric matrix.\*
- 2) It has at least  $4(n - 1)$  infinitely large off-diagonal elements.

---

\*It can be structurally symmetric with all symmetric elements.

3) All the  $2n$  diagonal elements are also infinitely large and thus can be expressed as

$$J_{22} = 1/\mu[H] \quad (2.47)$$

for  $\mu > 0$  and  $\mu \rightarrow 0$  where

$H_{ij}$  be the element of  $k$  at the  $i^{\text{th}}$  row and  $j^{\text{th}}$  column

$H_{ij} = 0$  if no connection between buses  $i$  and  $j$

$= \mu \epsilon_{ij}$  if it is not an infinitely stiff connection

$= \epsilon_{ij}$  if it is an infinitely stiff connection

where  $\epsilon_{ij}$ 's are non-zero real numbers in the same order of magnitudes.

In order to simplify the expressions in the following proofs, let

$$\Delta W = [\Delta W_S^t \Delta W_C^t]^t = [\Delta P_S^t \Delta Q_S^t \Delta P_C^t \Delta Q_C^t]^t$$

$$\Delta X = [\Delta X_S^t \Delta X_C^t]^t = [\Delta \theta_S^t \Delta V_S^t \Delta \theta_C^t \Delta V_C^t]^t$$

**Property 2.5:** If there is an  $n - 1$  infinite admittance connecting all  $n$  buses forming a tree in the  $n$  bus test group, then

$$(i) \quad J_{22} \rightarrow [0] \quad (2.48)$$

(ii)  $\Delta X_C \rightarrow 0$  for any disturbances  $\Delta P$  and  $\Delta Q$

$$\text{i.e.} \begin{bmatrix} \Delta \theta_C \\ \Delta V_C \end{bmatrix} \rightarrow 0$$

Proof (i):

Since SSC holds in the A.C. model, it can be shown that

$$\begin{aligned} J_{22}^{-1} &= \{1/\mu[H]\}^{-1} \\ &= \mu\{[H]\}^{-1} \end{aligned} \quad (2.49)$$

but  $\mu > 0$  and  $\mu \rightarrow 0$  implies

$$J_{22} \rightarrow [0]$$

Proof (ii):

Assume that  $J_{11}$  and  $J_{22}$  are nonsingular square matrices, and let the corresponding partitioned Jacobian inverse be

$$J^{-1} = \begin{bmatrix} K_{11} & K_{12} \\ K_{21} & K_{22} \end{bmatrix} \quad (2.50)$$

such that

$$\begin{aligned} K_{11} &= [J_{11} - J_{12} J_{22}^{-1} J_{21}]^{-1} \\ K_{12} &= -K_{11} J_{12} J_{22}^{-1} \\ K_{21} &= -J_{22}^{-1} J_{21} K_{11} \\ K_{22} &= J_{22}^{-1} - J_{22}^{-1} J_{21} K_{12} \end{aligned} \quad (2.51)$$

Note that if  $J_{22}^{-1} \rightarrow 0$ , then

$$K_{12} \rightarrow [0]$$

$$K_{21} \rightarrow [0]$$

$$K_{22} \rightarrow [0]$$

Solving for  $\begin{bmatrix} \Delta X_s \\ \Delta X_c \end{bmatrix}$  in (2.45) and substituting (2.51) gives

$$\begin{bmatrix} \Delta X_s \\ \Delta X_c \end{bmatrix} = J^{-1} \begin{bmatrix} \Delta X_s \\ \Delta X_c \end{bmatrix} = \begin{bmatrix} K_{11} & 0 \\ 0 & 0 \end{bmatrix} \begin{bmatrix} \Delta W_s \\ \Delta W_c \end{bmatrix}$$

Therefore  $\Delta X_c \rightarrow [0]$  for any  $\Delta W_s$  and  $\Delta W_c$  and thus the test group is SSC.

As a result, the SSC sufficient condition has been shown to hold in the linearized A.C. loadflow model. A measure [9]

$$\begin{aligned} C(k,1) &= E\{(\Delta\theta_k - \Delta\theta_1)^2 + (\Delta V_k/V_k - \Delta V_1/V_1)^2\}^{\frac{1}{2}} \\ &= \{e_{k1}^t [S_\theta] e_{k1} + e_{k1}^t [S_v] e_{k1}\}^{\frac{1}{2}} \end{aligned} \quad (2.52)$$

$$\begin{aligned} E \left\{ \begin{bmatrix} \Delta P \\ \Delta Q \end{bmatrix} \right\} &= 0 \\ E \left\{ \begin{bmatrix} \Delta P \\ \Delta Q \end{bmatrix} [\Delta P^t \Delta Q^t] \right\} &= R \end{aligned}$$

is proposed and then shown to detect the SSC property. Let  $S_\theta$ ,  $S_v$ ,  $\lambda_s$ , and  $\lambda_c$  be defined as in the previous sections of this chapter. Additionally, let

$$\{\bar{e}_{k1}\}_j = \begin{cases} 1 & \text{for } j = k \text{ or } j = k + m \\ -1 & \text{for } j = 1 \text{ or } j = 1 + m \\ 0 & \text{otherwise} \end{cases} \quad (2.53)$$

$$S = E\{\bar{\lambda}\Delta X\Delta X^t\bar{\lambda}\} \quad (2.54)$$

with

$$\bar{\lambda} = \begin{bmatrix} \bar{\lambda}_s & 0 \\ 0 & \bar{\lambda}_c \end{bmatrix} \quad (2.55)$$

$$\bar{\lambda}_s = \begin{bmatrix} I & 0 \\ 0 & \lambda_s \end{bmatrix}$$

$$\bar{\lambda}_c = \begin{bmatrix} I & 0 \\ 0 & \lambda_c \end{bmatrix}$$

where

$\bar{\lambda}_s$  is  $2m \times 2m$  matrix

$\bar{\lambda}_c$  is  $2n \times 2n$  matrix

$\bar{\lambda}$  is  $2(m+n) \times 2(m+n)$  matrix

Then from (2.53), (2.54), and (2.55)

$$\begin{aligned}
 C(k,1) &= E\{[\Delta\theta_k - \Delta\theta_1]^2 + [\Delta V_k/V_k - \Delta V_1/V_1]\}^{\frac{1}{2}} \\
 &= \left\{ e_{k1}^t E\{\Delta\theta\Delta\theta^t\} e_{k1} + e_{k1}^t E\{\Delta\bar{V}\Delta\bar{V}^t\} e_{k1} \right\}^{\frac{1}{2}} \\
 &= \left\{ \bar{e}_{k1}^t E \left\{ \begin{bmatrix} \Delta\theta_s \\ \Delta V_s \\ \Delta\theta_c \\ \Delta V_c \end{bmatrix} [\Delta\theta_s^t \Delta\bar{V}_s^t \Delta\theta_c^t \Delta\bar{V}_c^t] \begin{bmatrix} \Delta\theta_s \\ \Delta V_s \\ \Delta\theta_c \\ \Delta V_c \end{bmatrix} \right\} \bar{e}_{k1} \right\}^{\frac{1}{2}} \\
 &= \left\{ \bar{e}_{k1}^t \bar{\lambda} E\{\Delta X \Delta X^t\} \bar{e}_{k1} \right\}^{\frac{1}{2}}
 \end{aligned} \tag{2.56}$$

Property 2.6: If  $k,1$  belong to SSC then

$C(k,1) \leq \epsilon$  for any small  $\epsilon > 0$

**Proof:**

Since

$$J^{-1} = \begin{bmatrix} K_{11} & K_{12} \\ K_{21} & K_{22} \end{bmatrix},$$

which is partitioned into the study and SSC groups, respectively,  
then

$$\Delta X \Delta X^t = \begin{bmatrix} K_{11} & K_{12} \\ K_{21} & K_{22} \end{bmatrix} \begin{bmatrix} \Delta W_s \\ \Delta W_c \end{bmatrix} [\Delta W_s^t \Delta W_c^t] \begin{bmatrix} K_{11} & K_{12} \\ K_{21} & K_{22} \end{bmatrix}^t \quad (2.57)$$

But from property 2.5 we get

$$K_{12} \rightarrow [0]$$

$$K_{21} \rightarrow [0]$$

$$K_{22} \rightarrow [0]$$

so that

$$\Delta X \Delta X^t \rightarrow \begin{bmatrix} K_{11} \Delta W_s \Delta W_s^t K_{11}^t & 0 \\ 0 & 0 \end{bmatrix} \quad (2.58)$$

In order to detect the SSC group in the A.C. model, again we can artificially create a set of loss-of-generation (real and reactive power) contingencies such that  $E\{\Delta W \Delta W^t\}$  has all elements on the principle diagonal non-zero. Therefore, when measuring the coherency between each pair of buses in the system we get



$$\begin{aligned}
C(k,1) &= \left\{ \bar{e}_{k1}^t E \left\{ \bar{\lambda}_{\Delta} X_{\Delta} X_{\Delta}^t \bar{\lambda} \right\} \bar{e}_{k1} \right\}^{\frac{1}{2}} \\
&= \left\{ \bar{e}_{k1}^t E \left\{ \begin{bmatrix} \bar{\lambda}_s & 0 \\ 0 & \bar{\lambda}_c \end{bmatrix} \begin{bmatrix} \Delta X_s \\ \Delta X_c \end{bmatrix} \begin{bmatrix} \Delta X_s^t & \Delta X_c^t \end{bmatrix} \begin{bmatrix} \bar{\lambda}_s & 0 \\ 0 & \bar{\lambda}_c \end{bmatrix} \right\} \bar{e}_{k1} \right\}^{\frac{1}{2}} \\
&\rightarrow \left\{ \bar{e}_{k1}^t E \left\{ \begin{bmatrix} \bar{\lambda}_s & 0 \\ 0 & \bar{\lambda}_c \end{bmatrix} \begin{bmatrix} K_{11} \Delta W_s \Delta W_s^t K_{11}^t & 0 \\ 0 & 0 \end{bmatrix} \begin{bmatrix} \bar{\lambda}_s & 0 \\ 0 & \bar{\lambda}_c \end{bmatrix} \right\} \bar{e}_{k1} \right\}^{\frac{1}{2}} \\
&= \left\{ \bar{e}_{k1}^t E \left\{ \begin{bmatrix} \bar{\lambda}_s K_{11} \Delta W_s \Delta W_s^t K_{11}^t \bar{\lambda}_s & 0 \\ 0 & 0 \end{bmatrix} \right\} \bar{e}_{k1} \right\}^{\frac{1}{2}} \\
&= \left\{ \bar{e}_{k1}^t \left\{ \begin{bmatrix} \bar{\lambda}_s K_{11} E \{ \Delta W_s \Delta W_s^t \} K_{11}^t \bar{\lambda}_s & 0 \\ 0 & 0 \end{bmatrix} \right\} \bar{e}_{k1} \right\}^{\frac{1}{2}}
\end{aligned}$$

since

$$C(k,1) \rightarrow \left\{ \bar{e}_{k1}^t \left\{ \begin{bmatrix} \bar{\lambda}_s K_{11} E \{ \Delta W_s \Delta W_s^t \} K_{11}^t \bar{\lambda}_s & 0 \\ 0 & 0 \end{bmatrix} \right\} \bar{e}_{k1} \right\}^{\frac{1}{2}}$$

Therefore  $C(k,1) \rightarrow 0$  if both buses  $k$  and  $1$  belong to the SSC group.

## 2.6. The Limited Sources and Weak Boundaries

Physically for each source bus or generator bus there is a set of lower and upper limits of reactive power injection, i.e.,



$Q_{\min,i} \leq Q_i \leq Q_{\max,i}$  at source or generator bus  $i$ . Whenever  $Q_i$  hits one of the limits, the reactive power injection will stay there. As far as we are concerned in the loadflow solutions, this particular source bus now is regarded as a load bus, and it can no longer take action in responding to any reactive power disturbances to match demands beyond its capability. If a stiffly connected group always has the reactive power demands exceeding the total capability of the group, eventually all its source buses will be converted into load buses. Under this situation, due to the fact that the reactive power cannot be transmitted over long distance (across weak boundaries), this group will lose the voltage stability.

If each stiffly connected group is regarded as a single bus, this group with heavy reactive load will be regarded as a load bus to those interconnected networks. One may ask if this is the case then can a set of guidelines or operational constraints be developed for each of these stiffly connected groups based on our understanding about the behavior of each individual bus. The answer is yes. If the constraints and rules for voltage stability can be developed at each bus then these constraints can be generalized to the groups. We will show this in Chapter 4 using the sensitivity analysis.

The weak transmission boundaries for a power system are the branches that connect the buses in different SSC groups. It is clear that these boundaries are referred to as weak because none of the branches that connect the buses in these groups has infinite admittance where within each SSC group of buses there is an infinite

2012

2013

2014

2015

2016

2017

2018

2019

2020

2021

2022

2023

2024

2025

2026

2027

2028

2029

2030

2031

2032

2033

2034

2035

2036

admittance path connecting all buses. In practical networks the SSC groups will not be connected by infinite admittance branches but rather the collection of buses within each such group are more stiffly interconnected than the buses between such groups. Operating conditions such as loadflow can possibly modify the SSC groups in a network. Moreover, the SSC groups defined based on phase, voltage, and both voltage and phase (current) may be different. The next chapter will investigate the SSC groups based on the phase, voltage, and current coherency measures.

The weak transmission boundaries can cause the security and stability problems for power systems. It was shown that the phase coherency measure (regulated loss of generated contingencies) based on inertial loadflow identified the weak transmission boundaries that decoupled the dynamics of the classical transient stability model in [1]. This decoupling could cause the phase oscillations between regions in power systems that have recently been observed. Furthermore, the weak boundaries identified by the phase coherency measure have been shown to identify the branches that are severely affected by any line outage or loss of generation contingency in a 49 bus test system. Thus the branches in the weak boundaries are the insecure elements in the network and once identified indicate the contingencies that could most severely affect system security by affecting particular branches or groups of branches in these weak boundaries.

The above study [1] was performed for thermal and steady state phase stability problems. The weak boundaries will be shown in Chapter 4 to prevent changes in reactive load from being reflected to reactive sources in other SSC groups. Thus, sources in one SSC group will not provide reactive power for reactive load requirements in another SSC group.

Furthermore, the weak boundaries will be shown in Chapter 4 to require voltage support for load buses be provided by the voltages established at reactive source buses in an SSC group. The voltage at load buses in one SSC group of load and generator buses will therefore not be significantly affected by the voltage magnitudes established at source buses in other SSC groups. It is thus clear that voltage control is local within each SSC group. Therefore, if reactive load increases or decreases, the source buses in an SSC group must compensate. If the reactive load continues to change such that all source buses in an SSC group reach the upper or lower limit, these source buses in the SSC can no longer provide voltage control. Additional changes in reactive load will also cause large voltage changes within the SSC group as the network attempts to provide reactive power through the weak boundaries.

It is thus clear that there must be sufficient positive and negative reactive reserve in each SSC group to preserve voltage stability problem and is investigated in the computational results on the 30 bus New England system given in Chapter 5.

## CHAPTER 3

### DETERMINATION OF WEAK TRANSMISSION BOUNDARIES FOR THE 30 BUS NEW ENGLAND SYSTEM

#### 3.1. Introduction

The purpose of this chapter is to determine the weak transmission boundaries for phase, voltage magnitude, and current on a 30 bus New England system. The weak transmission boundary for phase is based on a phase coherency used to determine the coherent groups to be aggregated to produce dynamic equivalents [3] for transient stability studies. This same phase rms coherency measure evaluated for all inertial loadflow simulated loss of generation contingencies was shown [1] (a) to detect the weak transmission boundaries to cause the phase oscillation problem based on an analysis of the classical transient stability model, and (b) to determine the weak transmission boundaries and the associated branches that experience thermal or phase stability problems for line outage or inertial loadflow simulated loss of generation contingencies.

The weak phase transmission boundary based on the rms phase coherency measure is evaluated in this chapter based on load contingencies at all buses in the network rather than just loss of generation contingencies. The loss of load disturbances at all buses should be more robust and should establish the weak transmission boundaries

between groups of load and generation buses and not just between groups of generator buses. The weak transmission based on this phase coherency measure should establish the boundaries and associated branches that are vulnerable to phase stability problems. The weak phase transmission boundaries are determined for three cases: active power load disturbances at every bus, reactive power load disturbances at every bus, and complex power load disturbances at every bus. It is found that the weak phase transmission boundaries for active and complex power disturbances are quite similar and reflect the electrical distance from the swing bus. This occurred because the mismatch due to the loss of load is eliminated by a similar loss of generation at the swing bus causing a power flow to the swing bus from the disturbed bus. The weak phase boundaries for loss of reactive disturbance had no pattern and reflect the weak coupling of phase and reactive power.

A voltage coherency measure is used to determine the weak voltage transmission boundaries for loss of load at all buses. The weak voltage transmission boundaries reflect the boundaries between groups of PQ and PV buses where voltage security and stability problems should occur. This is confirmed by the results in Chapter 5 based on a set of multiple loss of generation and line outage contingencies. The weak voltage transmission boundaries between groups of PV and PQ buses are determined by converting all PV buses to PQ buses so that the PV buses can experience voltage swings that will reflect the stiffness of the transmission grid and not the action of the voltage controls. The weak voltage transmission boundary for active power



and reactive power disturbances encircle PQ and PV buses that are all interconnected and lie in a small geographical area. The weak boundaries for reactive power disturbances and real power disturbances are quite similar showing that weak voltage boundaries are sensitive to both active and reactive power flows. The principal difference between the weak voltage transmission boundaries for active and reactive power disturbances is that there appears to be additional separation of groups of buses near the swing bus for real power disturbances, and the groups of buses for reactive power disturbances appear to be based more on local transmission network characteristics.

A current coherency measure is used to determine the weak current transmission boundaries for loss of load disturbances at all buses. The weak current transmission boundaries represent the boundaries between groups of PV and PQ buses where thermal security problems should occur. All PV buses are converted to PQ buses so that the PV buses can experience both phase and voltage swings that are determined by the network and not the voltage controls. The weak current boundaries determined for active and complex power disturbances are identical. Moreover, the weak current boundaries are very similar to the weak phase transmission boundaries, reflecting that the phase stability and thermal overload problems are related and are likely to occur on the same transmission boundaries. This was tacitly assumed in the recent EPRI study

All computer simulations in this chapter as well as in Chapter 5 use the 30 bus New England system. This system has 10 generator buses, 20 load buses, and 37 branches as shown by Figure 3.1. The solved loadflow data or the base case data is listed in Appendix 1, using common format for loadflow data exchange.

The phase, voltage, and current coherency measures defined in Chapter 2 were derived based on a linearized loadflow model and a probabilistic disturbance model. Although the coherency measures defined in this manner were shown to detect the SSC groups, it is not convenient for computing the rms measure.

It can be shown that the phase and current coherency measures can be evaluated using measures

$$S_{\theta} = \left\{ \sum_{i \in I} (\Delta\delta_k(i) - \Delta\delta_1(i))^2 \right\}^{\frac{1}{2}} \quad (3.1)$$

$$S_V = \left\{ \sum_{i \in I} \left( \frac{\Delta V_k(i)}{V_k} - \frac{\Delta V_1(i)}{V_1} \right)^2 \right\}^{\frac{1}{2}} \quad (3.2)$$

$$S = \left\{ \sum_{i \in I} \left\{ (\Delta\delta_k(i) - \Delta\delta_1(i))^2 + \left( \frac{\Delta V_k(i)}{V_k} - \frac{\Delta V_1(i)}{V_1} \right)^2 \right\} \right\}^{\frac{1}{2}} \quad (3.3)$$

where  $\Delta\delta_k(i)$  is the phase deviation and  $\Delta V_k(i)$  is the voltage deviation at bus  $k$  for contingency  $i$ . The set of contingencies  $\{I\}$  must be selected so that it models the statistical description of the disturbance.

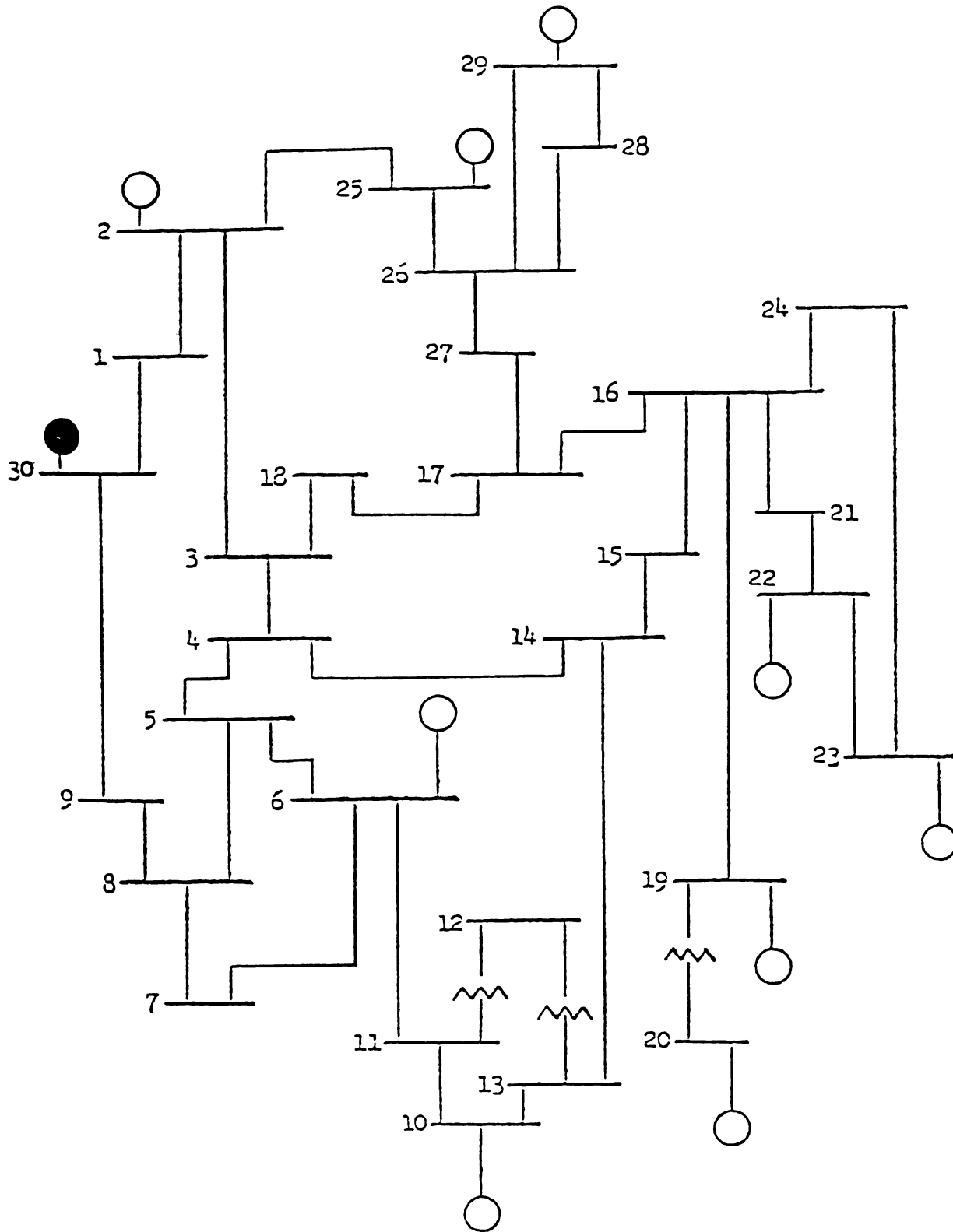


Figure 3.1. The original 30 bus New England system.

It can be shown in a manner similar to that in [2] that if the set of contingencies  $i \in I$  are a set of load disturbances at each of the  $N$  buses in the network, the statistics of the disturbance will be an identity matrix and the coherency measure is strictly based on the relative stiffness of the network model connecting buses  $k$  and  $l$ . The phase, voltage, and current coherency measures are evaluated for a set of  $N$  100 MW loss of active power disturbances at each of the  $N$  buses. The phase, voltage, and current coherency measures are also evaluated for a set of  $N$  100 MVAR loss of reactive power disturbances at all  $N$  network buses as well as a set of  $N$  100 MW and 100 MVAR loss of complex load disturbances at all  $N$  buses. The weak transmission boundaries are determined for each coherency measure for all three sets of active, reactive, and complex power disturbances.

An improved current rms coherency measure is now proposed.

Let

$$\Delta I_k(i) = \frac{\Delta V_k(i) e^{j\Delta\theta_k(i)}}{|Z_{k1}| e^{j\gamma_{k1}}}$$

where  $|Z_{k1}|$  and  $\gamma_{k1}$  are the magnitude and phase of the impedance of the branch connecting buses  $k$  and  $l$ . The natural logarithm is a monotonically increasing function of the argument, and thus will preserve the relative magnitude of  $\Delta I_k(i)$  and  $\Delta I_l(i)$ . Therefore define  $\Delta I_{kl}(i)$

$$\begin{aligned}
\Delta I_{k1}(i)^* &= \ln \Delta I_k(i) - \ln \Delta I_1(i) \\
&= \ln \frac{\Delta V_k(i)}{|Z_{k1}|} + j(\Delta \theta_k(i) - \gamma_{k1}) \\
&\quad - \ln \frac{\Delta V_1(i)}{|Z_{1k}|} + j(\Delta \theta_1(i) - \gamma_{1k}) \\
&= \ln \frac{(\Delta V_k(i))}{\Delta V_1(i)} + j(\Delta \theta_k(i) - \Delta \theta_1(i))
\end{aligned}$$

The improved rms current coherency measure is defined as

$$\begin{aligned}
&\left\{ \sum_{i \in I} |\Delta I_{k1}^*| \right\} \\
&= \sum_{i \in I} \left\{ \left\{ \ln \frac{\Delta V_k(i)}{\Delta V_1(i)} \right\}^2 + (\theta_k(i) - \theta_1(i))^2 \right\}^{\frac{1}{2}} \quad (3.4)
\end{aligned}$$

The rms current coherency measure can be shown to detect stiffly interconnected groups of buses and is zero if the  $\Delta V_k(i) = \Delta V_1(i)$  and  $\Delta \theta_k(i) = \Delta \theta_1(i)$  which indicates buses  $k$  and  $1$  are coherent.

The identification of weak transmission boundaries is based on a grouping method that utilizes the coherency measures evaluated for all bus pairs  $k$  and  $1$ . The grouping method is based on the commutative rule [2]. This rule for forming a group requires that a group be formed if and only if all the generators are coherent with respect to each other; that is, if the Group  $G1$  is a group containing

buses A and B, then bus C is added to this group if and only if generator C is coherent with A, and C is coherent with B. This method has been used [2,3] for clustering generators in coherent groups for producing dynamic equivalents of the system for transient stability studies.

The values of the coherency measures are ranked from the smallest to the largest forming a ranking table; then the groups are formed based on the following algorithm:

(1) Form the first group (a pair) from the smallest coherency measure at rank 1,  $r = 1$ .

(2) Decide which of the following possibilities apply to buses  $k, l$  at the rank  $r = r + 1$ .

(3) If  $r = N \times \frac{(N - 1)}{2}$ , stop.  $N$  = number of buses.

(a) If neither  $k$  nor  $l$  has been previously identified as belonging to a group, then this pair becomes a new group.

(b) If bus  $k(l)$  belongs to a group but bus  $l(k)$  does not, then

(i) If  $l(k)$  has been previously recognized as coherent with all members of the group to which  $k(l)$  belongs except for  $k(l)$ , then add  $l(k)$  to the group containing  $k(l)$ .

(ii) If  $l(k)$  has not been found previously to be coherent with all other members of the group to which  $k(l)$  belongs, then recognize that  $k$  and  $l$  are coherent but do not add  $l(k)$  to the coherent group containing  $k(l)$ . Return to (2).

- (c) If buses  $k$  and  $l$  belong to different groups, then
    - (i) If all possible bus pairs which can be selected from the members of the two groups except  $k$  and  $l$  have been previously recognized as being coherent, then merge the two groups to form a single group containing all members of the separate group.
    - (ii) If at least one pair of buses which can be selected from the two groups other than  $k$  and  $l$  has not yet been recognized as a coherent pair, then recognize the pair  $k$  and  $l$  as coherent but do not merge the groups.
- Return to (2).

The algorithm continues the procedure to the bottom of the ranking table, and when every bus pair is checked, it terminates. As one proceeds down the ranking table, individual buses are included in groups and later groups are merged to form larger groups. As groups are merged, the boundaries between groups should be continuously weaker since a coherency measure between bus pairs indicates stiff connection of the buses, and the coherency measures are ranked from the smallest to the largest in this ranking table. Thus, the boundaries may be ranked from the weakest to strongest based on the reverse order of the group formation; that is, the last two groups to be lumped into a single group have the weakest boundary between them, and the second weakest belongs to the second-to-the-last group aggregated, etc.

The commutative grouping rules assure that all the buses in a group formed have stiff connection by requiring a bus to join the group if and only if it is coherent with all the buses in the group, and groups are merged if and only if all the buses in group one are coherent with every bus in group two. This ensures at least  $n - 1$  stiff connections exist between buses in an  $n$  bus group.

Now to sum up the procedure for identifying vulnerable boundaries, the following steps are given:

- (1) Compute the coherency measure  $C(k,1)$  for all bus pairs.
- (2) Rank the coherency measures from smallest to largest and form a ranking table.
- (3) Form groups by the commutative grouping rules and set a group formation table.
- (4) Rank the boundaries from the weakest to the strongest based on the reverse order in the group formation table.

A Fortran computer program has been developed to implement this procedure. It requires files of the base cases loadflow angles and loadflow simulations of all loss of load contingencies to compute the coherency measure. The output gives the groups of buses in reverse order to formation indicating the increasingly stronger boundaries as existing groups are broken up to form larger numbers of groups.

### 3.2. Weak Phase Transmission Boundaries

The weak phase transmission boundaries are identified based on the rms coherency measure (3.1) evaluated for loss of load disturbances at every bus. As indicated above, the rms coherency measure



has been utilized to (1) determine groups to be aggregated to produce dynamic equivalents; (2) to identify the weak transmission boundaries that cause decoupling leading to phase oscillation problems based on classical transient stability model; and (3) to identify weak boundaries that experience thermal overload and steady state stability problems for line outage and loss of generation contingencies. The rms phase coherency measure has previously been simulated for strictly loss of generation contingencies using an inertial loadflow simulation. The results in this section are based on loss of load contingencies and a conventional loadflow simulation which reduces the generation of the swing bus to compensate for the loss of load. The inertial loadflow would reduce the power at every generator bus in proportion to the ratio of its inertia to the total inertia of all generators in the system.

#### Case 1: Real power loss of load disturbances

The phase coherency measure is computed for the set of 100 MW loss of load disturbances and the grouping method is utilized to identify the stiffly connected groups and associated weak transmission boundaries. Figures 3.2, 3.3, and 3.4 show the weak boundaries for a 3, 4, and 6 group partition of the network. The three-group partition shows the three weakest transmission boundaries. The largest group contains the swing bus (bus 30), most of the load buses in the network, as well as generator buses 2 and 6. All of the remaining buses are grouped based on their electrical distance to the swing bus. The large group III containing the swing bus is split in the

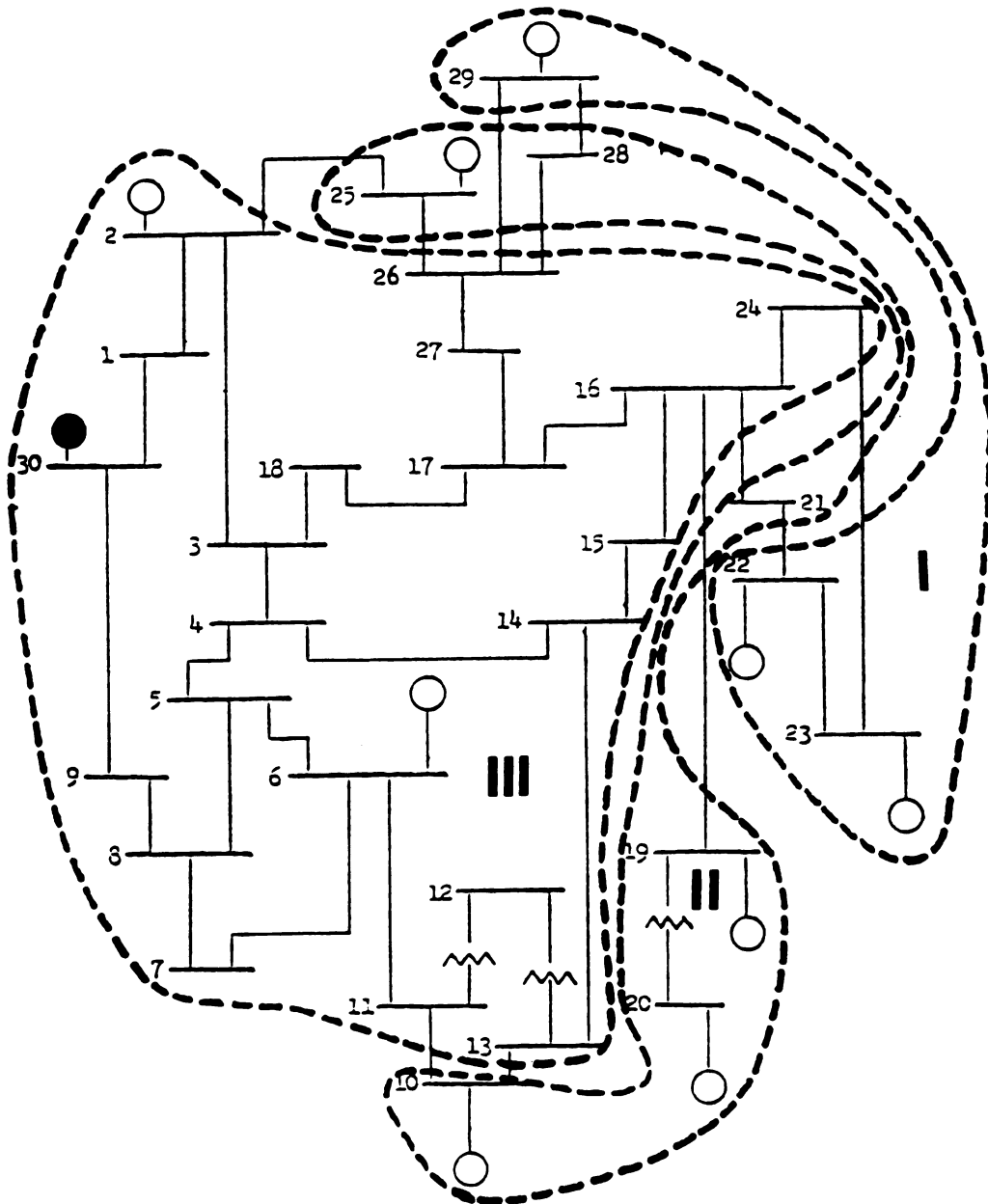


Figure 3.2. The weak boundaries for a 3-group partition based on real power disturbance and phase rms coherency measure.

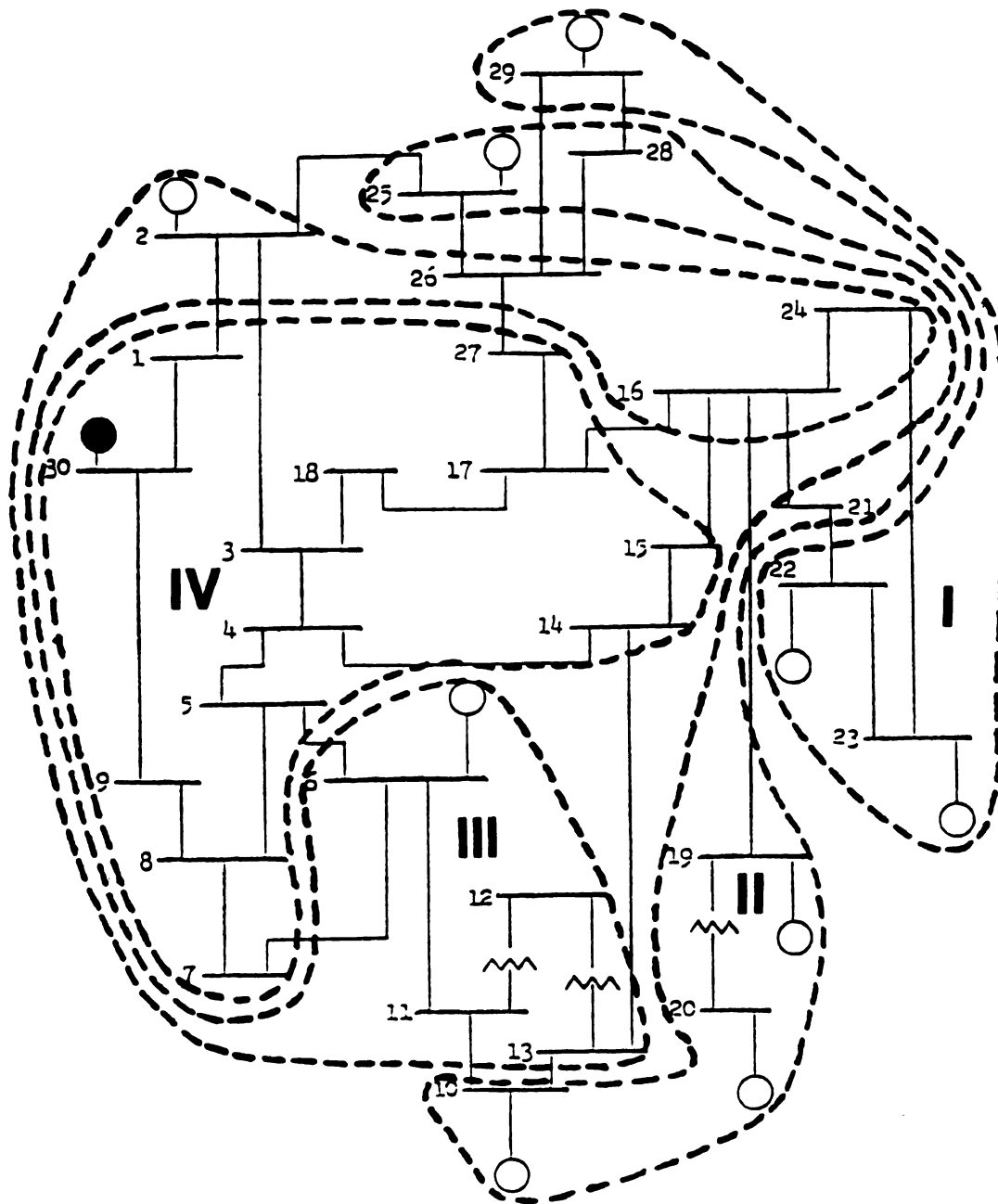


Figure 3.3. The weak boundaries for a 4-group partition based on real power disturbance and phase rms coherency measure.

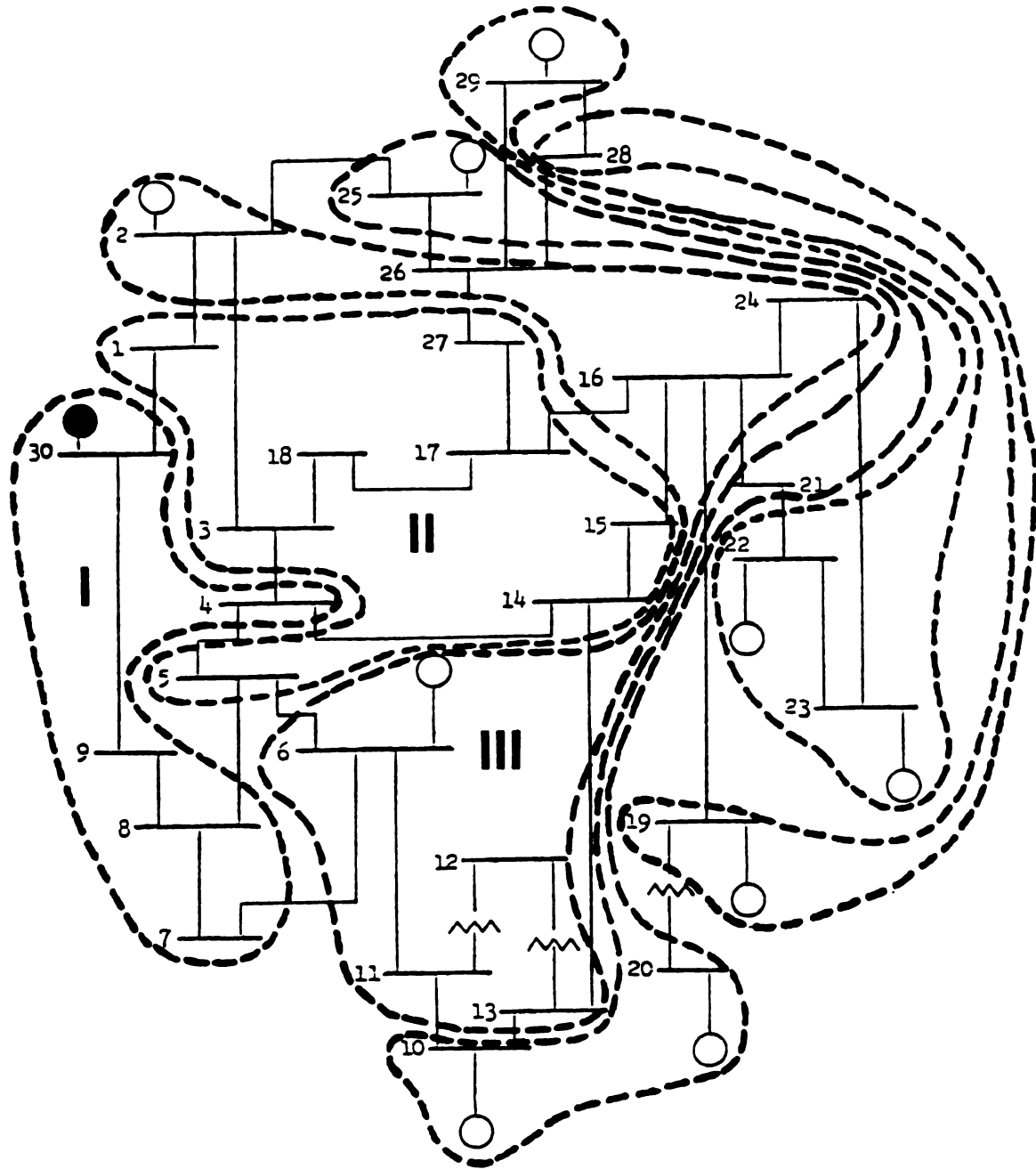


Figure 3.4. The weak boundaries for a 6-group partition based on real power disturbance and phase rms coherency measure.

four-group partition separating generator buses 2 and 6 from a group of buses containing the swing bus. The buses joining generators 2 and 6 in this group are again the buses in group III furthest electrically from the swing bus. Both groups II and IV in four-group partition are further split in the six-group partition again based on electrical distance to the swing bus.

The groupings of buses based on electrical distance to the swing bus appear to be based on the method of simulating the loss of 100 MW load contingencies. The loss of 100 MW in active power is matched by a decrease in 100 MW of generation at the swing bus causing an active power flow to the swing bus from the particular disturbed bus. This method of simulating loss of load contingencies identifies the sequence of continually weaker transmission boundaries between the swing bus and the rest of the system.

An alternate method of simulating the loss of load contingencies is an inertial loadflow where the 100 MW of generation required to match the 100 MW of load is distributed to all generators based on their inertia. This procedure used in [1] would identify the weak transmission boundaries for the inadvertent flows caused by the decrease in frequency after loss of load contingencies. The weak boundaries based on the use of a swing bus to match loss of generation would be based on an operating procedure which utilizes a single generator in the utility to perform regulation or alternatively is an equivalent external system representation.

A set of weak phase boundaries could also be identified by simulating loss of load contingencies using distribution factors to allocate the 100 MW decrease in generation among the generators in a utility.

The comparison of results of determining the stiffly interconnected groups for this same system based on an inertial loadflow simulation of loss of generation contingencies and based on this set of loss of load simulated contingencies indicates the weak transmission boundaries are similar. Thus it appears that the weak transmission boundaries depend more on the network rather than the type of contingency (loss of load or loss of generation) and the type of simulation (inertial distribution or swing bus).

The weakest boundaries are those observed in the three-group partition and the boundaries formed by splitting these three groups into four and six groups are successively stronger. It was observed based on a study of 49 bus system in [1] that the branches in the weaker phase transmission boundaries experience thermal overloads more often and more severely than the branches in stronger phase boundaries. Moreover, it was observed that all thermal overloads for a set of multiple line outage and all loss of generation contingencies occurred on branches in these weak boundaries.

The branches in the weak phase transmission boundaries should be vulnerable to steady state stability problems rather than the thermal overload problems. The weak current transmission boundaries based on the current coherency measure (3.4) should determine the branches that

experience thermal overloads. However, the results obtained for the weak current transmission boundaries in section 3.4 indicate they are nearly identical to the phase transmission boundaries, thus explaining why thermal overloads would occur on the weak phase transmission boundaries.

#### Case 2: Reactive loss of load disturbances

The weak phase transmission boundaries were determined based on a set of 100 MVAR loss of load disturbances at every network bus. The results from this case do not have any value for applications. Moreover, the grouping and weak boundary identification are not creditable. The groups are formed based on the weak coupling of reactive power disturbances to the phase deviation. Since the results have no value for applications and show no viable weakness of the transmission grid, the numerical results will not be shown here.

#### Case 3: Complex loss of load disturbances

The weak phase transmission boundaries were determined based on a set of 100 MW and 100 MVAR loss of load disturbances at every network bus. The results of three-, four-, and five-group partition are shown in Figures 3.5, 3.6, and 3.7, respectively. The coherent groups in each case are very similar to the groups obtained from case 1 with only real power disturbances. The reason for this similarity is due to the fact that phase response is not sensitive to the reactive disturbances. These results also show slight differences on the groups obtained for the real and complex disturbances.

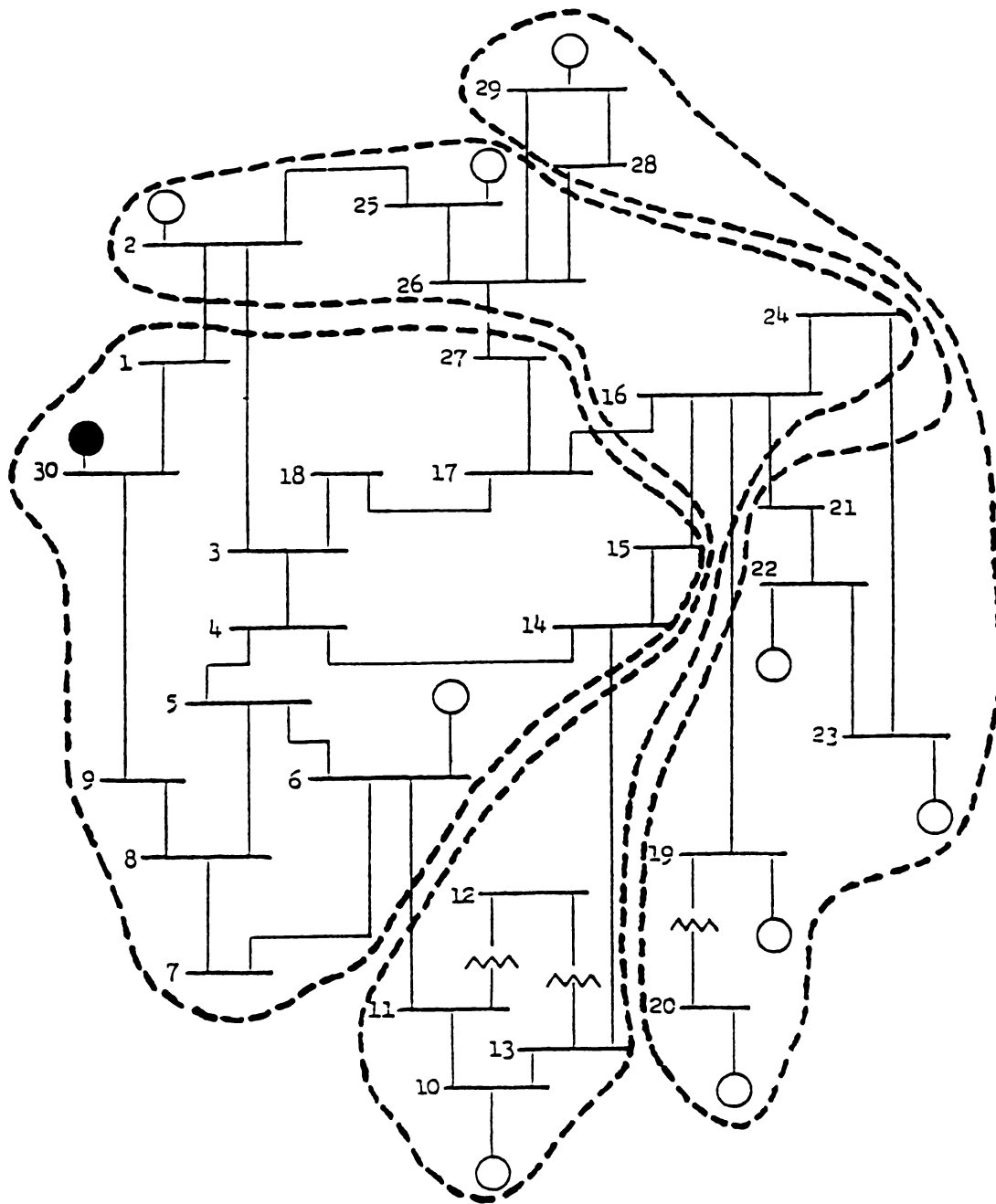


Figure 3.5. The weak boundaries for a 3-group partition based on complex power disturbance and phase rms coherency measure.



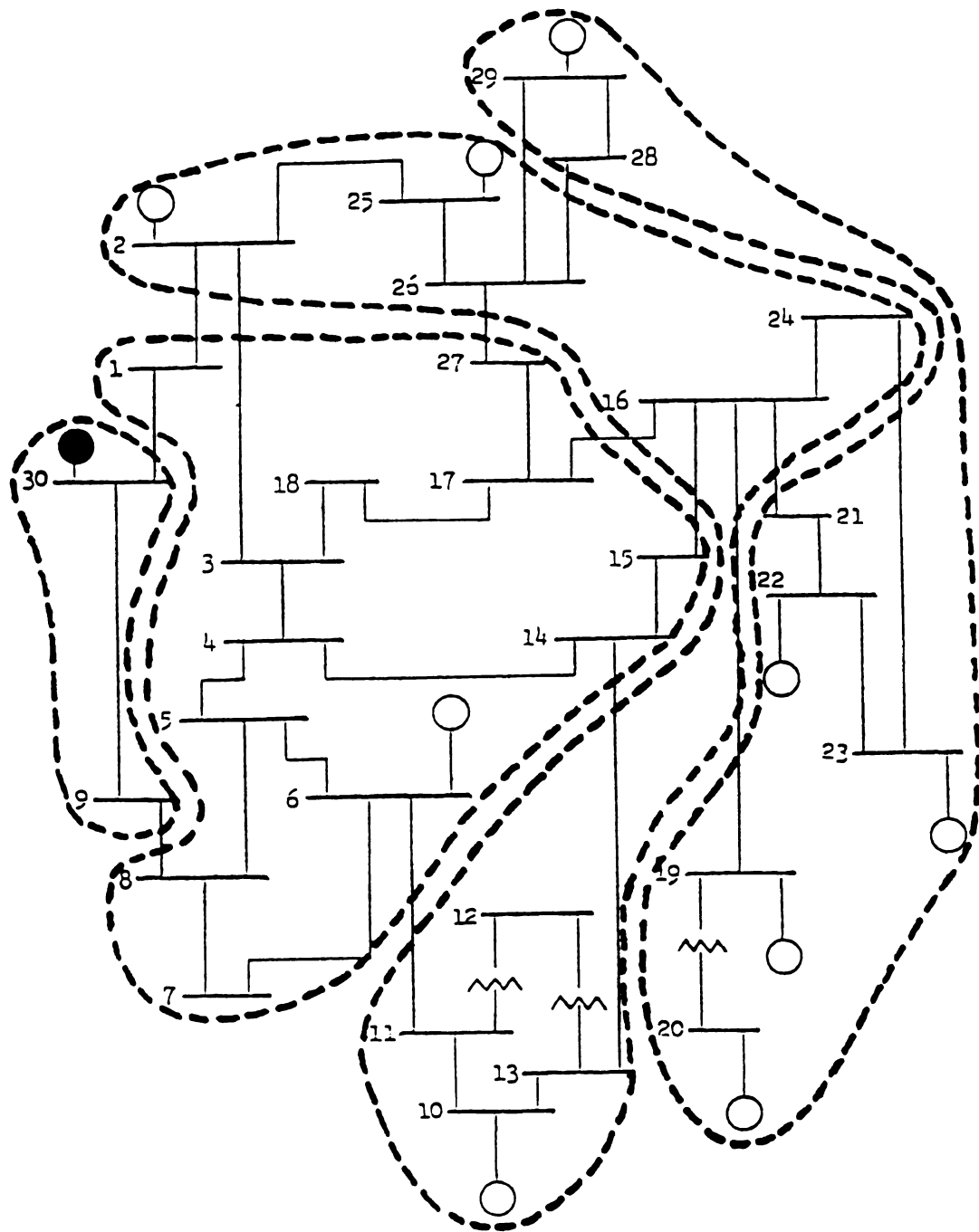


Figure 3.6. The weak boundaries for a 4-group partition based on real power disturbance and phase rms coherency measure.

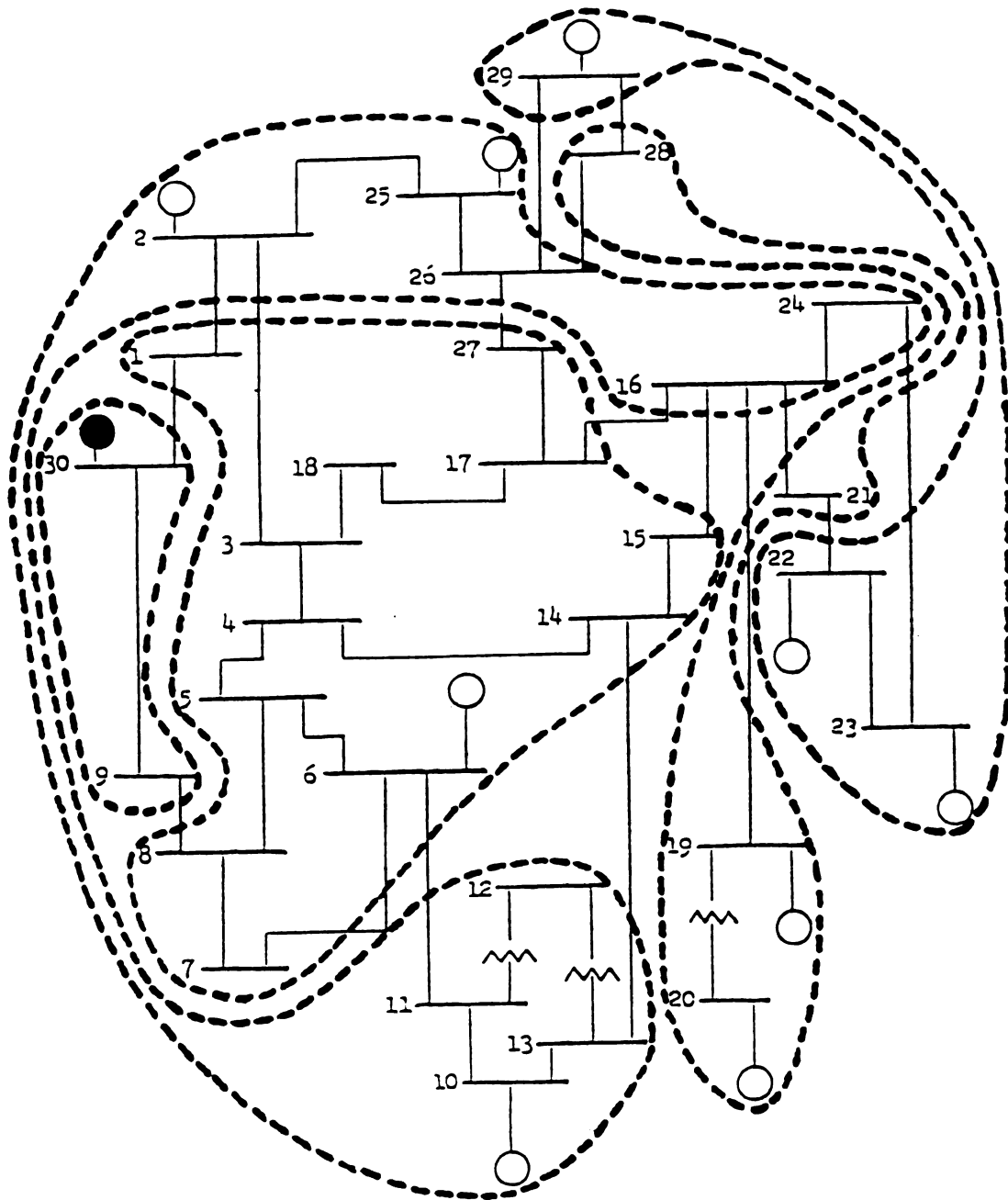


Figure 3.7. The weak boundaries for a 5-group partition based on real power disturbance and phase rms coherency measure.

### 3.3. Weak Voltage Transmission Boundaries

Weak voltage transmission boundaries are known to be much more local than the phase transmission boundaries identified in the previous section. Previous efforts have focused on identification of local voltage control areas for the purpose of providing proper voltage control. Recent papers have documented efforts to identify the voltage control areas based on the magnitude of elements in sensitivity matrices [15]. No effort has been made to determine and rank the weak transmission boundaries for the purpose of voltage security assessment. The identification and ranking voltage of weak transmission boundaries would indicate the branches and boundaries where voltage security problems exist and where line outage, loss of generation, or loss of switchable capacitors, or reactors could lead to voltage collapse, low voltage profiles, or voltage oscillations.

#### Case 1: Real power loss of load disturbance

The weak transmission boundaries based on the voltage coherency measure evaluated for the set of 100 MW real power loss of load contingencies are shown in Figure 3.8, 3.9, and 3.10 for the 3, 4, and 6 group partition of the system. The local nature of the stiffly interconnected groups or voltage control areas is clear in each case. The transmission boundary and the associated branches are the location where large voltage deviations occur for loss of load or generation contingencies as shown in Chapter 5. Moreover, line outages of branches in these boundaries will be shown to severely aggravate the voltage security or stability problems.

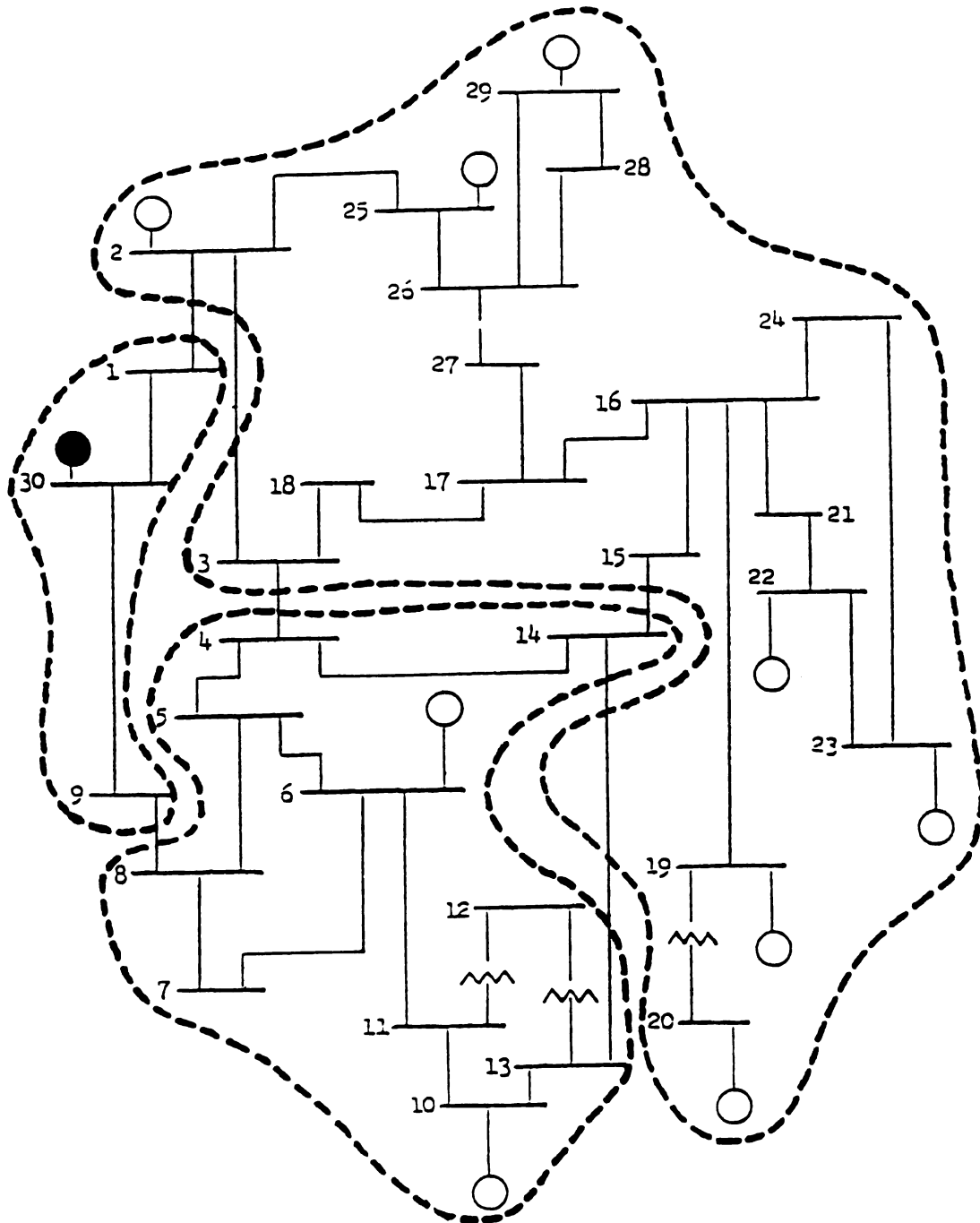


Figure 3.8. The weak boundaries for a 3-group partition based on real power disturbance and voltage rms coherency measure.

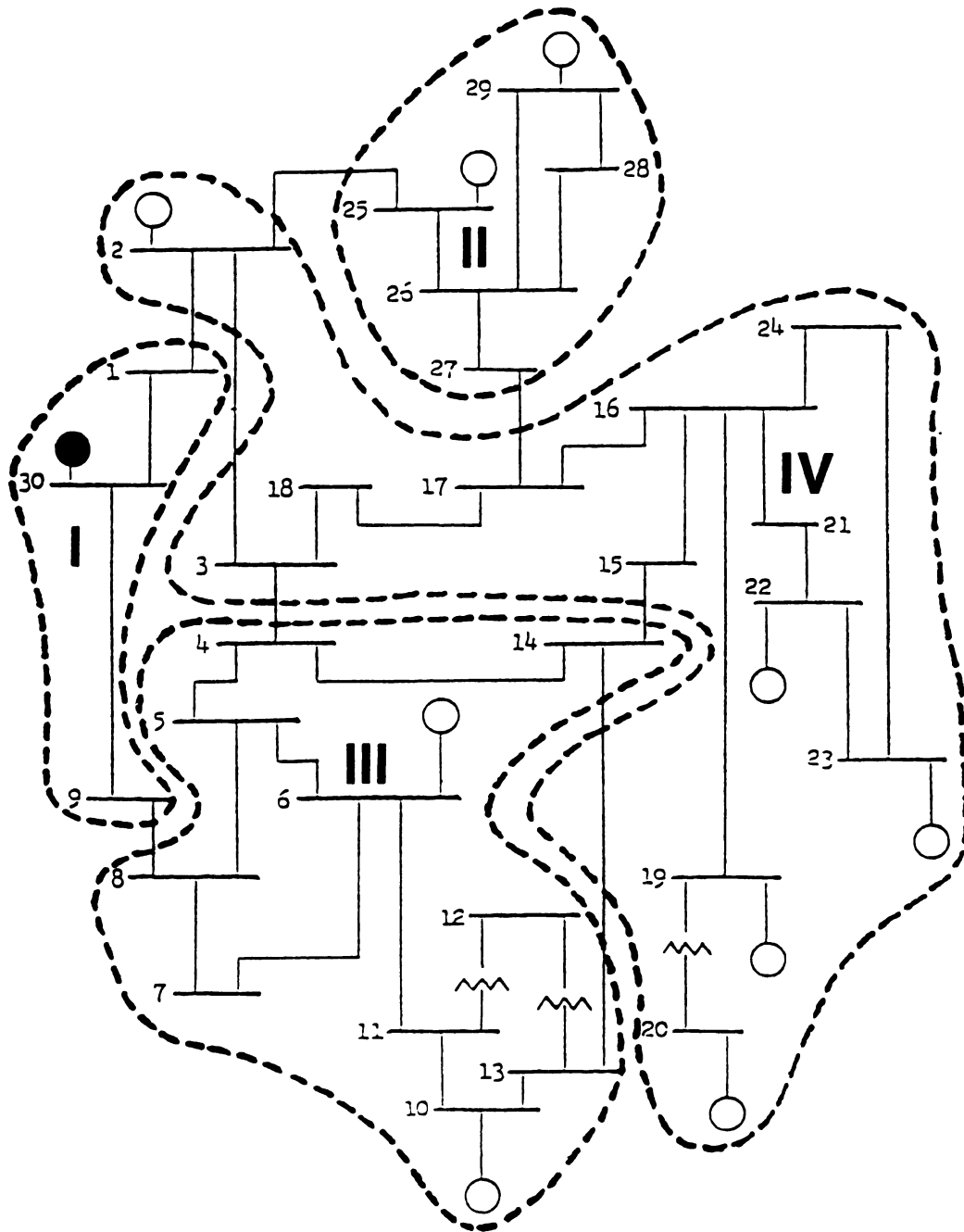


Figure 3.9. The weak boundaries for a 4-group partition based on real power disturbance and voltage rms coherency measure.

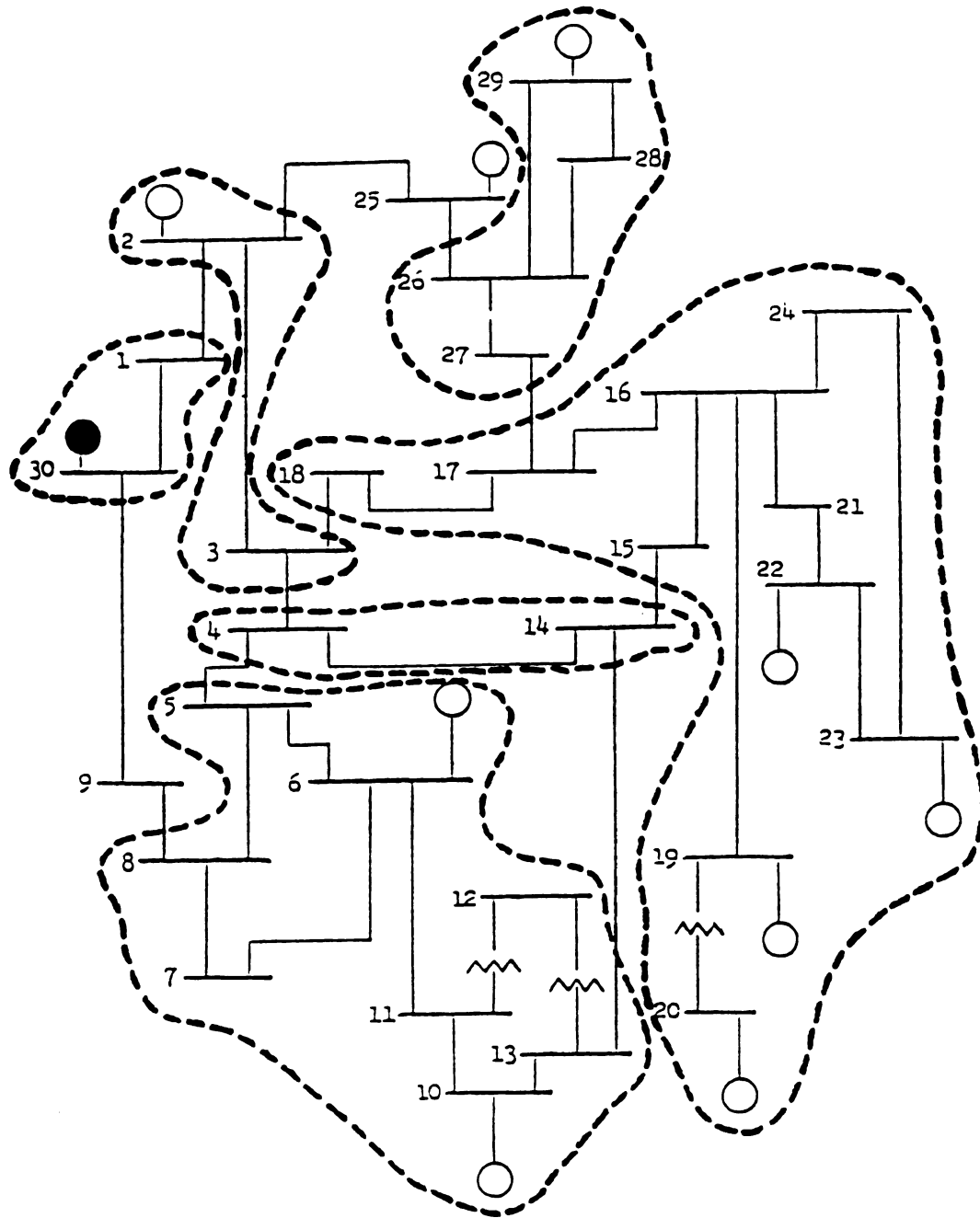


Figure 3.10. The weak boundaries for a 6-group partition based on real power disturbance and voltage rms coherency measure.

The three-group partition shown in Figure 3.8 has both reactive sources (generators) and loads in each local area. The weak boundary, which divides the system, is clearly defined by the lines connecting the following pairs of buses: (1,2), (3,4), (8,9), and (14,15).

This is the weakest boundary of the system. The reactive power supply in each of these groups must be sufficient to meet the local loads. The four-group partition of the system, shown in Figure 3.9, also has local control areas composed of both sources and loads.

The weak boundary in this case is defined by the following lines: (1,2), (3,4), (8,9), (14,15), (2,25), and (17,27). The difference between the three-group and four-group boundaries is that the latter contains additional but less vulnerable elements (2,25) and (17,27). For a very large system this procedure for identifying and ranking the boundaries and branches in terms of voltage security provides the system planner or the operator a very useful on-line tool to predict the worst contingencies that would affect the weakest transmission boundaries. Corrective actions could then be determined to relieve this vulnerability. The weak boundaries could also be displayed graphically on the control panel to the system operator. The operator would thus have a better picture to select the correct zones to perform the contingency analysis.

Another interesting case is shown in Figure 3.10, where the system is divided into six groups. From the base case data it is found that bus 4 is carrying 500.0 MW and 184.0 MVAR load, and bus 14 is an intermediate bus which has no load and no generation. These

two buses are at the center of the system and electrically close to the swing bus making them a sort of buffer zone between different control areas. The results for loss-of-reactive-load contingencies are similar to those for the loss-of-real-load contingencies. But the difference of these results is that they can identify the local voltage control areas more precisely and always maintain sources and load buses in each control area. This six-group partition based on real power disturbance did not have a source in the bus 4 and bus 14 group. The interesting result of the identification of weak transmission boundaries for real power loss of contingencies is that the weak voltage boundaries identified for reactive power disturbances in Case 2 are also vulnerable based on real power disturbances.

#### Case 2: Reactive loss of load disturbances

The weak voltage transmission boundaries are identified based on the voltage rms coherency measure evaluated for the set of loss of 100 MVAR reactive load disturbances at each bus. Since reactive power is much more strongly related to voltage than is real power, the weak voltage transmission boundaries should be identified based on the set of reactive power loss of local disturbances rather than the loss of real power load disturbances. The five and six group partition of the network using the reactive power disturbances, shown in Figures 3.11 and 3.12 respectively, are similar to the four-group partition in Figure 3.9 for real power disturbance. Group IV in Figure 3.9 is split into three groups in both the five and six group partition shown in Figures 3.11 and 3.12 for reactive power



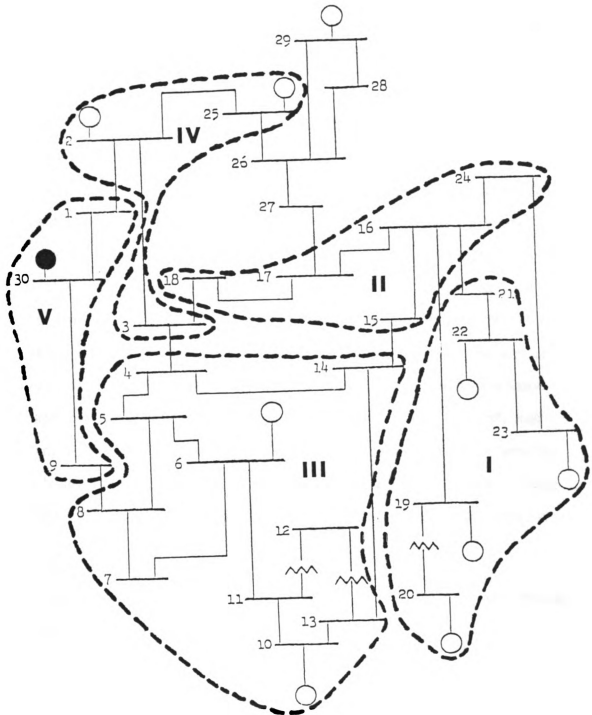


Figure 3.11. The weak boundaries for a 5-group partition based on reactive power disturbance and voltage rms coherency measure.

disturbance. Group II in Figure 3.10 is ungrouped in Figures 3.11 and 3.12, which suggests it is a group separate from the other groups in these 5 and 6 group partitions. Finally, group III in the five-group partition in Figure 3.11 is broken into two groups each with a source in the six-group partition in Figure 3.12. Note that all groups in Figures 3.11 and 3.12 have a source bus and surrounding load buses except for group II. Group II is a buffer zone between groups I and II, and group IV and the ungrouped buses. Figure 3.13 shows the partition of the network based on the voltage coherency measure evaluated for reactive disturbance when the generator bus is regulated. Note that all the generators and closely related load buses form a single group because their voltage controls hold their terminal voltages constant. These groups really reflect the action of voltage controls rather than the voltage control areas and weak voltage transmission boundaries in the network. This is confirmed by the results in Chapter 5 that indicate the weak voltage transmission boundaries of Figure 3.11 are indeed the location where voltage problems occur for loss of generation and line outage contingencies.

#### 3.4. Weak Current Transmission Boundaries

Weak current transmission boundaries should indicate the boundaries and branches where thermal overload problems should occur.

The three-group partition of the transmission grid based on the current coherency measure evaluated for real power and for complex power disturbances are identical and shown in Figure 3.14. This three-group partition based on the current coherency measure is

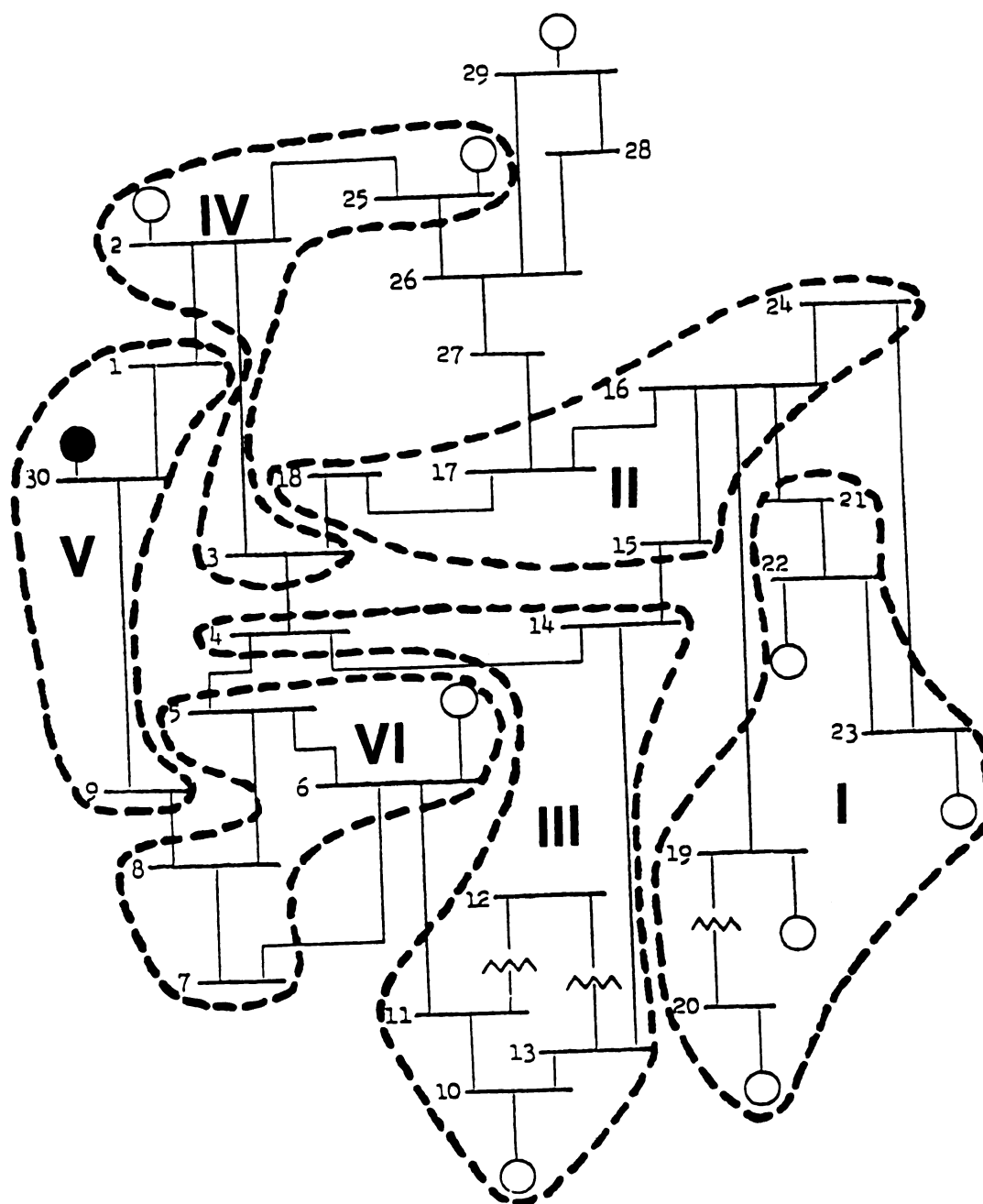


Figure 3.12. The weak boundaries for a 6-group partition based on reactive power disturbance and voltage rms coherency measure .

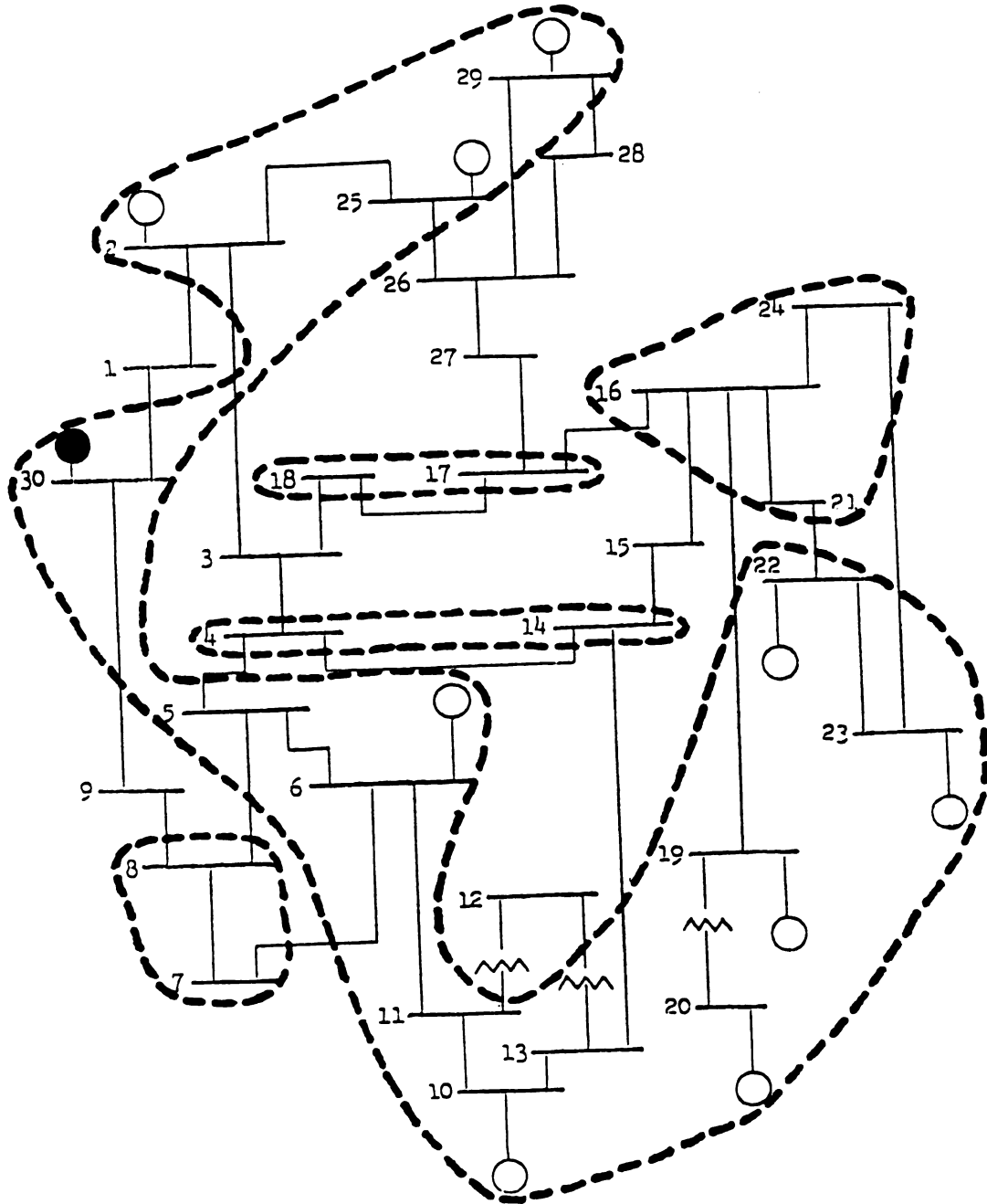


Figure 3.13. The weak boundaries for a 5-group partition based on reactive power disturbance and voltage rms coherency measure when all generator buses are regulated.

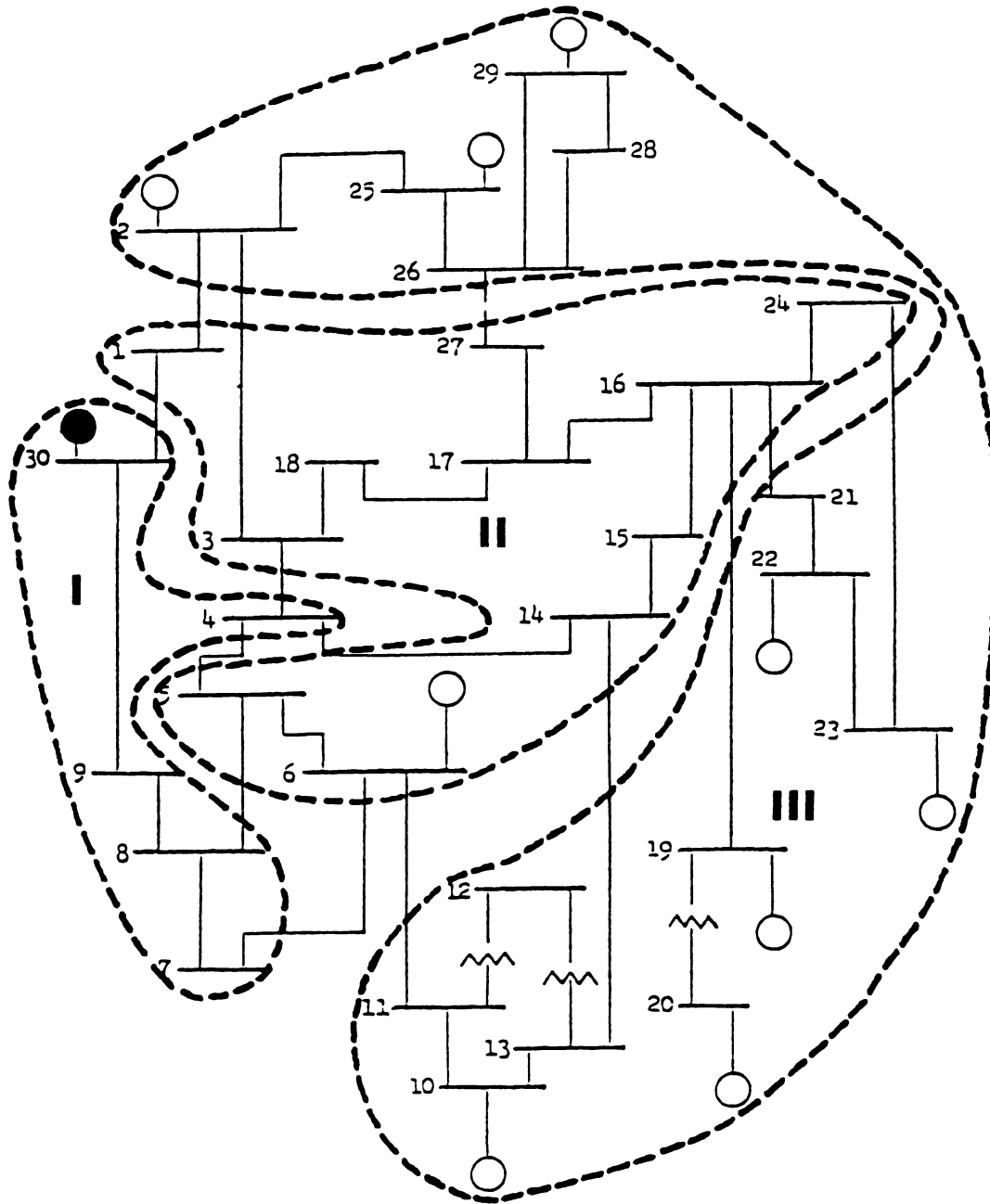


Figure 3.14. The weak boundaries for a 3-group partition based on the current coherency measure for both real and complex power disturbances.

similar to the six-group partition (but not the three-group partition) based on the phase coherency measure shown in Figure 3.4 that group III in Figure 3.14 is broken into four groups. This suggests that the thermal overload security problems may be more severe on boundaries closer to the swing bus and that phase stability problems may be more severe on the weak boundaries of the subgroups that compose group III in Figure 3.14. However, the results suggest that thermal overload problems will likely occur on the weak phase boundaries. This severity of the violations and the number of contingencies causing thermal problems on a boundary are not likely to be proportional to the ranking of the weak phase boundaries.

## CHAPTER 4

### CONDITIONS FOR VOLTAGE CONTROLLABILITY, OBSERVABILITY, AND STABILITY

#### 4.1. Introduction

The objective of this chapter is to lay the groundwork for the study of the structural causes of voltage stability problems. This is accomplished by first developing sensitivity analysis based on the linearized loadflow equations in section 4.2. A set of sensitivity matrices is defined which relates the voltage magnitudes at load buses and reactive power injections at the generator buses to the voltage at generator buses and the reactive and real power at load buses. Two algebraic equations are developed by this sensitivity analysis in section 4.2. The first equation relates the voltage at PQ buses to the voltage at PV (reactive source) buses and the reactive load at PQ buses. Since the voltage at PV buses acts as a control and the load at PQ buses acts as a disturbance to the voltage at PQ buses, the equation is called the controllability equation. The other equation will reflect the reactive demands of the system at the source buses. Since under normal operations the reactive demands from PQ can be observed at or reflected to the source buses by this equation, it is called the observability equation.

The voltage stability of an interconnected power system can be affected by the lack of resources and the weakened boundary between two regions. An example mathematical model of five buses system will be introduced and the corresponding sensitivity matrices will be determined in section 4.3 under light-load conditions.

In section 4.4 a set of theorems for voltage stability will be derived based on the controllability and observability equations. Finally, in section 4.5 we will integrate the two parallel approaches about voltage stability problems, which will post the very useful local and global operational constraints for the interconnected power systems.

#### 4.2. The Model Development

It is intended to establish the relationship among the various controlled and observed variables of the system in this section. This leads to a set of sensitivity matrices which can be derived from the following loadflow equations:

$$f_{P_G}(\delta, \theta, E, V) = 0$$

$$f_{P_L}(\delta, \theta, E, V) = 0$$

$$f_{Q_G}(\delta, \theta, E, V) = 0$$

$$f_{Q_L}(\delta, \theta, E, V) = 0$$

where



$f_{P_G}$  is the vector of the real power flow equations at all generator (PV) buses

$f_{Q_G}$  is the vector of reactive power flow equations at all generator (PV) buses

$f_{P_L}$  is the vector of the real power flow equations at load (PQ) buses where voltage  $V$  is not controlled

$f_{Q_L}$  is the vector of reactive power flow equations at all load (PQ) buses where voltage  $V$  is not controlled

$E$  is the vector of voltage magnitude at the generator (PV) buses

$V$  is the vector of voltage magnitude at the load (PQ) buses

$\delta$  is the vector of phase angle at the generator (PV) buses

$\theta$  is the vector of phase angle at the load (PQ) buses

Then the Jacobian matrix which relates the change of input vector

$$\Delta X = [\Delta\delta, \Delta\theta, \Delta E, \Delta V]^t ; \quad \Delta E_i \triangleq \frac{E_i - E_{i0}}{E_i} , \quad \Delta V_i \triangleq \frac{V_i - V_{i0}}{V_i} .$$

to the change of output function

$$\Delta f(\delta, \theta, E, V) = \begin{bmatrix} \Delta f_{P_G}(\delta, \theta, E, V) \\ \Delta f_{P_L}(\delta, \theta, E, V) \\ \Delta f_{Q_G}(\delta, \theta, E, V) \\ \Delta f_{Q_L}(\delta, \theta, E, V) \end{bmatrix} \quad (4.1)$$

is

$$J = \begin{bmatrix} A_1 & B_1 & C_1 & D_1 \\ A_2 & B_2 & C_2 & D_2 \\ A_3 & B_3 & C_3 & D_3 \\ A_4 & B_4 & C_4 & D_4 \end{bmatrix} \quad (4.2)$$

so that the following expression can be written

$$\begin{bmatrix} \Delta P_G \\ \Delta P_L \\ \Delta Q_G \\ \Delta Q_L \end{bmatrix} = \begin{bmatrix} A_1 & B_1 & C_1 & D_1 \\ A_2 & B_2 & C_2 & D_2 \\ A_3 & B_3 & C_3 & D_3 \\ A_4 & B_4 & C_4 & D_4 \end{bmatrix} \begin{bmatrix} \Delta \delta \\ \Delta \theta \\ \Delta E \\ \Delta V \end{bmatrix} \quad (4.3)$$

If the phase angle changes at generator buses are assumed to be neglectable in the calculation of voltage magnitudes, then  $\Delta \delta$  can be set to zero to solve for  $\Delta \theta$  in (4.3) using

$$\Delta P_L = B_2 \Delta \theta + C_2 \Delta E + D_2 \Delta V \quad (4.4)$$

to obtain

$$\Delta \theta = B_2^{-1} (\Delta P_L - C_2 \Delta E - D_2 \Delta V) \quad (4.5)$$

Substituting for  $\Delta \theta$  in (4.3) when  $\Delta \delta = 0$ , the following expressions for  $\Delta Q_G$  and  $\Delta Q_L$  are obtained

$$\begin{aligned} \Delta Q_G &= B_3 \Delta \theta + C_3 \Delta E + D_3 \Delta V \\ &= (D_3 - B_3 B_2^{-1} D_2) \Delta V + (C_3 - B_3 B_2^{-1} C_2) \Delta E + B_3 B_2^{-1} \Delta P_L \end{aligned} \quad (4.6)$$

$$\begin{aligned} \Delta Q_L &= B_4 \Delta \theta + C_4 \Delta E + D_4 \Delta V \\ &= (D_4 - B_4 B_2^{-1} D_2) \Delta V + (C_4 - B_4 B_2^{-1} C_2) \Delta E + B_4 B_2^{-1} \Delta P_L \end{aligned} \quad (4.7)$$

Solving for  $\Delta V$  in (4.7) the following expression is obtained

$$\begin{aligned}\Delta V = & - [D_4 - B_4 B_2^{-1} D_2]^{-1} [C_4 - B_4 B_2^{-1} C_2] \Delta E \\ & + [D_4 - B_4 B_2^{-1} D_2]^{-1} [\Delta Q_L - B_4 B_2^{-1} \Delta P_L]\end{aligned}$$

Now define the following sensitivity matrices:

$$S_{VE} = - [D_4 - B_4 B_2^{-1} D_2]^{-1} [C_4 - B_4 B_2^{-1} C_2] \quad (4.8)$$

$$S_{Q_L V} = [D_4 - B_4 B_2^{-1} D_2] \quad (4.9)$$

Then the above expression for  $\Delta V$  becomes

$$\Delta V = [S_{VE}] \Delta E + [S_{Q_L V}]^{-1} [\Delta Q_L - B_4 B_2^{-1} \Delta P_L] \quad (4.10)$$

where  $S_{VE}$  relates the voltage vector  $V$  at the PQ (reactive load) buses to the voltage vector  $E$  at PV (reactive generation) generator buses and  $S_{Q_L V}$  relates the vector of reactive power disturbances at the load buses  $Q_L$  to the change in voltage  $V$ .

Note that the voltages at load buses are controlled by the voltages at generator buses. In order to have the proper controllability in the system, the matrix  $S_{VE}$  must have all positive elements. This implies that changes in any elements of  $E$  will cause changes in like sign in all elements of  $V$ . Similarly, the sensitivity matrix  $S_{Q_L V}^{-1}$  must have non-negative elements and be nonsingular so

that changes in any element of reactive injections  $Q_L$  will cause changes of like sign in all elements of  $V$ .

Now substituting  $\Delta V$  in the expression in (4.6), the following expression is obtained

$$\begin{aligned} \Delta Q_G = & [(C_3 - B_3 B_2^{-1} C_2) - (D_3 - B_3 B_2^{-1} D_2)(D_4 - B_4 B_2^{-1} D_2)^{-1} \\ & (C_4 - B_4 B_2^{-1} C_2)] \Delta E \\ & + (D_3 - B_3 B_2^{-1} D_2)(D_4 - B_4 B_2^{-1} D_2)^{-1} (\Delta Q_L - B_4 B_2^{-1} \Delta P_L) \\ & + B_3 B_2^{-1} \Delta P_L \end{aligned}$$

Now define another set of sensitivity matrices

$$\begin{aligned} S_{Q_G E} = & (C_3 - B_3 B_2^{-1} C_2) - (D_3 - B_3 B_2^{-1} D_2)(D_4 - B_4 B_2^{-1} D_2)^{-1} \\ & (C_4 - B_4 B_2^{-1} C_2) \end{aligned} \quad (4.11)$$

$$S_{Q_G Q_L} = - (D_3 - B_3 B_2^{-1} D_2)(D_4 - B_4 B_2^{-1} D_2)^{-1} \quad (4.12)$$

Then the expression for  $\Delta Q_G$  becomes

$$\Delta Q_G = [S_{Q_G E}] \Delta E - [S_{Q_G Q_L}] (\Delta Q_L - B_4 B_2^{-1} \Delta P_L) + B_3 B_2^{-1} \Delta P_L \quad (4.13)$$

If the system is assumed to be operating normally, then a positive reactive power injection  $\Delta Q_L$  at any load buses will induce a negative power injection  $\Delta Q_G$  at all generator buses. As a result, the matrix  $S_{Q_G Q_L}$  must have all positive elements under normal conditions. The reactive injections at generators should increase with increase in the magnitudes of the generator voltages  $E$ , so that the matrix  $S_{Q_G E}$  normally must have nonsingular with non-negative elements.

Based on the controllability and observability equations a set of theorems regarding necessary conditions for voltage stability will be derived. Changes in voltage  $\Delta E$  at PV (source) buses and changes in reactive injection  $Q_L$  at PQ (load) buses are considered the control and disturbance input.

The state of the network is considered to be the voltage  $V$  at PQ (load) buses. The network governed by (4.10) is said to be stable if a vector of solely positive (negative) incremental changes  $\Delta E$  on one or more elements of  $E$  will cause only positive (negative) increments on elements of  $V$ , and if a vector of solely positive (negative) increments  $\Delta Q_L$  on one or more elements of  $Q_L$  will cause only positive (negative) increments in  $V$ . If there exists a vector of solely positive (negative) incremental changes on elements of  $E$  which produces no change on any of the elements of  $V$ , the network is said to be structurally uncontrollable. Likewise, if some vector of solely positive (negative) incremental change on elements of  $Q_L$  produces no change on any of the elements of  $V$ , the network is said to be uncontrollable. The network is said to be structurally

unstable if there exists a vector of solely positive incremental changes  $\Delta E$  that will produce a vector  $\Delta V$  that has one or more negative incremental changes.

Similarly, a network is said to be unstable if there exists some vector of positive (negative) incremental changes  $\Delta Q_L$  that will produce a vector  $\Delta V$  with one or more negative elements. Thus from equation (4.10), the network is stable and controllable if (a)  $S_{VE}$  has no negative elements and no zero rows, and (b) the square matrix  $S_{Q_L V}$  is positive definite with no negative elements. The network is uncontrollable if either  $S_{VE}$  has no negative elements but has one or more rows, or if  $S_{Q_L V}$  is positive semi-definite. A system is unstable if  $S_{VE}$  has one or more negative elements, or if  $S_{Q_L V}$  is indefinite (or negative definite) or has negative elements. A power system network that is structurally uncontrollable will have multiple solutions, and a structurally unstable network will have no solution and experience voltage collapse or voltage rise.

The reactive injection  $\Delta Q_G$  at PV buses governed by (4.13) is considered an output of the network because it is the reactive power reflected to or requested of PV buses. If one or more PV buses cannot serve the requested reactive injection due to constraints

$$Q_{G_i, \min} \leq Q_{G_i} \leq Q_{G_i, \max}$$

then the reactive injection at that bus is set to  $Q_{G_i, \min}$  or  $Q_{G_i, \max}$  and the bus converts from a PV bus to PQ bus. In this case the system loses some degree of voltage controllability due to the lack

of reactive source at that bus. If all PV buses in a local area are converted to PQ buses, then a voltage collapse will occur as discussed in Chapter 2.

$Q_G$  is considered an output and (4.13) is an output equation for the network. Either one of the following two conditions will cause the output stability of the network:

1) If some vector of solely positive (negative) incremental changes  $\Delta Q_G$  in  $Q_G$  do not cause a vector of solely positive (negative) changes  $\Delta E_G$  in  $E_G$ , or

2) If some vector of solely negative (positive) incremental changes  $\Delta Q_L$  in  $Q_L$  do not cause a vector of solely positive (negative) change in  $Q_G(\Delta Q_G)$ ,

then the network loses observability. It is said to be structurally output unstable.

If the square sensitivity matrix  $[S_{Q_G E}]^{-1}$  is positive definite with no negative elements, and sensitivity matrix  $S_{Q_G Q_L}$  has no negative elements or zero columns, then the network is said to be observable and output stable. If the matrix  $S_{Q_G E}$  is semi-definite or  $S_{Q_G Q_L}$  has no negative elements but one or more zero columns, then the network is said to be unobservable. A network is output unstable if either  $S_{Q_G E}$  is indefinite or has negative elements, or if  $S_{Q_G Q_L}$  has one or more negative elements.

Now let us summarize the above concepts in more rigorous mathematical format. The following definitions and facts are needed for our theorems [13].

Definition: A real matrix  $A$  is called positive if all of its elements have positive value,  $A > 0$ .  $A$  is non-negative if all of its elements are non-negative,  $A \geq 0$ .

Definition: A real  $n \times n$  matrix  $A = (a_{ij})$  with  $a_{ij} \leq 0$  for all  $i \neq j$  is an M-matrix, if  $A$  is nonsingular, and  $A^{-1} \geq 0$ .

Fact 1: If  $A = (a_{ij})$  is a real symmetric and nonsingular  $n \times n$  irreducible matrix, where  $a_{ij} \leq 0$  for all  $i \neq j$ , then  $A^{-1} \geq 0$  if and only if  $A$  is positive definite.

Fact 2: The Jacobian matrix of the linearized loadflow equation for any non-islanded power system network is irreducible.

From the discussion of the controllability and observability equations the following theorems are established.

Theorem 1: A necessary condition for the network to be controllable and stable is that  $S_{Q_L V}$  be an M-matrix.

Theorem 2: A necessary condition for the network to be observable and output stable is that  $S_{Q_G E}$  be an M-matrix.

Theorem 3: A necessary condition for the network to be controllable and stable is that  $S_{V E}$  be a positive matrix.

Theorem 4: A necessary condition for the network to be observable is that  $S_{Q_G Q_L}$  be a positive matrix.

The necessary conditions that will cause  $S_{Q_L V}$  and  $S_{Q_G E}$  to be M matrices and  $S_{V E}$  and  $S_{Q_G Q_L}$  to be positive will be investigated for light load conditions in Section 4.4. The conditions that assure the above properties in these sensitivity matrices will indicate the



causes for loss of observability and controllability induced stability problems.

Facts 1 and 2 indicate that a necessary and sufficient condition for the matrices  $S_{Q_L V}$  and  $S_{Q_G E}$  to be M matrices is that these matrices be positive definite if the network is not islanded or has nonsymmetric transmission elements. Therefore one can investigate the satisfaction or the degree of satisfaction of the M matrix condition by computing the eigenvalues of these matrices and noting the magnitude of the small positive eigenvalues if a loss of controllability or observability is possible and the negative eigenvalues if a loss of controllability or observability induced voltage stability has occurred.

It is emphasized here that the sensitivity matrix  $S_{VE}$  is the matrix which reflects the voltage controllability of the system and  $S_{Q_G Q_L}$  represents the reactive power observability of the system. They will be discussed in detail later.

In the analysis that follows, different forms of loadflow equations and Jacobians are required for the analysis. The polar form is given first and then the hybrid form. Relationships between the elements in the bus admittance matrix are also given which will be useful in this analysis.

$$\bar{Y}_{ij} = Y_{ij}(\cos \gamma_{ij} + j \sin \gamma_{ij}) = -G_{ij} + jB_{ij}$$

$$S_{ij} = V_i V_j Y_{ij} \quad (4.14)$$

$$\theta_{ij} = \theta_i - \theta_j$$

Then the power injections can be written in the polar form as

$$P_i = \sum_{j=1}^n V_i V_j Y_{ij} \cos (\theta_{ij} - \gamma_{ij})$$

$$Q_i = \sum_{j=1}^n V_i V_j Y_{ij} \sin (\theta_{ij} - \gamma_{ij})$$

$$\partial P_i / \partial \theta_i = - (Q_i - V_i^2 B_{ii}) \quad (4.15)$$

$$\partial P_i / \partial \theta_j = S_{ij} \sin (\theta_{ij} - \gamma_{ij}) \quad (4.16)$$

$$\partial Q_i / \partial \theta_i = P_i - V_i^2 G_{ii} \quad (4.17)$$

$$\partial Q_i / \partial \theta_j = -S_{ij} \cos (\theta_{ij} - \gamma_{ij}) \quad (4.18)$$

$$V_i \partial P_i / \partial V_i = P_i + V_i^2 G_{ii} \quad (4.19)$$

$$V_j \partial P_i / \partial V_j = S_{ij} \cos (\theta_{ij} - \gamma_{ij}) \quad (4.20)$$

$$V_i \partial Q_i / \partial V_i = Q_i - V_i^2 B_{ii} \quad (4.21)$$

$$V_j \partial Q_i / \partial V_j = S_{ij} \sin (\theta_{ij} - \gamma_{ij}) \quad (4.22)$$

where

$\bar{Y}_{ij}$  is the  $(i,j)^{th}$  element of bus admittance matrix

$\bar{Y}_{i0}$  is the shunt capacitance at bus  $i$

$\bar{Y}_{Lij}$  is the admittance of line that connects bus  $i$  and bus  $j$

$\bar{Y}_{Lij} = G_{ij} - jB_{ij}$  with  $G_{ij} \geq 0$  and  $B_{ij} \geq 0$

The elements of the bus admittance matrix satisfy

$$\bar{Y}_{ij} = -Y_{Lij} = -G_{ij} + jB_{ij} \quad i \neq j$$

$$\bar{Y}_{ii} = \sum_{j=1, j \neq i}^n \bar{Y}_{Lij} + \bar{Y}_{i0} = - \sum_{j=1, j \neq i}^n \bar{Y}_{ij} + \bar{Y}_{i0}$$

where

$$\text{Re}\{\bar{Y}_{ij}\} = Y_{ij} \cos (\gamma_{ij}) = -G_{ij}$$

$$\text{Im}\{\bar{Y}_{ij}\} = Y_{ij} \sin (\gamma_{ij}) = B_{ij}$$

$$\text{Re}\{\bar{Y}_{i0}\} = G_{i0} \geq 0$$

$$\text{Im}\{\bar{Y}_{i0}\} = B_{i0} \geq 0 \text{ for capacitor}$$

$$\begin{aligned}
\bar{Y}_{ii} &= \sum_{j=1, j \neq i}^n (G_{ij} - jB_{ij}) + (G_{i0} + jB_{i0}) \\
&= \left\{ \sum_{j=1, j \neq i}^n G_{ij} \right\} + G_{i0} + j \left\{ \sum_{j=1, j \neq i}^n -B_{ij} \right\} + B_{i0} \quad (4.23)
\end{aligned}$$

$$\text{Re}\{\bar{Y}_{ii}\} = G_{ii} = \sum_{j=1, j \neq i}^n (G_{ij}) + G_{i0}$$

$$\text{Im}\{\bar{Y}_{ii}\} = B_{ii} = \sum_{j=1, j \neq i}^n (-B_{ij}) + B_{i0}$$

Note that based on the above properties of the admittance matrix that the following property holds

$$\begin{aligned}
\sum_{j=1}^n \bar{Y}_{ij} &= \sum_{j=1, j \neq i}^n \bar{Y}_{ij} + \bar{Y}_{ii} \\
&= \sum_{j=1, j \neq i}^n \bar{Y}_{ij} + \left\{ - \sum_{j=1, j \neq i}^n \bar{Y}_{ij} + \bar{Y}_{i0} \right\} \\
&= \bar{Y}_{i0} = G_{i0} + jB_{i0} \quad (4.24)
\end{aligned}$$

$$\text{Re} \left\{ \sum_{j=1}^n \bar{Y}_{ij} \right\} = G_{i0} \quad (4.25)$$

$$\text{Im} \left\{ \sum_{j=1}^n \bar{Y}_{ij} \right\} = B_{i0} \quad (4.26)$$

The loadflow equations can now be written in hybrid form as

$$P_i = \sum_{j=1}^n V_i V_j [-G_{ij} \cos (\theta_i - \theta_j) + B_{ij} \sin (\theta_i - \theta_j)] \quad (4.27)$$

$$Q_i = \sum_{j=1}^n V_i V_j [-G_{ij} \sin (\theta_i - \theta_j) + B_{ij} \cos (\theta_i - \theta_j)] \quad (4.28)$$

so that

$$\partial P_i / \partial \theta_i = -Q_i - V_i^2 B_{ii} \quad (4.15)$$

$$\partial P_i / \partial \theta_j = V_i V_j [-G_{ij} \sin \theta_{ij} - B_{ij} \cos \theta_{ij}] \quad (4.29)$$

$$\partial Q_i / \partial \theta_i = P_i - V_i^2 G_{ii} \quad (4.17)$$

$$\partial Q_i / \partial \theta_j = V_i V_j [-G_{ij} \cos \theta_{ij} - B_{ij} \sin \theta_{ij}] \quad (4.30)$$

$$V_i \partial P_i / \partial V_i = P_i + V_i^2 G_{ii} \quad (4.19)$$

$$V_j \partial P_i / \partial V_j = V_i V_j [-G_{ij} \cos \theta_{ij} + B_{ij} \sin \theta_{ij}] \quad (4.31)$$

$$V_i \partial Q_i / \partial V_i = Q_i - V_i^2 B_{ii} \quad (4.21)$$

$$V_j \partial Q_i / \partial V_j = V_i V_j [-G_{ij} \sin \theta_{ij} - B_{ij} \cos \theta_{ij}] \quad (4.32)$$

Both the polar form and the hybrid form will be used frequently in the analysis of Sections 4.3-4.5.

#### 4.3. The Controllability and Observability Equations and the Sensitivity Matrices Under Light Load Conditions

In this section, the sensitivity model of (4.3) will be developed for the case of the light load conditions. Light load conditions are assumed to satisfy the following conditions:

- 1) The network has no real or reactive power dissipation.
- 2) The R/X ratios are constant over all the transmission lines of the system ( $G_{ij}/B_{ij} = \alpha$ ,  $i \neq j$ ).
- 3)  $V_i = V_j = 1$  p.u.

$$\theta_i = \theta_j \rightarrow \theta_{ij} = 0$$

These assumptions are made to perform the analysis of the conditions that will assure  $S_{VE}$  and  $S_{Q_G Q_L}$  to be positive, and the  $S_{Q_L V}$  and  $S_{Q_G E}$  to be M matrices for light load conditions in Sections 4.4 and 4.5. Under the above assumptions the loadflow equations become

$$P_i = \sum_{j=1}^n V_i V_j Y_{ij} \cos (\theta_{ij} - \gamma_{ij}) = \sum_{j=1}^n Y_{ij} \cos (\gamma_{ij})$$

$$Q_i = \sum_{j=1}^n V_i V_j Y_{ij} \sin (\theta_{ij} - \gamma_{ij}) = - \sum_{j=1}^n Y_{ij} \sin (\gamma_{ij})$$

Recall that

$$\operatorname{Re}\{Y_{ii}\} = G_{ii} = \sum_{j=1, j \neq i}^n G_{ij} + G_{i0}$$

$$\operatorname{Im}\{Y_{ii}\} = B_{ii} = \sum_{j=1, j \neq i}^n (-B_{ij}) + B_{i0}$$

Then (4.15)-(4.22) can be rewritten as follows:

$$\partial P_i / \partial \theta_i = -Q_i - V_i^2 B_{ii} \quad (4.15)$$

$$= \sum_{j=1}^n Y_{ij} \sin(\gamma_{ij}) - B_{ii}$$

$$= B_{i0} - B_{ii}$$

$$= B_{i0} - \left\{ \sum_{j=1, j \neq i}^n (-B_{ij}) + B_{i0} \right\}$$

$$= \sum_{j=1, j \neq i}^n B_{ij}$$

$$\partial P_i / \partial \theta_j = S_{ij} \sin(\theta_{ij} - \gamma_{ij}) \quad (4.16)$$

$$= -Y_{ij} \sin(\gamma_{ij}) \quad i \neq j$$

$$= -B_{ij}$$





$$\partial Q_i / \partial \theta_i = P_i - V_i^2 G_{ii} \quad (4.17)$$

$$\begin{aligned} &= \sum_{j=1}^n Y_{ij} \cos (\gamma_{ij}) - G_{ii} \\ &= G_{i0} - \left\{ \sum_{j=1, j \neq i}^n (-G_{ij} + G_{i0}) \right\} \\ &= - \sum_{j=1, j \neq i}^n G_{ij} \end{aligned}$$

$$\partial Q_i / \partial \theta_j = -S_{ij} \cos (\theta_{ij} - \gamma_{ij}) \quad (4.18)$$

$$\begin{aligned} &= -Y_{ij} \cos (\gamma_{ij}) \\ &= G_{ij} \end{aligned}$$

$$V_i \partial P_i / \partial V_i = P_i + V_i^2 G_{ii} \quad (4.19)$$

$$\begin{aligned} &= \sum_{j=1}^n Y_{ij} \cos (\gamma_{ij}) + G_{ii} \\ &= G_{i0} + \sum_{j=1, j \neq i}^n G_{ij} + G_{i0} \\ &= \sum_{j=1, j \neq i}^n G_{ij} + 2G_{i0} \end{aligned}$$

$$V_j \partial P_i / \partial V_j = S_{ij} \cos (\theta_{ij} - \gamma_{ij}) \quad (4.20)$$

$$= Y_{ij} \cos (\gamma_{ij}) \quad i \neq j$$

$$= -G_{ij}$$

$$V_i \partial Q_i / \partial V_i = Q_i - V_i^2 B_{ii} \quad (4.21)$$

$$= - \sum_{j=1}^n Y_{ij} \sin (\gamma_{ij}) - B_{ii}$$

$$= -B_{i0} - B_{ii}$$

$$= -B_{i0} - \left\{ \sum_{j=1, j \neq i}^n (-B_{ij}) + B_{i0} \right\}$$

$$= \sum_{j=1, j \neq i}^n B_{ij} - 2B_{i0}$$

$$V_j \partial Q_i / \partial V_j = S_{ij} \sin (\theta_{ij} - \gamma_{ij}) \quad (4.22)$$

$$= -Y_{ij} \sin (\gamma_{ij}) \quad i \neq j$$

$$= -B_{ij}$$

Now a general five-bus model is presented in order to make the analysis of Sections 4.4 and 4.5 more manageable. The results obtained in the analysis can be generalized to any network.

Let the five bus system be indexed from 1 to 5, where buses 1 and 2 are generator (PV) buses and buses 3 and 4 are load (PQ) buses. Then the corresponding Jacobian matrix (4.2) in polar form is shown in Figure 4.1.

Note that in the sensitivity matrices, all diagonal terms are solely defined by the real/reactive power injections at each bus minus the multiplication of the voltage magnitude square and the real/imaginary part of the diagonal term of the admittance matrix. This interesting feature brings the concerns of the voltage problem to the operational constraints at each individual bus, which will be analyzed in the next section.

The submatrices of the Jacobian are now determined for this five bus system for light load conditions as

$$\begin{aligned}
 A_1 &= \begin{bmatrix} -Q_1 - V_1^2 B_{11} & S_{12} \sin(\theta_{12} - \gamma_{12}) \\ S_{21} \sin(\theta_{21} - \gamma_{21}) & -Q_2 - V_2^2 B_{22} \end{bmatrix} \\
 &= \begin{bmatrix} \sum_{j \neq 1} B_{1j} & -B_{12} \\ -B_{21} & \sum_{j \neq 2} B_{2j} \end{bmatrix} \\
 A_2 &= \begin{bmatrix} S_{31} \sin(\theta_{31} - \gamma_{31}) & S_{32} \sin(\theta_{32} - \gamma_{32}) \\ S_{41} \sin(\theta_{41} - \gamma_{41}) & S_{42} \sin(\theta_{42} - \gamma_{42}) \end{bmatrix} \\
 &= \begin{bmatrix} -B_{31} & -B_{32} \\ -B_{41} & -B_{42} \end{bmatrix}
 \end{aligned}$$

$-Q_1 - V_1^2 B_{11}$	$S_{12} \sin(\theta_{12} - \Gamma_{12})$	$S_{13} \sin(\theta_{13} - \Gamma_{13})$	$S_{14} \sin(\theta_{14} - \Gamma_{14})$	$P_1 + V_1^2 G_{11}$	$S_{12} \cos(\theta_{12} - \Gamma_{12})$	$S_{13} \cos(\theta_{13} - \Gamma_{13})$	$S_{14} \cos(\theta_{14} - \Gamma_{14})$
$S_{21} \sin(\theta_{21} - \Gamma_{21})$	$-Q_2 - V_2^2 B_{22}$	$S_{23} \sin(\theta_{23} - \Gamma_{23})$	$S_{24} \sin(\theta_{24} - \Gamma_{24})$	$S_{21} \cos(\theta_{21} - \Gamma_{21})$	$P_2 + V_2^2 G_{22}$	$S_{23} \cos(\theta_{23} - \Gamma_{23})$	$S_{24} \cos(\theta_{24} - \Gamma_{24})$
.....	.....	.....	.....	.....	.....	.....	.....
$S_{31} \sin(\theta_{31} - \Gamma_{31})$	$S_{32} \sin(\theta_{32} - \Gamma_{32})$	$-Q_3 - V_3^2 B_{33}$	$S_{34} \sin(\theta_{34} - \Gamma_{34})$	$S_{31} \cos(\theta_{31} - \Gamma_{31})$	$S_{32} \cos(\theta_{32} - \Gamma_{32})$	$P_3 + V_3^2 G_{33}$	$S_{34} \cos(\theta_{34} - \Gamma_{34})$
$S_{41} \sin(\theta_{41} - \Gamma_{41})$	$S_{42} \sin(\theta_{42} - \Gamma_{42})$	$S_{43} \sin(\theta_{43} - \Gamma_{43})$	$-Q_4 - V_4^2 B_{44}$	$S_{41} \cos(\theta_{41} - \Gamma_{41})$	$S_{42} \cos(\theta_{42} - \Gamma_{42})$	$S_{43} \cos(\theta_{43} - \Gamma_{43})$	$P_4 + V_4^2 G_{44}$
.....	.....	.....	.....	.....	.....	.....	.....
$P_1 - V_1^2 G_{11}$	$-S_{12} \cos(\theta_{12} - \Gamma_{12})$	$-S_{13} \cos(\theta_{13} - \Gamma_{13})$	$-S_{14} \cos(\theta_{14} - \Gamma_{14})$	$Q_1 - V_1^2 B_{11}$	$S_{12} \sin(\theta_{12} - \Gamma_{12})$	$S_{13} \sin(\theta_{13} - \Gamma_{13})$	$S_{14} \sin(\theta_{14} - \Gamma_{14})$
$-S_{21} \cos(\theta_{21} - \Gamma_{21})$	$P_2 - V_2^2 G_{22}$	$-S_{23} \cos(\theta_{23} - \Gamma_{23})$	$-S_{24} \cos(\theta_{24} - \Gamma_{24})$	$S_{21} \sin(\theta_{21} - \Gamma_{21})$	$Q_2 - V_2^2 B_{22}$	$S_{23} \sin(\theta_{23} - \Gamma_{23})$	$S_{24} \sin(\theta_{24} - \Gamma_{24})$
.....	.....	.....	.....	.....	.....	.....	.....
$-S_{31} \cos(\theta_{31} - \Gamma_{31})$	$-S_{32} \cos(\theta_{32} - \Gamma_{32})$	$P_3 - V_3^2 G_{33}$	$-S_{34} \cos(\theta_{34} - \Gamma_{34})$	$S_{31} \sin(\theta_{31} - \Gamma_{31})$	$S_{32} \sin(\theta_{32} - \Gamma_{32})$	$Q_3 - V_3^2 B_{33}$	$S_{34} \sin(\theta_{34} - \Gamma_{34})$
$-S_{41} \cos(\theta_{41} - \Gamma_{41})$	$-S_{42} \cos(\theta_{42} - \Gamma_{42})$	$-S_{43} \cos(\theta_{43} - \Gamma_{43})$	$P_4 - V_4^2 G_{44}$	$S_{41} \sin(\theta_{41} - \Gamma_{41})$	$S_{42} \sin(\theta_{42} - \Gamma_{42})$	$S_{43} \sin(\theta_{43} - \Gamma_{43})$	$Q_4 - V_4^2 B_{44}$

Figure 4.1. The Jacobian matrix of five-bus system in polar form.

$$A_3 = \begin{bmatrix} P_1 - V_1^2 G_{11} & -S_{12} \cos (\theta_{12} - \gamma_{12}) \\ -S_{21} \cos (\theta_{21} - \gamma_{21}) & P_2 - V_2^2 G_{22} \end{bmatrix}$$

$$= \begin{bmatrix} -\sum_{j \neq 1} G_{1j} & G_{12} \\ G_{21} & -\sum_{j \neq 2} G_{2j} \end{bmatrix}$$

$$A_4 = \begin{bmatrix} -S_{31} \cos (\theta_{31} - \gamma_{31}) & -S_{32} \cos (\theta_{32} - \gamma_{32}) \\ -S_{41} \cos (\theta_{41} - \gamma_{41}) & -S_{42} \cos (\theta_{42} - \gamma_{42}) \end{bmatrix}$$

$$= \begin{bmatrix} G_{31} & G_{32} \\ G_{41} & G_{42} \end{bmatrix}$$

$$B_1 = \begin{bmatrix} S_{13} \sin (\theta_{13} - \gamma_{13}) & S_{14} \sin (\theta_{14} - \gamma_{14}) \\ S_{23} \sin (\theta_{23} - \gamma_{23}) & S_{24} \sin (\theta_{24} - \gamma_{24}) \end{bmatrix}$$

$$= \begin{bmatrix} -B_{13} & -B_{14} \\ -B_{23} & -B_{24} \end{bmatrix}$$

$$B_2 = \begin{bmatrix} -Q_3 - V_3^2 B_{33} & S_{34} \sin (\theta_{34} - \gamma_{34}) \\ S_{43} \sin (\theta_{43} - \gamma_{43}) & -Q_4 - V_4^2 B_{44} \end{bmatrix}$$

$$= \begin{bmatrix} \sum_{j \neq 3} B_{3j} & -B_{34} \\ -B_{43} & \sum_{j \neq 4} B_{4j} \end{bmatrix}$$

$$B_3 = \begin{bmatrix} -S_{13} \cos (\theta_{13} - \gamma_{13}) & -S_{14} \cos (\theta_{14} - \gamma_{14}) \\ -S_{23} \cos (\theta_{23} - \gamma_{23}) & -S_{24} \cos (\theta_{24} - \gamma_{24}) \end{bmatrix}$$

$$= \begin{bmatrix} G_{13} & G_{14} \\ G_{23} & G_{24} \end{bmatrix}$$

$$B_4 = \begin{bmatrix} P_3 - V_3^2 G_{33} & -S_{34} \cos (\theta_{34} - \gamma_{34}) \\ -S_{43} \cos (\theta_{43} - \gamma_{43}) & P_4 - V_4^2 G_{44} \end{bmatrix}$$

$$= \begin{bmatrix} -\sum_{j \neq 3} G_{3j} & G_{34} \\ G_{43} & -\sum_{j \neq 4} G_{4j} \end{bmatrix}$$

$$C_1 = \begin{bmatrix} P_1 + V_1^2 G_{11} & S_{12} \cos (\theta_{12} - \gamma_{12}) \\ S_{21} \cos (\theta_{21} - \gamma_{21}) & P_2 + V_2^2 G_{22} \end{bmatrix}$$

$$= \begin{bmatrix} \sum_{j \neq 1} G_{1j} + 2G_{10} & -G_{12} \\ -G_{21} & \sum_{j \neq 2} G_{2j} + 2G_{20} \end{bmatrix}$$

$$C_2 = \begin{bmatrix} S_{31} \cos (\theta_{31} - \gamma_{31}) & S_{32} \cos (\theta_{32} - \gamma_{32}) \\ S_{41} \cos (\theta_{41} - \gamma_{41}) & S_{42} \cos (\theta_{42} - \gamma_{42}) \end{bmatrix}$$

$$= \begin{bmatrix} -G_{31} & -G_{32} \\ -G_{41} & -G_{42} \end{bmatrix}$$

$$C_3 = \begin{bmatrix} Q_1 - V_1^2 B_{11} & S_{12} \sin (\theta_{12} - \gamma_{12}) \\ S_{21} \sin (\theta_{21} - \gamma_{21}) & Q_2 - V_2^2 B_{22} \end{bmatrix}$$

$$= \begin{bmatrix} \sum_{j \neq 1} B_{1j} - 2B_{10} & -B_{12} \\ -B_{21} & \sum_{j \neq 2} B_{2j} - 2B_{20} \end{bmatrix}$$

$$C_4 = \begin{bmatrix} S_{31} \sin (\theta_{31} - \gamma_{31}) & S_{32} \sin (\theta_{32} - \gamma_{32}) \\ S_{41} \sin (\theta_{41} - \gamma_{41}) & S_{42} \sin (\theta_{42} - \gamma_{42}) \end{bmatrix}$$

$$= \begin{bmatrix} -B_{31} & -B_{32} \\ -B_{41} & -B_{42} \end{bmatrix}$$

$$D_1 = \begin{bmatrix} S_{13} \cos (\theta_{13} - \gamma_{13}) & S_{14} \cos (\theta_{14} - \gamma_{14}) \\ S_{23} \cos (\theta_{23} - \gamma_{23}) & S_{24} \cos (\theta_{24} - \gamma_{24}) \end{bmatrix}$$

$$= \begin{bmatrix} -G_{13} & -G_{14} \\ -G_{23} & -G_{24} \end{bmatrix}$$

$$D_2 = \begin{bmatrix} P_3 + V_3^2 G_{33} & S_{34} \cos (\theta_{34} - \gamma_{34}) \\ S_{43} \cos (\theta_{43} - \gamma_{43}) & P_4 + V_4^2 G_{44} \end{bmatrix}$$

$$= \begin{bmatrix} \sum_{j \neq 3} G_{3j} + 2G_{30} & G_{34} \\ G_{43} & \sum_{j \neq 4} G_{4j} + 2G_{40} \end{bmatrix}$$



$$\begin{aligned}
D_3 &= \begin{bmatrix} S_{13} \sin(\theta_{13} - \gamma_{13}) & S_{14} \sin(\theta_{14} - \gamma_{14}) \\ S_{23} \sin(\theta_{23} - \gamma_{23}) & S_{24} \sin(\theta_{24} - \gamma_{24}) \end{bmatrix} \\
&= \begin{bmatrix} -B_{13} & -B_{14} \\ -B_{23} & -B_{24} \end{bmatrix} \\
D_4 &= \begin{bmatrix} Q_3 - v_3^2 B_{33} & S_{34} \sin(\theta_{34} - \gamma_{34}) \\ S_{43} \sin(\theta_{43} - \gamma_{43}) & Q_4 - v_4^2 B_{44} \end{bmatrix} \\
&= \begin{bmatrix} \sum_{j \neq 3} B_{3j} - 2B_{30} & -B_{34} \\ -B_{43} & \sum_{j \neq 4} B_{4j} - 2B_{40} \end{bmatrix}
\end{aligned}$$

From equations (4.8), (4.9), (4.11), and (4.12) the sensitivity matrices can be expressed as

$$S_{VE} = S_{Q_L V}^{-1} M_{VE} \quad (4.33)$$

$$S_{Q_G Q_L} = M_{Q_G Q_L} S_{Q_L V}^{-1} \quad (4.34)$$

$$S_{Q_G E} = M_{Q_G E} - S_{Q_G Q_L} S_{Q_L V}^{-1} S_{VE} \quad (4.35)$$

where  $S_{Q_L V}$ ,  $M_{VE}$ ,  $M_{Q_G Q_L}$ ,  $M_{Q_G E}$  are given below:

$$\begin{aligned}
 S_{Q_L V} &= [D_4 - B_4 B_2^{-1} D_2] \\
 &= \begin{bmatrix} \sum_{j \neq 3} B_{3j} - 2B_{30} & -B_{34} \\ -B_{43} & \sum_{j \neq 4} B_{4j} - 2B_{40} \end{bmatrix} \\
 &\quad - \begin{bmatrix} -\sum_{j \neq 3} G_{3j} & G_{34} \\ G_{43} & -\sum_{j \neq 4} G_{4j} \end{bmatrix} \\
 &\quad \left\{ \begin{bmatrix} \sum_{j \neq 3} B_{3j} & -B_{34} \\ -B_{43} & \sum_{j \neq 4} B_{4j} \end{bmatrix} \right\}^{-1} \\
 &\quad \begin{bmatrix} \sum_{j \neq 3} G_{3j} + 2G_{30} & -G_{34} \\ -G_{43} & \sum_{j \neq 4} G_{4j} + 2G_{40} \end{bmatrix} \\
 &= \begin{bmatrix} \sum_{j \neq 3} B_{3j} - 2B_{30} & -B_{34} \\ -B_{43} & \sum_{j \neq 4} B_{4j} - 2B_{40} \end{bmatrix}
 \end{aligned}$$

$$\begin{aligned}
& + \begin{bmatrix} \sum_{j \neq 3} G_{3j} & -G_{34} \\ -G_{43} & \sum_{j \neq 4} G_{4j} \end{bmatrix} \\
& \left\{ \begin{bmatrix} \sum_{j \neq 3} B_{3j} & -B_{34} \\ -B_{43} & \sum_{j \neq 4} B_{4j} \end{bmatrix} \right\}^{-1} \\
& \begin{bmatrix} \sum_{j \neq 3} G_{3j} + 2G_{30} & -G_{34} \\ -G_{43} & \sum_{j \neq 4} G_{4j} + 2G_{40} \end{bmatrix}
\end{aligned}$$

$$M_{VE} = - [C_4 - B_4 B_2^{-1} C_2]$$

$$\begin{aligned}
& = - \left\{ \begin{bmatrix} -B_{31} & -B_{32} \\ B_{41} & -B_{42} \end{bmatrix} \right. \\
& \left. - \begin{bmatrix} -\sum_{j \neq 3} G_{3j} & G_{34} \\ G_{43} & -\sum_{j \neq 4} G_{4j} \end{bmatrix} \left\{ \begin{bmatrix} \sum_{j \neq 3} B_{3j} & -B_{34} \\ -B_{43} & \sum_{j \neq 4} B_{4j} \end{bmatrix} \right\}^{-1} \right.
\end{aligned}$$

$$\begin{aligned}
& \left\{ \begin{bmatrix} -G_{31} & -G_{32} \\ -G_{41} & -G_{42} \end{bmatrix} \right\} \\
& = \left\{ \begin{bmatrix} B_{31} & B_{32} \\ B_{41} & B_{42} \end{bmatrix} \right. \\
& + \left. \begin{bmatrix} \sum_{j \neq 3} G_{3j} & -G_{34} \\ -G_{43} & \sum_{j \neq 4} G_{4j} \end{bmatrix} \left\{ \begin{bmatrix} \sum_{j \neq 3} B_{3j} & -B_{34} \\ -B_{43} & \sum_{j \neq 4} B_{4j} \end{bmatrix} \right\}^{-1} \right. \\
& \left. \begin{bmatrix} G_{31} & G_{32} \\ G_{41} & G_{42} \end{bmatrix} \right\}
\end{aligned}$$

$$M_{Q_G Q_L} = - [D_3 - B_3 B_2^{-1} D_2]$$

$$= - \left\{ \begin{bmatrix} -B_{13} & -B_{14} \\ -B_{23} & -B_{24} \end{bmatrix} \right\}$$

$$- \begin{bmatrix} G_{13} & G_{14} \\ G_{23} & G_{24} \end{bmatrix} \left\{ \begin{bmatrix} \sum_{j \neq 3} B_{3j} & -B_{34} \\ -B_{43} & \sum_{j \neq 4} B_{4j} \end{bmatrix} \right\}^{-1}$$

$$\left[ \begin{array}{cc} \sum_{j \neq 3} G_{3j} + 2G_{30} & -G_{34} \\ -G_{43} & \sum_{j \neq 4} G_{4j} + 2G_{40} \end{array} \right]$$

$$= \begin{bmatrix} B_{13} & B_{14} \\ B_{23} & B_{24} \end{bmatrix}$$

$$+ \begin{bmatrix} G_{13} & G_{14} \\ G_{23} & G_{24} \end{bmatrix} \left\{ \begin{bmatrix} \sum_{j \neq 3} B_{3j} & -B_{34} \\ -B_{43} & \sum_{j \neq 4} B_{4j} \end{bmatrix} \right\}^{-1}$$

$$\left[ \begin{array}{cc} \sum_{j \neq 3} G_{3j} + 2G_{30} & -G_{34} \\ -G_{43} & \sum_{j \neq 4} G_{4j} + 2G_{40} \end{array} \right]$$

$$M_{QGE} = [C_3 - B_3 B_2^{-1} C_2]$$

$$= \begin{bmatrix} \sum_{j \neq 1} B_{1j} - 2B_{10} & -B_{12} \\ -B_{21} & \sum_{j \neq 2} B_{2j} - 2B_{20} \end{bmatrix}$$

$$- \begin{bmatrix} G_{13} & G_{14} \\ G_{23} & G_{24} \end{bmatrix} \left\{ \begin{bmatrix} \sum_{j \neq 3} B_{3j} & -B_{34} \\ -B_{43} & \sum_{j \neq 4} B_{4j} \end{bmatrix} \right\}^{-1}$$

$$\begin{bmatrix} -G_{31} & -G_{32} \\ -G_{41} & -G_{42} \end{bmatrix}$$

$$= \begin{bmatrix} \sum_{j \neq 1} B_{1j} - 2B_{10} & -B_{12} \\ -B_{21} & \sum_{j \neq 2} B_{2j} - 2B_{20} \end{bmatrix}$$

$$+ \begin{bmatrix} G_{13} & G_{14} \\ G_{23} & G_{24} \end{bmatrix} \left\{ \begin{bmatrix} \sum_{j \neq 3} B_{3j} & -B_{34} \\ -B_{43} & \sum_{j \neq 4} B_{4j} \end{bmatrix} \right\}^{-1}$$

$$\begin{bmatrix} G_{31} & G_{32} \\ G_{41} & G_{42} \end{bmatrix}$$

At this point all important equations that are needed for sensitivity analysis in sections 4.4 and 4.5 have been derived. Thus the sufficient conditions for voltage stability are derived in the next two sections.

#### 4.4. The Theorems for Local and Global Voltage Stability

The system that will be studied here is assumed to be operated under light load conditions, as it is defined in the previous section. The local control at load buses will be discussed first. Setting  $\Delta P_L = 0$  in (4.8), the following expression relating the voltage  $V$  at PQ bus to the control voltage  $E$  at PV buses and the reactive load disturbance  $\Delta Q_L$  at PQ buses is obtained

$$V = [S_{VE}]\Delta E + [S_{Q_L V}]\Delta Q_L$$

It is shown in section 4.2 that for proper control of  $\Delta V$  the sensitivity matrices  $S_{VE}$  must have all positive elements and  $S_{Q_L V}$  must be positive definite. One way to show the positive definiteness is using the properties of M-matrix, which will be shown later.

The positiveness of both  $S_{VE}$  and  $S_{Q_G E}$  and the positive definiteness of  $S_{Q_G E}$  and  $S_{Q_L V}$  are the basis for proper voltage control. If these properties are violated the loss of voltage control would immediately result. Thus, the large capacitances of long transmission lines or underground transmission lines will have been shown to cause voltage control problems for light load conditions. These problems are known to exist and are often solved by removing these

long transmission lines or underground transmission under light load conditions.

All elements of the sensitivity matrix  $S_{VE} = S_{QL}^{-1} M_{VE}$  in (4.10) must be positive for the PV buses to properly support voltage at PQ buses. If  $S_{VE}$  loses its positiveness, indicating a loss of controllability, then there are some PV buses that have no effect or have reversed effect on some PQ buses. It will cause a loss of voltage stability. This loss of controllability and stability would be seen if raising  $E$  at PV buses has no effect at all on raising  $V$  at particular PQ buses and if increasing  $E$  at some PV buses actually would cause decreases in  $V$  at some PQ buses, respectively.

Theorem 5: Under light load condition, a sufficient condition for  $S_{VE}$  to be positive is that  $S_{QL}$  be an M-matrix and the R/X ratios of all lines are equal.

Proof:

Recall that

$$M_{VE} = - [C_4 - B_4 B_2^{-1} C_2]$$

$$= \left\{ \begin{bmatrix} B_{31} & B_{32} \\ B_{41} & B_{42} \end{bmatrix} + \begin{bmatrix} \sum_{j \neq 3} G_{3j} & -G_{34} \\ -G_{43} & \sum_{j \neq 4} G_{4j} \end{bmatrix} \right\} \left\{ \begin{bmatrix} \sum_{j \neq 3} B_{3j} & -B_{34} \\ -B_{43} & \sum_{j \neq 4} B_{4j} \end{bmatrix} \right\}^{-1}$$





$$\begin{aligned}
 & \left[ \begin{array}{cc} G_{31} & G_{32} \\ G_{41} & G_{42} \end{array} \right] \\
 & \approx \left[ \begin{array}{cc} B_{31} & B_{32} \\ B_{41} & B_{42} \end{array} \right] + (R/X) \left[ \begin{array}{cc} G_{31} & G_{32} \\ G_{41} & G_{42} \end{array} \right] \\
 & = (1 + (R/X)^2) \left[ \begin{array}{cc} B_{31} & B_{32} \\ B_{41} & B_{42} \end{array} \right]
 \end{aligned}$$

Since all  $B_{ij}$ 's are positive, matrix  $M_{VE}$  is always positive. Since  $S_{QLV}$  is assumed to be an M matrix, then  $S_{VE} = S_{QLV}^{-1} M_{VE}$  is always positive.

Next, a sufficient condition for  $S_{QGQL}$  to be positive, which in part assures observability, is considered. Recall that if  $\Delta P_L = 0$ , equation (4.13) becomes

$$\Delta Q_G \approx [S_{QGE}] \Delta E - [S_{QGQL}] \Delta Q_L$$

$$S_{QGQL} = M_{QGQL} S_{QLV}^{-1} \quad (4.34)$$

$$S_{QGE} = M_{QGE} - S_{QGQL} S_{QLV} S_{VE} \quad (4.35)$$

Theorem 6: Under light load condition, a sufficient condition

that  $S_{Q_G Q_L}$  be positive is that

- 1)  $S_{Q_L V}$  be an M-matrix,
- 2) the shunt conductances  $G_{i0}$  are negligible at all buses, and
- 3) R/X ratios of all lines are equal.

Proof:

Since

$$\begin{aligned}
 M_{Q_G Q_L} &= - [D_3 - B_3 B_2^{-1} D_2] \\
 &= \left\{ \begin{bmatrix} B_{13} & B_{23} \\ B_{14} & B_{24} \end{bmatrix} \right. \\
 &\quad + \begin{bmatrix} G_{13} & G_{14} \\ G_{23} & G_{24} \end{bmatrix} \left\{ \begin{bmatrix} \sum_{j \neq 3} B_{3j} & -B_{34} \\ -B_{43} & \sum_{j \neq 4} B_{4j} \end{bmatrix} \right\}^{-1} \\
 &\quad \left. \begin{bmatrix} \sum_{j \neq 3} G_{3j} + 2G_{30} & -G_{34} \\ -G_{43} & \sum_{j \neq 4} G_{4j} + 2G_{40} \end{bmatrix} \right\} \\
 &\approx \begin{bmatrix} B_{13} & B_{23} \\ B_{14} & B_{24} \end{bmatrix} + \begin{bmatrix} G_{13} & G_{14} \\ G_{23} & G_{24} \end{bmatrix} (R/X)
 \end{aligned}$$

$$\begin{aligned}
&= \begin{bmatrix} B_{13} & B_{23} \\ B_{14} & B_{24} \end{bmatrix} + (R/X)^2 \begin{bmatrix} B_{13} & B_{14} \\ B_{23} & B_{24} \end{bmatrix} \\
&= (1 + (R/X)^2) \begin{bmatrix} B_{13} & B_{14} \\ B_{23} & B_{24} \end{bmatrix}
\end{aligned}$$

then  $M_{Q_G Q_L}$  is positive. Assuming that  $S_{Q_L V}$  is an M matrix, then

$S_{Q_G Q_L} = M_{Q_G Q_L} S_{Q_L V}^{-1}$  is a positive matrix.

Remarks:  $S_{Q_G Q_L}$  must be positive if a positive reactive load injection  $Q_L$  is to produce a negative reactive generator injection at PV buses. If  $S_{Q_G Q_L}$  has negative elements a continual voltage rise or voltage collapse would occur based on the change in  $\Delta Q_L$  because the reactive sources would not compensate for changes in  $\Delta Q_L$  but actually reduce support.

Theorem 7: Under light load condition, a sufficient condition for  $S_{Q_L V}$  to be an M-matrix is

- 1) if  $D_4$  is an M-matrix, and
- 2) R/X ratios of all lines are equal.

Proof:

$$\begin{aligned}
S_{Q_L V} &= [D_4 - B_4 B_2^{-1} D_2] \\
&= \begin{bmatrix} \sum_{j \neq 3} B_{3j} - 2B_{30} & -B_{34} \\ -B_{43} & \sum_{j \neq 4} B_{4j} - 2B_{40} \end{bmatrix}
\end{aligned}$$

$$\begin{aligned}
& + \left[ \begin{array}{cc} \sum_{j \neq 3} G_{3j} & -G_{34} \\ -G_{43} & \sum_{j \neq 4} G_{4j} \end{array} \right]^{112} \\
& \left\{ \left[ \begin{array}{cc} \sum_{j \neq 3} B_{3j} & -B_{34} \\ -B_{43} & \sum_{j \neq 4} B_{4j} \end{array} \right] \right\}^{-1} \\
& \left[ \begin{array}{cc} \sum_{j \neq 3} G_{3j} + 2G_{30} & -G_{34} \\ -G_{43} & \sum_{j \neq 4} G_{4j} + 2G_{40} \end{array} \right] \\
& = \left[ \begin{array}{cc} \sum_{j \neq 3} B_{3j} - 2B_{30} & -B_{34} \\ -B_{43} & \sum_{j \neq 4} B_{4j} - 2B_{40} \end{array} \right] \\
& + (R/X) \left[ \begin{array}{cc} \sum_{j \neq 3} G_{3j} + 2G_{30} & -G_{34} \\ -G_{43} & \sum_{j \neq 4} G_{4j} + 2G_{40} \end{array} \right]
\end{aligned}$$

The above matrix

$$S_{Q_L V} = \left(1 + \left(\frac{R}{X}\right)^2\right) \begin{bmatrix} \sum_{j \neq 3} B_{3j} - \frac{2B_{30}}{[1 + (\frac{R}{X})^2]} & -B_{34} \\ -B_{43} & \sum_{j \neq 4} B_{4j} - \frac{2B_{40}}{[1 + (\frac{R}{X})^2]} \end{bmatrix} \cong [1 + (\frac{R}{X})^2] D_4$$

If  $G_{30} = G_{40} = 0$  for light load conditions  $B_3$  and  $B_4 > 0$ , and  $D_4$  is assumed to be an M matrix, then  $S_{Q_L V}$  must be an M matrix. From fact 2, since  $S_{Q_L V}$  is irreducible, then it is also positive definite.

Remarks:  $S_{Q_L V}$  can be positive definite, but could also be semi-definite, indefinite, or even negative definite, since it depends on the shunt  $B_{i0}$ 's in  $D_4$ .  $B_{i0}$  can represent either shunt capacitances of transmission lines or switchable shunt capacitors banks at each bus. Under light load conditions switchable shunt capacitors banks would never be in the network.  $D_4$  could be indefinite or negative definite if the shunt capacitance ( $B_{30}, B_{40}$ ) of a long or an underground transmission system was sufficient to overcome the positive definiteness of  $D_4$  with these shunt capacitances eliminated. The shunt capacitance of the transmission line not only makes  $D_4$  less positive definite but possibly indefinite or negative definite. The shunt capacitance can also possibly make  $S_{Q_L V}$  indefinite or negative definite. If  $S_{Q_L V}$  should ever become negative definite, the effects of load  $Q_L$  injection on voltage would be reversed from normal conditions. More important, the positiveness of the matrices  $S_{VE}$ ,  $S_{Q_G Q_L}$ , and the positive definiteness of  $S_{Q_G E}$ , can only be assured if  $S_{Q_L V}$  is positive definite.

Theorem 8: Under light load condition, a sufficient condition

for  $S_{QGE}$  is positive definite is that

- 1)  $S_{QLV}$  be an M-matrix ( $D_4$  be an M-matrix),
- 2) R/X ratios of all lines are equal, and
- 3) Matrix

$$\begin{bmatrix} C_3 & D_3 \\ C_4 & D_4 \end{bmatrix}$$

is positive definite.

Proof:

We know that  $S_{QGE} = M_{QGE} - S_{QGQL} S_{QLV} S_{VE}$ . Since  $B_{i0}$ 's and  $G_{i0}$ 's are assumed to be negligible,  $S_{QLV}$  can be expressed as from Theorem 7.

$$\begin{aligned} S_{QLV} &\cong \begin{bmatrix} \sum_{j \neq 3} B_{3j} & -B_{34} \\ -B_{43} & \sum_{j \neq 4} B_{4j} \end{bmatrix} \\ &+ (R/X) \begin{bmatrix} \sum_{j \neq 3} G_{3j} & -G_{34} \\ -G_{43} & \sum_{j \neq 4} G_{4j} \end{bmatrix} \\ &= \begin{bmatrix} \sum_{j \neq 3} B_{3j} & -B_{34} \\ -B_{43} & \sum_{j \neq 4} B_{4j} \end{bmatrix} \end{aligned}$$

$$\begin{aligned}
& + (R/X)^2 \begin{bmatrix} \sum_{j \neq 3} B_{3j} & -B_{34} \\ -B_{43} & \sum_{j \neq 4} B_{4j} \end{bmatrix} \\
& = (1 + (R/X)^2) \begin{bmatrix} \sum_{j \neq 3} B_{3j} & -B_{34} \\ -B_{43} & \sum_{j \neq 4} B_{4j} \end{bmatrix}
\end{aligned}$$

The matrix product  $S_{Q_G Q_L} S_{Q_L V} S_{V E}$  becomes

$$\begin{aligned}
S_{Q_G Q_L} S_{Q_L V} S_{V E} &= (-M_{Q_G Q_L}) S_{Q_L V}^{-1} (-M_{V E}) \\
&= \left\{ (1 + (R/X)^2) \begin{bmatrix} B_{13} & B_{14} \\ B_{23} & B_{24} \end{bmatrix} \right. \\
&\quad (1 + (R/X)^2)^{-1} \left\{ \begin{bmatrix} \sum_{j \neq 3} B_{3j} & -B_{34} \\ -B_{43} & \sum_{j \neq 4} B_{4j} \end{bmatrix} \right\}^{-1} \\
&\quad \left. (1 + (R/X)^2) \begin{bmatrix} B_{31} & B_{32} \\ B_{41} & B_{42} \end{bmatrix} \right\}
\end{aligned}$$



$$= (1 + (R/X)^2) \left\{ \begin{bmatrix} B_{13} & B_{14} \\ B_{23} & B_{24} \end{bmatrix} \right\}$$

$$\left\{ \begin{bmatrix} \sum_{j \neq 3} B_{3j} & -B_{34} \\ -B_{43} & \sum_{j \neq 4} B_{4j} \end{bmatrix} \right\}^{-1} \begin{bmatrix} B_{31} & B_{32} \\ B_{41} & B_{42} \end{bmatrix}$$

The matrix  $M_{QGE}$  can now be expressed as

$$M_{QGE} = [C_3 - B_3 B_2^{-1} C_2]$$

$$= \begin{bmatrix} \sum_{j \neq 1} B_{1j} - 2B_{10} & -B_{12} \\ -B_{21} & \sum_{j \neq 2} B_{2j} - 2B_{20} \end{bmatrix}$$

$$+ \begin{bmatrix} G_{13} & G_{14} \\ G_{23} & G_{24} \end{bmatrix} \left\{ \begin{bmatrix} \sum_{j \neq 3} B_{3j} & -B_{34} \\ -B_{43} & \sum_{j \neq 4} B_{4j} \end{bmatrix} \right\}^{-1}$$

$$\begin{bmatrix} G_{31} & G_{32} \\ G_{41} & G_{42} \end{bmatrix}$$

$$\approx \begin{bmatrix} \sum_{j \neq 1} B_{1j} & -B_{12} \\ -B_{21} & \sum_{j \neq 2} B_{2j} \end{bmatrix}$$

$$+ \begin{bmatrix} G_{13} & G_{14} \\ G_{23} & G_{24} \end{bmatrix} \left\{ \begin{bmatrix} \sum_{j \neq 3} B_{3j} & -B_{34} \\ -B_{43} & \sum_{j \neq 4} B_{4j} \end{bmatrix} \right\}^{-1}$$

$$\begin{bmatrix} G_{31} & G_{32} \\ G_{41} & G_{42} \end{bmatrix}$$

$$= \begin{bmatrix} \sum_{j \neq 1} B_{1j} & -B_{12} \\ -B_{21} & \sum_{j \neq 2} B_{2j} \end{bmatrix}$$

$$+ (R/X)^2 \begin{bmatrix} B_{13} & B_{14} \\ B_{23} & B_{24} \end{bmatrix} \left\{ \begin{bmatrix} \sum_{j \neq 3} B_{3j} & -B_{34} \\ -B_{43} & \sum_{j \neq 4} B_{4j} \end{bmatrix} \right\}^{-1}$$

$$\begin{bmatrix} B_{31} & B_{32} \\ B_{41} & B_{42} \end{bmatrix}$$

The matrix  $S_{QGE}$  now becomes

$$S_{QGE} = M_{QGE} - S_{QGQL} S_{QLV} S_{VE}$$

$$= \begin{bmatrix} \sum_{j \neq 1} B_{1j} & -B_{12} \\ -B_{21} & \sum_{j \neq 2} B_{2j} \end{bmatrix}$$

$$+ (R/X)^2 \begin{bmatrix} B_{13} & B_{14} \\ B_{23} & B_{24} \end{bmatrix} \left\{ \begin{bmatrix} \sum_{j \neq 3} B_{3j} & -B_{34} \\ -B_{43} & \sum_{j \neq 4} B_{4j} \end{bmatrix} \right\}^{-1}$$

$$\begin{bmatrix} B_{31} & B_{32} \\ B_{41} & B_{42} \end{bmatrix} - (1 + (R/X)^2) \left\{ \begin{bmatrix} B_{13} & B_{14} \\ B_{23} & B_{24} \end{bmatrix} \right\}$$

$$\left\{ \begin{bmatrix} \sum_{j \neq 3} B_{3j} & -B_{34} \\ -B_{43} & \sum_{j \neq 4} B_{4j} \end{bmatrix} \right\}^{-1}$$

$$\begin{bmatrix} B_{31} & B_{32} \\ B_{41} & B_{42} \end{bmatrix}$$

$$\begin{aligned}
&= \begin{bmatrix} \sum_{j \neq 1} B_{1j} & -B_{12} \\ -B_{21} & \sum_{j \neq 2} B_{2j} \end{bmatrix} \\
&- \left\{ \begin{bmatrix} B_{13} & B_{14} \\ B_{23} & B_{24} \end{bmatrix} \right\} \\
&\left\{ \begin{bmatrix} \sum_{j \neq 3} B_{3j} & -B_{34} \\ -B_{43} & \sum_{j \neq 4} B_{4j} \end{bmatrix} \right\}^{-1} \begin{bmatrix} B_{31} & B_{32} \\ B_{41} & B_{42} \end{bmatrix} \\
&= C_3 - D_3 D_4^{-1} C_4
\end{aligned}$$

given that the matrices

$$\begin{bmatrix} C_3 & D_3 \\ C_4 & D_4 \end{bmatrix}$$

and  $D_4$  are both positive definite. The inverse matrix has the form  $(C_3 - D_3 D_4^{-1} C_4)$  and since the inverse matrix is positive definite if the original matrix is positive definite, the submatrix  $[C_3 - D_3 D_4^{-1} C_4]$  is positive definite.

Remarks: If  $S_{Q_G E}$  is positive definite then increasing voltage at PV buses requires a large positive reactive injection. However, if  $S_{Q_G E}$  is semi-definite, then raising E at some PV buses has no effect on raising  $Q_G$  at these buses. If  $S_{Q_G E}$  is indefinite, then raising E at PV buses could indeed require reduced positive reactive injection which is contrary to how a power system is supposed to support voltage.

The above results indicate that if  $S_{Q_L V}$  is negative definite, then a controllability induced loss of stability can occur directly or because  $S_{V E}$  has negative elements and a loss of observability induced loss of stability can occur because  $S_{Q_G Q_L}$  has negative elements or  $S_{Q_G E}$  is negative definite. The results for light load conditions indicate that for  $S_{Q_L V}$  to be positive definite  $D_4$  must be positive definite, and for  $S_{Q_G E}$  to be positive definite both  $D_4$  and  $\begin{bmatrix} C_3 & D_4 \\ C_3 & D_4 \end{bmatrix}$  must be positive definite. These matrices will be negative definite if the capacitive admittance at generator or load bus exceeds half the sum of all branch admittance connected to that bus. This explains the operation practice of switching out certain long transmission lines with large shunt capacitive admittance under light load conditions.

Although an analysis is not performed for normal or heavy load conditions, it is hypothesized that the admittance of switchable shunt capacitance at any bus should also be less than half the admittance of all branch elements connected to that bus. This hypothesis will be studied experimentally in Chapter 5.

The above analysis is quite important because it has been known that capacitance from long transmission lines can cause voltage problems under light load conditions but the above analysis is the first that analytically derives a limit on the capacitive admittance at a bus to assure voltage controllability and observability induced stability. Deriving a similar limit for normal and heavy load conditions is a subject for future research.

#### 4.5. Theorems Integrating the Weak Boundaries and Sensitivity Analysis

In this section, two parallel approaches of the identification of weak boundary and sensitivity analysis are integrated, and summarize the corresponding mathematical results as theorems. In order to show that the SSC groups preserve their coherency structure in all sensitivity matrices, the following model of a three SSC group network is introduced.

$$\Delta P_G = [\Delta P_{G1} \Delta P_{G2} \Delta P_{G3}]^t$$

$$\Delta P_L = [\Delta P_{L1} \Delta P_{L2} \Delta P_{L3}]^t$$

$$\Delta Q_G = [\Delta Q_{G1} \Delta Q_{G2} \Delta Q_{G3}]^t$$

$$\Delta Q_L = [\Delta Q_{L1} \Delta Q_{L2} \Delta Q_{L3}]^t$$

$$\Delta \delta = [\Delta \delta_1 \Delta \delta_2 \Delta \delta_3]^t .$$

$$\Delta\theta = [\Delta\theta_1 \Delta\theta_2 \Delta\theta_3]^t$$

$$\Delta E = [\Delta E_1 \Delta E_2 \Delta E_3]^t$$

$$\Delta V = [\Delta V_1 \Delta V_2 \Delta V_3]^t \quad (4.36)$$

The partitioned Jacobian matrix for this three-SSC-group system can be expressed as in Figure 4.2.

Property 1: All submatrices in Figure 4.2 are square matrices.

Definition: (Dominant diagonal block) If a square matrix is partitioned such that the absolute value of any nonzero element in its diagonal blocks is strictly greater than the absolute value of any element off the diagonal blocks, then those diagonal blocks are called dominant diagonal blocks of the matrix.

Property 2: Matrices  $B_2$ ,  $B_4$ ,  $C_3$ ,  $D_2$ , and  $D_4$  have dominant diagonal blocks corresponding to the three SSC groups.

Property 3: Let matrices

$$A_{m \times k} = \begin{bmatrix} A_{11} & A_{12} \\ A_{21} & A_{22} \end{bmatrix} \quad \text{and} \quad B_{k \times n} = \begin{bmatrix} B_{11} & B_{12} \\ B_{21} & B_{22} \end{bmatrix}$$

If the submatrices  $A_{11}$ ,  $A_{22}$ ,  $B_{11}$ , and  $B_{22}$  are dominant diagonal blocks in  $A$  and  $B$  respectively, then the product matrix  $C = AB$  also has the corresponding diagonal blocks dominant.

[illegible]

Figure 4.2. The partitioned Jacobian matrix of a three-SSC group network.



Property 4: The inverse of a matrix with dominant diagonal blocks has the same diagonal blocks dominant.

It is essential to prove the following property, and then use the mathematical induction to complete the proof of Property 4. If matrix

$$H = \begin{bmatrix} H_{11}/\mu & H_{12} \\ H_{21} & H_{22}/\mu \end{bmatrix} \quad (4.37)$$

where

- (1)  $H_{11}$  and  $H_{22}$  are nonsingular square matrices, and
- (2)  $H_{11}/\mu$  and  $H_{22}/\mu$  are dominant diagonal blocks in  $H$ , when  $\mu \rightarrow 0$ , then the inverse of  $H$ , which can be written as

$$H^{-1} = \begin{bmatrix} K_{11} & K_{12} \\ K_{21} & K_{22} \end{bmatrix} \quad (4.38)$$

with the same partitioning as  $H$ , also have dominant diagonal blocks.

**Proof:**

By the inverse matrix lemma the following results are obtained:

$$(i) \quad K_{11} = [H_{11}/\mu - H_{12}(\mu H_{22}^{-1})H_{21}]^{-1}$$

when  $\mu \rightarrow 0$ , so that

$$K_{11} \cong (\mu)[H_{11}]^{-1}$$

$$(ii) \quad K_{12} = - [K_{11}H_{12}(H_{22}/\mu)^{-1}]$$

when  $\mu \rightarrow 0$

$$K_{12} \cong -(\mu)^2 [H_{11}^{-1}H_{12}H_{22}^{-1}]$$

$$(iii) \quad K_{21} = - [(H_{22}/\mu)^{-1}H_{21}K_{11}]$$

when  $\mu \rightarrow 0$

$$K_{21} \cong -(\mu)^2 H_{22}^{-1}H_{21}H_{11}^{-1}]$$

$$(iv) \quad K_{22} = \mu H_{22}^{-1} - H_{22}^{-1}H_{21}K_{12}$$

when  $\mu \rightarrow 0$

$$\begin{aligned} K_{22} &\cong \mu H_{22}^{-1} - \mu H_{22}^{-1}H_{21} - (\mu)^2 [H_{11}^{-1}H_{12}H_{22}^{-1}] \\ &\cong (\mu)[H_{22}]^{-1} \end{aligned}$$

Summarizing (i) to (iv), the following relationships hold:

$$K_{11} \cong (\mu)[H_{11}]^{-1}$$

$$K_{12} \cong -(\mu)^2 [H_{11}^{-1}H_{12}H_{22}^{-1}]$$

$$K_{21} \cong -(\mu)^2 [H_{22}^{-1}H_{21}H_{11}^{-1}]$$

$$K_{22} \cong (\mu)[H_{22}]^{-1}$$

(4.39)

Therefore  $H^{-1}$  has diagonal dominant blocks as declared.

Finally, the proof of Property 4 can be accomplished by mathematical induction as shown in the following example:

Let

$$H = \begin{bmatrix} H_{11}/\mu & H_{12} & H_{13} \\ H_{21} & H_{22}/\mu & H_{23} \\ H_{31} & H_{32} & H_{33}/\mu \end{bmatrix}$$

where  $\mu \rightarrow 0$ , and

$$H^{-1} = \begin{bmatrix} K_{11} & K_{12} & K_{13} \\ K_{21} & K_{22} & K_{23} \\ K_{31} & K_{32} & K_{33} \end{bmatrix}$$

The matrix can be partitioned into four blocks. Then by (4.39) it can be asserted that submatrix  $K_{33}$  is a dominant diagonal block.

Similarly, by symmetry, if  $H$  is partitioned such that

$$H^{-1} = \begin{bmatrix} K_{11} & K_{12} & K_{13} \\ K_{21} & K_{22} & K_{23} \\ K_{31} & K_{32} & K_{33} \end{bmatrix}$$

then the submatrix  $K_{11}$  is a dominant diagonal block. Also, when

$\mu \rightarrow 0$

$$\begin{bmatrix} K_{11} & K_{12} \\ K_{21} & K_{22} \end{bmatrix} \cong \begin{bmatrix} H_{11}/\mu & H_{12} \\ H_{21} & H_{22}/\mu \end{bmatrix}^{-1}$$

then by (4.39)  $K_{22}$  is a dominant diagonal block. Therefore Property 4 has been proven with three diagonal blocks and the generalization into  $r$  finite dominant diagonal blocks can be easily obtained by the reader.

Applying Property 1 to Property 4 under light load conditions, the following sensitivity matrices

$$\begin{aligned} S_{Q_L V} &= [D_4 - B_4 B_2^{-1} D_2] \\ &= (1 + (R/X)^2) \begin{bmatrix} \sum_{j \neq 3} B_{3j} & -B_{34} \\ -B_{43} & \sum_{j \neq 4} B_{4j} \end{bmatrix} \end{aligned}$$

and

$$\begin{aligned} S_{Q_G E} &= M_{Q_G E} - S_{Q_G Q_L} S_{Q_L V} S_{V E} \\ &= \begin{bmatrix} \sum_{j \neq 1} B_{1j} & -B_{12} \\ -B_{21} & \sum_{j \neq 2} B_{2j} \end{bmatrix} \\ &\quad - \left\{ \begin{bmatrix} B_{13} & B_{14} \\ B_{23} & B_{24} \end{bmatrix} \right\} \end{aligned}$$

$$\left\{ \begin{bmatrix} \sum_{j \neq 3} B_{3j} & -B_{34} \\ -B_{43} & \sum_{j \neq 4} B_{4j} \end{bmatrix} \right\}^{-1} \begin{bmatrix} B_{31} & B_{32} \\ B_{41} & B_{42} \end{bmatrix}$$

$$= C_3 - D_3 D_4^{-1} C_4$$

will both have dominant diagonal blocks.

In the following two theorems a detailed sensitivity model will be used, where one of the SSC group in the system has no source bus as shown in (4.40).

$$\begin{bmatrix} P_{G1} \\ P_{L1} \\ P_{L2} \\ Q_{G1} \\ Q_{L1} \\ Q_{L2} \end{bmatrix} = \begin{bmatrix} A_1^* & B_{11}^* & B_{12} & C_1^* & D_{11}^* & D_{12} \\ A_{21}^* & B_{211}^* & B_{212} & C_{21}^* & D_{211}^* & D_{212} \\ \hdashline A_{22} & B_{221} & B_{222}^* & C_{22} & D_{221} & D_{222}^* \\ \hdashline A_3^* & B_{31}^* & B_{32} & C_3^* & D_{31}^* & D_{32} \\ A_{41}^* & B_{411}^* & B_{412} & C_{41}^* & D_{411}^* & D_{412} \\ \hdashline A_{42} & B_{421} & B_{422}^* & C_{42} & D_{421} & D_{422}^* \end{bmatrix} \begin{bmatrix} Q_{G1} \\ Q_{L1} \\ Q_{L2} \\ V_{G1} \\ V_{L1} \\ V_{L2} \end{bmatrix} \quad (4.40)$$

This system has two SSC groups. The first group consists of both source and load buses which are denoted as  $G_1$  and  $L_1$ , respectively. The second SSC group has only load buses  $L_2$ . The original Jacobian

matrix for the sensitivity analysis is partitioned as shown in (4.40). Note that each SSC group will have the corresponding dominant diagonal blocks as shown above, where the submatrices with "\*" denote the dominant blocks. Those dominant blocks are larger than the other block by an order of  $1/\mu$ , where  $0 < \mu < 1$ . For example,  $D_{411}^* = \frac{1}{\mu} D_{411}$ , where  $D_{411}$  has the same order as  $D_{412}$  does. The leading subscript of each submatrix in (4.40) is identical to the subscript of the original submatrix of (4.2). The second or third subscript indicates the partitioned blocks of each original submatrix. Based on the above model (4.40) the following theorems can be proven, respectively.

Theorem 9: If there is no source in an SSC group, then  $S_{VE}$  has zero rows and loss of controllability occurs.

Proof:

It is known that from the original sensitivity model

$$S_{VE} = S_{QLV}^{-1} M_{VE}$$

$$S_{QLV} = [D_4 - B_4 B_2^{-1} D_2] \cong (1 + (R/X)^2) D_4$$

$$M_{VE} = -[C_4 - B_4 B_2^{-1} C_2] \cong (1 + (R/X)^2) (-C_4)$$

$$S_{VE} \cong D_4^{-1} (-C_4)$$

Now apply these results to the new model

$$S_{VE} = \begin{bmatrix} D_{411}^* & D_{412} \\ D_{421} & D_{422}^* \end{bmatrix}^{-1} \begin{bmatrix} -C_{41}^* \\ -C_{42} \end{bmatrix} \triangleq \begin{bmatrix} \frac{D_{411}}{\mu} & D_{412} \\ D_{421} & \frac{D_{422}}{\mu} \end{bmatrix}^{-1} \begin{bmatrix} \frac{-C_{41}}{\mu} \\ -C_{42} \end{bmatrix}$$

Let

$$D_4^{-1} = \begin{bmatrix} d_{11} & d_{12} \\ d_{21} & d_{22} \end{bmatrix}$$

Similar to (4.39) as  $\mu \rightarrow 0$ , then

$$d_{11} \cong (\mu)[D_{411}]^{-1}$$

$$d_{12} \cong -(\mu)^2[D_{411}^{-1}D_{412}D_{422}^{-1}]$$

$$d_{21} \cong -(\mu)^2[D_{422}^{-1}D_{421}D_{411}^{-1}]$$

$$d_{22} \cong (\mu)[D_{422}]^{-1}$$

(4.41)

and

$$S_{VE} = \begin{bmatrix} d_{11} \left( \frac{-C_{41}}{\mu} \right) + d_{12}(-C_{42}) \\ d_{21} \left( \frac{-C_{41}}{\mu} \right) + d_{22}(-C_{42}) \end{bmatrix}$$

$$\cong \begin{bmatrix} D_{411}^{-1}(-C_{41}) - (\mu)^2[D_{411}^{-1}D_{412}D_{422}^{-1}](-C_{42}) \\ -(\mu)[D_{422}^{-1}D_{421}D_{411}^{-1}](-C_{41}) + (\mu)(D_{422}^{-1})(-C_{42}) \end{bmatrix}$$

Therefore

$$S_{VE} \rightarrow \begin{bmatrix} D_{411}^{-1}(-C_{41}) \\ 0 \end{bmatrix} \text{ as } \mu \rightarrow 0$$

Thus the rows corresponding to the SSC groups without source bus will go to zero, as the stiffness of the SSC group with the source buses goes to infinity. A loss of controllability occurs for the SSC group without a reactive source bus.

Theorem 10: If there is no source in an SSC group, then  $S_{Q_G Q_L}$  has zero columns and loss of observability occurs.

Proof:

It is known that

$$S_{Q_G Q_L} = M_{Q_G Q_L} S_{Q_L}^{-1} V$$

$$M_{Q_G Q_L} = -[D_3 - B_3 B_2^{-1} D_2] \cong (1 + (R/X)^2)(-D_3)$$

$$S_{Q_L} V = D_4 - B_4 B_2^{-1} D_2 \cong (1 + (R/X)^2) D_4$$

$$S_{Q_G Q_L} = (-D_3)(D_4^{-1})$$

Applying these results to the new model



$$\begin{aligned}
S_{Q_G Q_L} &= -[D_{31}^* \ D_{32}] \begin{bmatrix} D_{411}^* & D_{412} \\ D_{421} & D_{422}^* \end{bmatrix}^{-1} \\
&= \left[ \left( \frac{-D_{31}}{\mu} \right) (-D_{32}) \right] \begin{bmatrix} \frac{D_{411}}{\mu} & D_{412} \\ D_{421} & \frac{D_{422}}{\mu} \end{bmatrix}^{-1}
\end{aligned}$$

matrix  $D_4^{-1}$ , where

$$D_4^{-1} = \begin{bmatrix} d_{11} & d_{12} \\ d_{21} & d_{22} \end{bmatrix},$$

has dominant diagonal blocks given in (4.41). Matrix  $S_{Q_G Q_L}$  is

$$\begin{aligned}
S_{Q_G Q_L} &= \left[ -\frac{D_{31}}{\mu} d_{11} - D_{32} d_{21}, \frac{D_{31}}{\mu} d_{12} - D_{32} d_{22} \right] \\
&\cong \left[ (-D_{31})[D_{411}^{-1}] + (-D_{32})(-\mu^2)[D_{422}^{-1} D_{421} D_{411}^{-1}], \right. \\
&\quad \left. (-D_{31})(-\mu)[D_{411}^{-1} D_{412} D_{422}^{-1}] + (-D_{32})(\mu) D_{422}^{-1} \right]
\end{aligned}$$

Therefore

$$S_{Q_G Q_L} \rightarrow [(-D_{31})(D_{411}^{-1}) \quad 0] \text{ as } \mu \rightarrow 0.$$

Thus the columns corresponding to the SSC groups without source buses will go to zero as the stiffness of the SSC group with source buses goes to infinity. A loss of observability thus occurs for the SSC group without a reactive source.

From the above results, the effects of the weak boundaries corresponding to the SSC groups (or the stiffly interconnected groups) can be determined. If the dependent and independent variables of the linear loadflow model are rearranged, then a partitioned Jacobian matrix and a set of partitioned sensitivity matrices can be obtained with dominant diagonal blocks corresponding to the SSC groups. By the definition of SSC group, each SSC group can be modeled as a single bus with respect to the whole system. Then, the constraints derived for each bus in section 4.4 must be satisfied by the SSC group for the voltage stability of the whole system. In other words, the SSC group can be modeled as an equivalent bus to obtain a new Jacobian matrix and carry out the sensitivity analysis. The following is immediately valid from the new Jacobian matrix with the equivalent bus representing each SSC group.

Theorem 11: A sufficient condition for the equivalent sensitivity matrix  $\bar{S}_{Q_L V}$  to be an M matrix is that the sum of  $B_{i0}$  over all buses in the SSC group should not exceed the sum of  $B_{ij}$  over all transmission lines of the weak boundary surrounding the SSC group.

Proof:

Let  $\Delta Q_L = S_{Q_L V} \Delta V_L$  where

$$\Delta Q_L = [\Delta Q_1 \ \Delta Q_2 \ \Delta Q_3 \ \Delta Q_4 \ \Delta Q_5 \ \Delta Q_6 \ \Delta Q_7]^t$$

$$\Delta V_L = [\Delta V_1 \ \Delta V_2 \ \Delta V_3 \ \Delta V_4 \ \Delta V_5 \ \Delta V_6 \ \Delta V_7]^t$$

They are the deviations of reactive power injections and voltages at all load buses, respectively.

Without loss of generality, let buses {1, 2, 3, 4} belong to Group 1 and buses {5, 6, 7} belong to Group 2. Then the controllability equation can be transformed in the linear space as the following:

$$U = \left[ \begin{array}{cccc|ccc} 1 & 0 & 0 & 0 & 0 & 0 & 0 \\ 0 & 1 & 0 & 0 & 0 & 0 & 0 \\ 0 & 0 & 1 & 0 & 0 & 0 & 0 \\ 1 & 1 & 1 & 1 & 0 & 0 & 0 \\ \hline 0 & 0 & 0 & 0 & 1 & 0 & 0 \\ 0 & 0 & 0 & 0 & 0 & 1 & 0 \\ 0 & 0 & 0 & 0 & 1 & 1 & 1 \end{array} \right]$$

and

$$U \Delta Q_L = U [S_{Q_L V}] U^T (U^T)^{-1} \Delta V_L$$

$$= \bar{S}_{QV} (U^T)^{-1} \Delta V_L$$

$$\Delta \bar{Q}_L \triangleq \bar{S}_{Q_L V} \Delta \bar{V}_L$$

where

$$\bar{s}_{Q_L V} \triangleq U [s_{Q_L V}] U^T \quad (4.42)$$

$$\Delta \bar{V}_L \triangleq (U^T)^{-1} \Delta V_L$$

$$(U^T)^{-1} = \begin{bmatrix} 1 & 0 & 0 & -1 & \vdots & 0 & 0 & 0 \\ 0 & 1 & 0 & -1 & \vdots & 0 & 0 & 0 \\ 0 & 0 & 1 & -1 & \vdots & 0 & 0 & 0 \\ 0 & 0 & 0 & 1 & \vdots & 0 & 0 & 0 \\ \hdashline 0 & 0 & 0 & 0 & \vdots & 1 & 0 & -1 \\ 0 & 0 & 0 & 0 & \vdots & 0 & 1 & -1 \\ 0 & 0 & 0 & 0 & \vdots & 0 & 0 & 1 \end{bmatrix}$$

Therefore

$$\Delta \bar{V}_L = \begin{bmatrix} \Delta V_1 - \Delta V_4 \\ \Delta V_2 - \Delta V_4 \\ \Delta V_3 - \Delta V_4 \\ \Delta V_4 \\ \Delta V_5 - \Delta V_7 \\ \Delta V_6 - \Delta V_7 \\ \Delta V_7 \end{bmatrix}$$

and

$$\Delta \bar{Q}_L \stackrel{\Delta}{=} U \Delta Q_L = \begin{bmatrix} \Delta Q_1 \\ \Delta Q_2 \\ \Delta Q_3 \\ \sum_{i=1}^4 \Delta Q_i \\ \Delta Q_5 \\ \Delta Q_6 \\ \sum_{i=5}^7 \Delta Q_i \end{bmatrix}$$

The matrix  $U$  in (4.42) sums up rows 1, 2, 3, 4, and rows 5, 6, 7 of  $S_{Q_L V}$ , then put the result in row 4 and row 7, respectively. The matrix  $U^T$  in (4.42) sums up the columns 1, 2, 3, 4 and columns 5, 6, 7 of the preprocessed matrix  $[US_{Q_L V}]$ . The result of the equivalent sensitivity matrix  $\bar{S}_{Q_L V}$  given in Figure 4.3 carries the information about the global constraints on area-shunt-capacitance on columns and rows 4 and 7. All admittances of the lines that interconnect groups are eliminated from the (4,4) and (7,7) elements during this transformation. The only terms left on the equivalent diagonal elements are capacitances of that group, and the negative of the sum of total admittances of its boundary. Therefore, if the total shunt capacitance of that group exceeds the total admittances of its boundary, then the corresponding diagonal element will no longer dominate that row and column. Furthermore, the equivalent sensitivity matrix  $S_{Q_L V}$  is irreducible and symmetric. Since the original  $S_{Q_L V}$  is positive

$S_{11}$	$S_{12}$	$S_{13}$	$\sum_{j=1}^4 S_{1j}$	$S_{15}$	$S_{16}$	$\sum_{j=5}^7 S_{1j}$
$S_{21}$	$S_{22}$	$S_{23}$	$\sum_{j=1}^4 S_{2j}$	$S_{25}$	$S_{26}$	$\sum_{j=5}^7 S_{2j}$
$S_{31}$	$S_{32}$	$S_{33}$	$\sum_{j=1}^4 S_{3j}$	$S_{35}$	$S_{36}$	$\sum_{j=5}^7 S_{3j}$
$\sum_{i=1}^4 S_{i1}$	$\sum_{i=1}^4 S_{i2}$	$\sum_{i=1}^4 S_{i3}$	$\sum_{j=1}^4 \sum_{i=1}^4 S_{ij}$	$\sum_{i=1}^4 S_{i5}$	$\sum_{i=1}^4 S_{i6}$	$\sum_{j=5}^7 \sum_{i=1}^4 S_{ij}$
$S_{51}$	$S_{52}$	$S_{53}$	$\sum_{j=1}^4 S_{5j}$	$S_{55}$	$S_{56}$	$\sum_{j=5}^7 S_{5j}$
$S_{61}$	$S_{62}$	$S_{63}$	$\sum_{j=1}^4 S_{6j}$	$S_{65}$	$S_{66}$	$\sum_{j=5}^7 S_{6j}$
$\sum_{i=5}^7 S_{i1}$	$\sum_{i=5}^7 S_{i2}$	$\sum_{i=5}^7 S_{i3}$	$\sum_{j=1}^4 \sum_{i=5}^7 S_{ij}$	$\sum_{i=5}^7 S_{i5}$	$\sum_{i=5}^7 S_{i6}$	$\sum_{j=5}^7 \sum_{i=5}^7 S_{ij}$

Figure 4.3. The equivalent sensitivity matrix  $\bar{S}_{Q_L v}$ .

definite, then  $\bar{S}_{Q_L V}$  must be diagonally dominant to be an M-matrix. Therefore the sum of the area shunt capacitance must not exceed the total admittances of the weak boundary of that area for  $\bar{S}_{Q_L V}$  to be an M matrix and for the system to remain controllable, observable, and stable from Theorems 5-8.

Now it becomes very clear that the voltage stability problems are not simply caused by the lack of reactive sources in an SSC group, but also are caused by the wrong type of sources (capacitor banks). The installation of the capacitor banks as reactive sources is much cheaper than the generation of synchronous condensers. Therefore when the reactive supply or reserve is not sufficient to meet the demand, it is preferred to install more capacitor banks in that area without knowing the side effects to the whole system. In summarizing all theoretical results up to this point, it is understood that

(1) from the proof and identification of weak boundaries of Chapter 2, there are weak boundaries to prevent the transmission of reactive supply over long distances; and

(2) from sensitivity analysis of this chapter, the weaker the boundary around an SSC group the less the amount of area reactive supply can rely on the capacitor banks.

Now one may ask why a utility does not eliminate the weak boundaries of the system by requiring all utilities to be uniformly stiffly interconnected, such that there will be no weak boundaries. At

this point it might appear to be a good idea, but any contingency and even system operations may break the uniformity of the interconnections. The cost-benefit considerations and the impossibility of obtaining rights of way for such redundant transmission makes such an idea impossible for the EHV transmission grid, although it can be approximated on distribution networks. The following property will show that such a uniform connectivity will cause the singularity for the suggested system. By pivotal condensation and mathematical induction the following property can be proven.

Property: Let  $c \neq 0$  and  $d$  be constants and  $A$  be an  $n \times n$  matrix with  $a_{ij} = c$  and  $a_{ij} = d$  if  $i \neq j$ . Then

$$\det \{A\} = (c - d)^{n-1} (c + (n - 1)d)$$

From the above property,  $A$  will be singular if and only if  $c = d$  or  $d = -(1/(n - 1))c$ . Physically, this implies that an isolated, uniformly interconnected non-SSC group can lose controllability and observability under light conditions, due to its structural uniformity.

In conclusion, one has to live with the existing weak boundaries in the large scale power networks. The voltage problems can be solved by understanding the impact and interference of weak boundaries to the system controllability and observability. The next chapter will establish experimentally the theoretical results developed in this chapter.



CHAPTER 5

VOLTAGE STABILITY AND SECURITY EVALUATION  
ON THE 30 BUS NEW ENGLAND SYSTEM

5.1. Introduction

A methodology for determining and ranking weak transmission boundaries for phase, voltage, or current variations was developed in Chapter 2. The methodology was applied to a 30 bus New England test system in Chapter 3. Voltage controllability, observability, and voltage stability were defined in Chapter 4. A necessary condition for controllability and stability was shown to be that  $S_{Q_L V}$  be an M matrix and that  $S_{V E}$  be positive. A necessary condition for observability and stability was shown to be that  $S_{Q_G E}$  be an M matrix and that  $S_{Q_G Q_L}$  be a positive matrix. It was shown that a sufficient condition for  $S_{Q_G Q_L}$  to have zero columns and  $S_{V E}$  to have zero rows and thus violate the necessary conditions for observability and controllability is that there exist no reactive sources in a stiffly interconnected group of buses. It is thus clear that having determined the stiffly interconnected groups for any operating condition, sufficient reactive power reserve must be maintained in each group to accommodate load change and loss of reactive source contingencies. A further sufficient condition for voltage stability under light load conditions is that the shunt capacitive admittance at all buses in a stiffly interconnected group must not exceed the admittance of the

lines in the weak boundary connecting the group to other stiffly interconnected groups. This condition may well justify the utility's practice of switching out some of the long transmission lines with large shunt capacitance under light load conditions.

Line outage and loss of generation contingencies are simulated for the same 30 bus New England system model used in Chapter 2 to test the methodology for determining and ranking weak transmission boundaries. The results of these simulations using a Philadelphia Electric (PE) Load Flow are presented in Section 5.2. The bus voltages in each stiffly interconnected group respond similarly for each contingency. Line outages of elements in the weak voltage boundaries are shown to cause large voltage drops at buses in load groups and large voltage increases at buses in supply groups. Loss of generators in a load group with insufficient reactive supply is shown to cause the same large voltage drops in load groups and large voltage increases in the supply groups. These results confirm that sufficient reactive reserve must be maintained in each group for proper voltage control and that the weak transmission boundaries decouple the voltage controls (reactive sources) in one group from supplying load in another group (loss of voltage controllability). The results confirm that the need for reactive support will be observed and thus occur locally unless insufficient reactive resources exist in a stiffly interconnected group. The reactive requirements can be observed across weak boundaries if there is insufficient resources in a group and thus cause the large voltage variations across the weak boundaries.

The study, performed in subsections 5.3 and 5.4, is intended to show that adding shunt capacitance in a stiffly interconnected group can cause loss of controllability, observability, and stability for non light load condition, confirming the analysis performed in Chapter 4 for light load conditions. An experiment is performed where a stiffly interconnected group with a weak transmission boundary is forced to be reactive resource deficient due to loss of generation contingencies. Capacitive reactive support and load is simultaneously increased at a bus in this group. The results indicate that the voltages at buses drop with increased capacitive admittance until the loadflow no longer converges. Moreover, eigenvalues of the Jacobian rapidly decrease to zero from large positive values as the capacitive admittance is increased. The elements in the eigenvectors associated with these rapidly decreasing eigenvalues experience sign changes and magnitude changes for those elements in the group experiencing the voltage collapse. Thus the addition of capacitances for voltage support can actually weaken the boundary around the group, causing a voltage collapse and a loss of voltage controllability and observability induced stability.

## 5.2. The Systematic Impacts of the Weak Boundary to the Voltage Stability

The original New England System is very stable because each group in the system has sufficient reactive sources. In order to observe the voltage problems, two strategies are applied in this

section to simulate contingencies which will cause the voltage stability problems:

(1) loss of generation contingencies that cause one group to have insufficient reactive supply, which then causes complex power to flow over the weak transmission boundary; and

(2) line outage contingencies that remove elements in weak transmission boundaries, which further weaken these boundaries. Several line outage and loss of generation contingencies were simulated. The effects of line outages of elements in weak boundaries always had much greater security problems than outages of branches within stiffly interconnected bus groups.

Case 1 is a multiple loss of generation and line outage contingency that both affect stiffly interconnected group IV in Figure 5.1. The loss of generation leaves the group with insufficient reactive supply and the line outage weakens the transmission boundary for that group. Note that the results for this case, presented in Table 5.1, show low voltage violations at several buses in this group. Moreover, high voltage violations are observed at generator buses in groups I and II.

Case 2 is a multiple loss of generation contingency of generators 6 and 10 in stiffly interconnected group IV in Figure 5.1. Note that in this case all voltage in this stiffly interconnected group have low voltage violations and the generator buses in a neighboring group have high voltage violations.

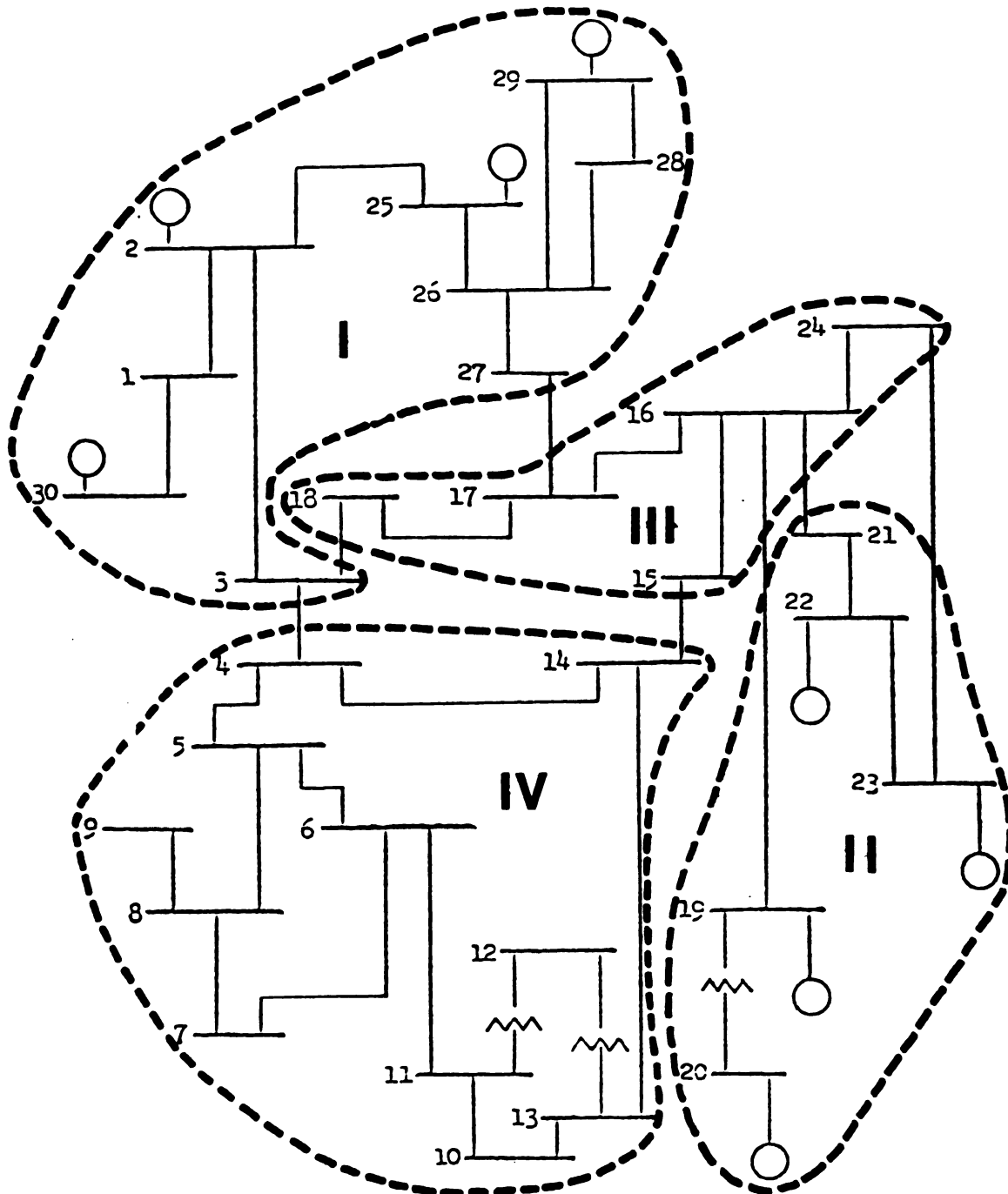


Figure 5.1. The four group partition based on reactive power disturbance and voltage rms coherency measure after generators 6 and 10 are removed.

Table 5.1. Summary of results for case 1.

---



---

<u>System configuration</u>	
Removed generator(s):	6
Removed line(s):	(4,3)
<u>Changes of load and shunt capacitance</u>	
Load:	none
Total:	N/A
Shunt capacitor(s);	none
<u>Abnormal voltages</u> ( $V < 0.95$ or $V > 1.05$ p.u.)	
Low:	$V_4 = 0.937$ $V_5 = 0.944$ $V_6 = 0.946$ $V_7 = 0.938$ $V_8 = 0.939$
High:	$V_{19} = 1.051$ $V_{22} = 1.051$ $V_{25} = 1.058$ $V_{29} = 1.051$

---

These results clearly show that buses in a stiffly connected group behave as a single bus for line outage and loss of generation contingencies. Furthermore, the large voltage variations across elements in the weak boundaries indicate that both a loss of voltage control and a loss of observability of the need for reactive support occur in these weak boundaries.

### 5.3. Local and Global Effects of Capacitance on Voltage Stability

The theoretical results in Chapter 4 indicate that under light load conditions a sufficient condition for voltage controllability requires that the magnitude of the shunt capacitance at any bus in a stiffly connected group be less than the admittance of all branches connected to that bus. Likewise, a sufficient condition for voltage controllability for light load conditions is that the sum of the admittance of all shunt capacitance in a stiffly connected group must be less than the sum of the admittance that connects this group to other groups and thus belongs to the weak boundary for that group. These results do not necessarily apply for non light load conditions.

A hypothesis, that replacing generation reactive support by capacitive reactive support can cause loss of voltage controllability and observability and lead to a voltage collapse, is tested. A special test case was developed to provide a test for the hypothesis. Generators 6 and 10 are removed from stiffly interconnected group IV in Figure 5.1. Generators 2, 25, and 29 make up for the lost real power generation evenly. Case 1 results in Table 5.1 suggest that these

generators also attempt to provide reactive support over the weak transmission boundary. Line (30,9) is removed to prevent the swing bus from directly supplying reactive support for group IV in Figure 5.1. The stiffly connected groups for this system were then recomputed and are given in Table 5.3 and Figure 5.1. The system at this point does not have sufficient reactive supply and the load-flow did not converge. A 600 MVAR shunt capacitor is placed at bus 11 in group 4 of Table 5.3 that should experience voltage problems. The capacitor is placed at bus 11 because it is located electrically between the buses where generators 6 and 10 were lost.

The summary of the abnormal voltages from the PE loadflow is shown in Table 5.4. There is no low voltage reported and the high voltages are right on their maximum desired limits, indicating that this case is normal.

Case 4 is shown in Table 5.5, where only a 500 MVAR shunt capacitor is inserted at bus 16. One low voltage is reported at bus 8, which indicates that group 4 has difficulty in importing reactive power across its weak boundary. At this point, the voltage problem still appears to be a local problem.

The results for Case 5 are shown in Table 5.6, where a smaller 400 MVAR capacitor is inserted. The voltage problem is spread over all the buses in group IV. It is clear from Cases 4-6 that the sensitivity to the capacitive reactive support appears to be large. Four cases were simulated with 700 MVAR, 800 MVAR, 900 MVAR, and 1000 MVAR capacitors, respectively. All of these cases have no low



Table 5.2. Summary of results for case 2.

---



---

<u>System configuration</u>				
Removed generator(s): 6, 10				
Removed line(s): none				
<u>Changes of load and shunt capacitance</u>				
Load: none				
Total: N/A				
Shunt capacitor(s): none				
<u>Abnormal Voltages</u> ( $V < 0.95$ or $V > 1.05$ p.u.)				
Low:	$V_4 = 0.917$	$V_5 = 0.909$	$V_6 = 0.908$	$V_7 = 0.902$
	$V_8 = 0.904$	$V_{10} = 0.914$	$V_{11} = 0.911$	$V_{12} = 0.897$
	$V_{13} = 0.917$	$V_{14} = 0.928$		
High:	$V_{19} = 1.051$	$V_{22} = 1.051$	$V_{25} = 1.058$	$V_{29} = 1.051$

---

Table 5.3. New groups obtained from the weak boundary identifications based on voltage measure.

---

---

Group 1

Generator(s): 2, 25, 29, 30

Load: 1, 3, 16, 27, 28

Group 2

Generator(s): 19, 20, 22, 23

Load: 21

Group 3

Generator(s): none

Load: 15, 16, 17, 18, 24

Group 4

Generator(s): none

Load: 4, 5, 6, 7, 8, 9, 10, 11, 12, 13, 14

---

Table 5.4. Summary of results for case 3.

---

---

<u>System configuration</u>			
Removed generator(s):	6, 10		
Removed line(s):	(30,9)		
<u>Changes of load and shunt capacitance</u>			
Load:	none		
Total:	N/A		
Shunt capacitor(s):	600 MVAR at bus 11		
<u>Abnormal voltages</u> ( $V < 0.95$ or $V > 1.05$ p.u.)			
Low:	none		
High:	$V_{19} = 1.051$	$V_{22} = 1.051$	$V_{25} = 1.058 \quad V_{29} = 1.051$

---

Table 5.5. Summary of results for case 4.

---

---

<u>System configuration</u>				
Removed generator(s):	6, 10			
Removed line(s):	(30,9)			
<u>Changes of load and shunt capacitance</u>				
Load:	none			
Total:	N/A			
Shunt capacitance:	500 MVAR at bus 11			
<u>Abnormal voltages</u> ( $V < 0.95$ or $V > 1.05$ p.u.)				
Low:	$V_8 = 0.948$			
High:	$V_{19} = 1.051$	$V_{22} = 1.051$	$V_{25} = 1.058$	$V_{29} = 1.051$

---

Table 5.6. Summary of results for case 5.

---

---

<u>System configuration</u>				
Removed generator(s):	6, 10			
Removed line(s):	(30,9)			
<u>Changes of load and shunt capacitance</u>				
Load:	none			
Total:	N/A			
Shunt capacitance:	400 MVAR at bus 11			
<u>Abnormal Voltages</u> ( $V < 0.95$ or $V > 1.05$ p.u.)				
Low:	$V_4 = 0.921$	$V_5 = 0.915$	$V_6 = 0.918$	$V_7 = 0.902$
	$V_8 = 0.899$	$V_9 = 0.905$	$V_{10} = 0.940$	$V_{11} = 0.941$
	$V_{12} = 0.924$	$V_{13} = 0.938$	$V_{14} = 0.938$	
High:	$V_{19} = 1.051$	$V_{22} = 1.051$	$V_{25} = 1.058$	$V_{29} = 1.051$

---

voltage reported, but all have several generator buses outside group 4 reach their upper voltage limits.

Case 4, where the 500 MVAR capacitor is insufficient to meet reactive load in group 4, is studied further to determine if increasing reactive power load and increasing capacitive reactive support at bus 11 can cause a weakening of the weak boundary between group 4 and the rest of the system. It was hypothesized that a loss of voltage stability and thus a voltage collapse as predicted in Theorem 11 for light load conditions would occur and this is confirmed in the following results. Case 4 is chosen to initiate the experiment because the low voltage at bus 8 indicates there is both insufficient reactive support within group 4 and a reliance reactive flow that crosses the weak transmission boundary.

Case 6 shows the loadflow results when 1250 MVAR of capacitive reactive support and 750 MVAR of reactive load injection are inserted at bus 11. Case 6 is identical to Case 4 in terms of having a net 500 MVAR of reactive support at bus 11. The results in Table 5.7 indicate that buses 4, 5, 6, 7, and 12 now have low voltage problems in addition to the low voltage at bus 8, which was also observed in Case 4. Several cases were run where the capacitive reactive support and reactive load injection at bus 11 were both increased in a manner that maintained a net 500 MVAR of reactive support. The PE loadflow failed to converge for all of these cases. These results from Cases 4, 6, and these additional cases indicate that capacitive reactive support in a stiffly interconnected group that is reactive resource

Table 5.7. Summary of results for Case 6.

---

---

<u>System configuration</u>				
Removed generator(s): 6, 10				
Removed line(s): (30,9)				
<u>Changes of load and shunt capacitance</u>				
Load:	750 MVAR at bus 11			
Total:	N/A			
Shunt capacitance:	1250 MVAR			
<u>Abnormal voltages:</u> ( $V < 0.95$ or $V > 1.05$ p.u.)				
Low:	$V_4 = 0.935$	$V_5 = 0.933$	$V_6 = 0.937$	$V_7 = 0.921$
	$V_8 = 0.918$	$V_{12} = 0.944$		
High:	$V_{19} = 1.051$	$V_{22} = 1.051$	$V_{25} = 1.058$	$V_{29} = 1.051$

---

deficient can cause a loss of controllability and observability across the weak transmission boundary that leads to voltage stability and voltage collapse. A stiffly interconnected group that had sufficient reactive support from 600 (Case 3) to 1000 MVAR of capacitance reactive power support did not have stability problems. Thus, it appears that capacitive support may only cause voltage stability problems when the group it has been inserted in still has insufficient reactive support and is also relying on weak transmission boundaries for support.

Case 6 shows that the voltage problem at bus 8 in Case 4 spreads over the entire group but the voltage at bus 11 can still be maintained within the desired range. It also indicates that the shunt capacitor solves the voltage problem at bus 11 locally, but the neighboring buses start to experience the low voltage problem.

In Chapters 2 and 3 the theory and the measures of weak boundary for a power system were developed, tested, and confirmed. In this chapter the effects of the weak boundary to the voltage stability are checked experimentally. Except for the base case, all the simulations are carried out under heavy load conditions. Using the same New England 30 bus model, a series of contingencies are simulated in section 5.2. It confirmed that the weak boundary will prevent the reactive power from being transferred from one SSC group to the other. Therefore the voltage problem can only be solved in the local area.



In this section and section 5.4 the effects of shunt capacitor under heavy load condition are investigated. In general, there are three sources of reactive power which can be used to support the voltage in the local area: (1) generators, (2) synchronous condensers, and (3) shunt capacitors. The costs of these different kinds of equipment are quite different and the shunt capacitor is the cheapest one among them. Since the side effects of the shunt capacitor were not well understood before this investigation, the system planner usually preferred to use the shunt capacitor as the supplemental device for reactive power supply for a local area. It is a widespread practice in the industry to install shunt capacitors as reactive supply to meet reactive load and support voltage in each local area.

The results obtained in this section can be further explained by the eigenvalue analysis of the sensitivity matrices in section 5.4. It will be shown that a large positive eigenvalue is reduced to nearly zero as the reactive load injection and capacitive supply are increased. The results obtained in this section are very important in today's power system planning and operations, because the system planners can easily concentrate on the fact that the capacitors can always keep the local bus within the desired voltage limit as it did in the above case at bus 11. When the system has a voltage collapse, it is really difficult to convince oneself that the capacitance at all-looks-normal bus 11 instead of some other factor caused the system collapse. Without the sensitivity analysis, eigenvalue

analysis combined with the identification of the weak boundary, the understanding of voltage problems for a large scale system is difficult. The sensitivity/eigenvalue analysis of Cases 3-6 is analyzed in the next subsection.

#### 5.4. The Effects of Shunt Capacitor on the Controllability and Observability of the Steady State Voltage Problem

The sensitivity matrices  $S_{QGE}$  and  $S_{QLV}$  are computed for Cases 3-6 and are displayed in Tables 5.8-5.11. The matrices are diagonally dominant and all the large elements lie in diagonally dominant blocks because the generator buses and load buses were reordered according to the buses in the four stiffly interconnected groups in Table 5.3. Thus, the ordering of buses in  $S_{QGE}$  is 2, 25, 29, 30, 19, 20, 22, 23. The  $S_{QGE}$  matrix has two diagonal sub-blocks of (2, 25, 29, 30) and (19, 20, 22, 23) which are the only two stiffly interconnected groups with PV (generator buses). The ordering of buses in  $S_{QLV}$  is (1, 3, 26, 27, 28), (21), (15, 16, 17, 18, 24), and (4, 5, 6, 7, 8, 9, 10, 11, 12, 13, 14), where the brackets represent the PQ (load) buses in the four stiffly interconnected groups in Table 5.3.

The eigenvalues and eigenvectors for the  $S_{QGE}$  and  $S_{QLV}$  matrices are also displayed in Tables 5.8-5.11 for Cases 3-6. In Case 3, with 600 MVAR capacitance, the  $S_{QLV}$  eigenvalue 6 in Table 5.8 is the smallest of the eigenvalues and has value 237. The largest elements of an eigenvector indicate the buses at which the eigenvalue has the most effect. Eigenvalue 6 has value .88 at bus 4 which lies in

Table 5.8a. Sensitivity matrix  $S_{Q_G^E}$  for Case 3.

Table 5.8b. Eigenvalues and eigenvectors of  $S_{Q_G^E}$  for Case 3.

Table 5.8a

```

      1      2      3      4      5      6      7      8
      1 111.16  81.88  12.24  18.06  4.88  00.00  -3.88  -1.83
      2 76.48  88.88  12.24  18.06  -1.22  00.00  00.00  00.00
      3 -3.10  12.88  21.11  15.48  00.00  00.00  00.00  00.00
      4 13.78  00.00  00.00  15.48  11.68  00.00  14.83  10.17
      5 3.84  -7.11  00.00  00.00  00.00  00.00  00.00  00.00
      6 00.00  00.00  00.00  00.00  00.00  00.00  00.00  00.00
      7 -2.41  00.00  00.00  00.00  00.00  00.00  00.00  00.00
      8 -1.84  00.00  00.00  00.00  00.00  00.00  00.00  00.00
      ***** MATRIX SQR *****

```

Table 5.8b

```

**EIGENVALUES**
      1 250.38.
**EIGENVECTORS**
      1 0011 188.88. 0011 121.81. 0011 00.00 0011 00.00 0011 00.00 0011 00.00
      2 0011 -74.00 0011 00.00 0011 00.00 0011 00.00 0011 00.00
      3 0011 00.00 0011 00.00 0011 00.00 0011 00.00 0011 00.00
      4 0011 -04.00 0011 00.00 0011 00.00 0011 00.00 0011 00.00
      5 0011 00.00 0011 00.00 0011 00.00 0011 00.00 0011 00.00
      6 0011 00.00 0011 00.00 0011 00.00 0011 00.00 0011 00.00
      7 0011 00.00 0011 00.00 0011 00.00 0011 00.00 0011 00.00
      8 0011 00.00 0011 00.00 0011 00.00 0011 00.00 0011 00.00

```

```

**EIGENVALUES**
      1 86.47.
**EIGENVECTORS**
      1 0011 14.24. 0011 00.00
      2 0011 00.00 0011 00.00
      3 0011 00.00 0011 00.00
      4 0011 00.00 0011 00.00
      5 0011 00.00 0011 00.00
      6 0011 00.00 0011 00.00
      7 0011 00.00 0011 00.00
      8 0011 00.00 0011 00.00

```

```

      1 0011 188.88. 0011 121.81. 0011 00.00 0011 00.00 0011 00.00 0011 00.00
      2 0011 -74.00 0011 00.00 0011 00.00 0011 00.00 0011 00.00
      3 0011 00.00 0011 00.00 0011 00.00 0011 00.00 0011 00.00
      4 0011 -04.00 0011 00.00 0011 00.00 0011 00.00 0011 00.00
      5 0011 00.00 0011 00.00 0011 00.00 0011 00.00 0011 00.00
      6 0011 00.00 0011 00.00 0011 00.00 0011 00.00 0011 00.00
      7 0011 00.00 0011 00.00 0011 00.00 0011 00.00 0011 00.00
      8 0011 00.00 0011 00.00 0011 00.00 0011 00.00 0011 00.00

```



**Table 5.8d. Eigenvalues and eigenvectors of  $S_{\mathbf{Q}_L \mathbf{V}}$  for Case 3.**

[illegible]

Table 5.8d (continued).

[illegible]

--EIGENVALUES--		20		21		22	
	18	19	20	21	22	23	24
--EIGENVECTORS--							
1	91	88	85	88	81	88	81
2	00	00	00	00	00	00	00
3	30	30	30	30	30	30	30
4	05	05	05	05	05	05	05
5	40	40	40	40	40	40	40
6	57	57	57	57	57	57	57
7	16	16	16	16	16	16	16
8	11	11	11	11	11	11	11
9	03	03	03	03	03	03	03
10	38	38	38	38	38	38	38
11	12	12	12	12	12	12	12
12	02	02	02	02	02	02	02
13	01	01	01	01	01	01	01
14	01	01	01	01	01	01	01
15	13	13	13	13	13	13	13
16	12	12	12	12	12	12	12
17	08	08	08	08	08	08	08
18	06	06	06	06	06	06	06
19	08	08	08	08	08	08	08
20	04	04	04	04	04	04	04
21	21	21	21	21	21	21	21
22	04	04	04	04	04	04	04

Table 5.9a. Sensitivity matrix  $S_{Q_E}$  for Case 4.

[illegible]

**Table 5.9b. Eigenvalues and eigenvectors of  $S_{QE}$  for Case 4.**

```

--EIGENVALUES--
      2      3      4      5      6      7
0011 175.91  0011 123.08  0011 2.87  0011 25.55  0011 88.51  0011
--EIGENVECTORS--
      280.48
0011 0011 77.00  0011 0011 0011 0011
0011 0011 08.00  0011 0011 0011 0011
0011 0011 01.00  0011 0011 0011 0011
0011 0011 00.00  0011 0011 0011 0011
0011 0011 00.00  0011 0011 0011 0011
0011 0011 02.00  0011 0011 0011 0011
0011 0011 00.00  0011 0011 0011 0011
0011 0011 00.00  0011 0011 0011 0011
0011 0011 72.00  0011 0011 0011 0011
0011 0011 68.00  0011 0011 0011 0011

```

```

**EIGENVALUES**
      ( 17 3
--EIGENVECTOR--
1      0.011      15.20      0.01
2      0.011      0.00      0.00
3      0.011      0.00      0.00
4      0.011      0.00      0.00
5      0.011      0.00      0.00
6      0.011      0.00      0.00
7      0.011      0.00      0.00
8      0.011      0.00      0.00

```



Table 5.9c. Sensitivity matrix  $S_{Q_LV}$  for Case 4.

1	68.54	1	2	3	4	5	6	7	8	9	10	11	12	13	14	15	16	17	18	19	20	21	22
2	0.00	166.72	0.00	0.00	0.00	0.00	0.00	0.00	0.00	0.00	0.00	0.00	0.00	0.00	0.00	0.00	0.00	0.00	0.00	0.00	0.00	0.00	
3	0.00	1.07	116.78	-2.02	0.00	0.00	0.00	0.00	0.00	0.00	0.00	0.00	0.00	0.00	0.00	0.00	0.00	0.00	0.00	0.00	0.00	0.00	
4	0.00	-2.42	-33.00	97.14	-40.17	19.16	0.00	-1.05	8.40	16.46	-73.78	-38.00	10.11	10.46	8.58	6.75	0.00	0.00	0.00	0.00	0.00	0.00	
5	0.00	0.07	17.55	4.56	0.00	4.48	0.00	3.74	-16.87	43.33	-18.57	2.38	2.01	0.07	-1.00	-1.00	0.00	0.00	0.00	0.00	0.00	0.00	
6	0.00	0.00	13.23	0.86	0.00	92.51	0.00	0.00	0.00	0.00	0.00	0.00	0.00	0.00	0.00	0.00	0.00	0.00	0.00	0.00	0.00		
7	0.00	0.00	-1.13	2.81	0.00	149.01	0.00	-7.12	74.55	-28.48	1.54	-4.57	-7.00	0.00	0.00	0.00	0.00	0.00	0.00	0.00	0.00		
8	0.00	0.00	7.83	-18.37	0.00	58.72	0.00	121.43	66.45	-48.20	5.56	-16.52	7.00	1.16	0.00	0.00	0.00	0.00	0.00	0.00	0.00		
9	0.00	0.00	15.31	46.59	0.00	72.07	0.00	80.78	416.55	-48.20	-27.20	-168.55	-2.24	0.86	0.00	0.00	0.00	0.00	0.00	0.00	0.00		
10	0.00	0.00	71.34	-18.55	0.00	3.12	0.00	-28.45	-44.42	188.32	-58.56	-18.22	-13.11	1.04	0.00	0.00	0.00	0.00	0.00	0.00	0.00		
11	0.00	0.00	0.00	1.87	0.00	-4.58	0.00	-15.58	-161.42	-18.56	3.50	184.75	-2.40	0.10	0.00	0.00	0.00	0.00	0.00	0.00	0.00		
12	0.00	0.00	0.00	0.00	0.00	0.00	0.00	-6.97	-6.31	-12.53	-3.35	184.75	1.28	0.20	0.00	0.00	0.00	0.00	0.00	0.00	0.00		
13	0.00	0.00	0.00	0.00	0.00	0.00	0.00	0.00	0.00	0.00	0.00	0.00	0.00	0.00	0.00	0.00	0.00	0.00	0.00	0.00	0.00		
14	0.00	0.00	0.00	0.00	0.00	0.00	0.00	0.00	0.00	0.00	0.00	0.00	0.00	0.00	0.00	0.00	0.00	0.00	0.00	0.00	0.00		
15	0.00	0.00	0.00	0.00	0.00	0.00	0.00	0.00	0.00	0.00	0.00	0.00	0.00	0.00	0.00	0.00	0.00	0.00	0.00	0.00	0.00		
16	0.00	0.00	0.00	0.00	0.00	0.00	0.00	0.00	0.00	0.00	0.00	0.00	0.00	0.00	0.00	0.00	0.00	0.00	0.00	0.00	0.00		
17	0.00	0.00	0.00	0.00	0.00	0.00	0.00	0.00	0.00	0.00	0.00	0.00	0.00	0.00	0.00	0.00	0.00	0.00	0.00	0.00	0.00		
18	0.00	0.00	0.00	0.00	0.00	0.00	0.00	0.00	0.00	0.00	0.00	0.00	0.00	0.00	0.00	0.00	0.00	0.00	0.00	0.00	0.00		
19	0.00	0.00	0.00	0.00	0.00	0.00	0.00	0.00	0.00	0.00	0.00	0.00	0.00	0.00	0.00	0.00	0.00	0.00	0.00	0.00	0.00		
20	0.00	0.00	0.00	0.00	0.00	0.00	0.00	0.00	0.00	0.00	0.00	0.00	0.00	0.00	0.00	0.00	0.00	0.00	0.00	0.00	0.00		
21	0.00	0.00	0.00	0.00	0.00	0.00	0.00	0.00	0.00	0.00	0.00	0.00	0.00	0.00	0.00	0.00	0.00	0.00	0.00	0.00	0.00		
22	0.00	0.00	0.00	0.00	0.00	0.00	0.00	0.00	0.00	0.00	0.00	0.00	0.00	0.00	0.00	0.00	0.00	0.00	0.00	0.00	0.00		

1	16	17	18	19	20	21	22
2	0.00	0.00	0.00	0.00	0.00	0.00	0.00
3	0.00	0.00	0.00	0.00	0.00	0.00	0.00
4	0.00	0.00	0.00	0.00	0.00	0.00	0.00
5	0.00	0.00	0.00	0.00	0.00	0.00	0.00
6	0.00	0.00	0.00	0.00	0.00	0.00	0.00
7	0.00	0.00	0.00	0.00	0.00	0.00	0.00
8	0.00	0.00	0.00	0.00	0.00	0.00	0.00
9	0.00	0.00	0.00	0.00	0.00	0.00	0.00
10	0.00	0.00	0.00	0.00	0.00	0.00	0.00
11	0.00	0.00	0.00	0.00	0.00	0.00	0.00
12	0.00	0.00	0.00	0.00	0.00	0.00	0.00
13	0.00	0.00	0.00	0.00	0.00	0.00	0.00
14	0.00	0.00	0.00	0.00	0.00	0.00	0.00
15	0.00	0.00	0.00	0.00	0.00	0.00	0.00
16	0.00	0.00	0.00	0.00	0.00	0.00	0.00
17	0.00	0.00	0.00	0.00	0.00	0.00	0.00
18	0.00	0.00	0.00	0.00	0.00	0.00	0.00
19	0.00	0.00	0.00	0.00	0.00	0.00	0.00
20	0.00	0.00	0.00	0.00	0.00	0.00	0.00
21	0.00	0.00	0.00	0.00	0.00	0.00	0.00
22	0.00	0.00	0.00	0.00	0.00	0.00	0.00

+\*\*\* MATRIX SOLV +\*\*\*

Table 5.9d. Eigenvalues and eigenvectors of  $S_{Q_L} v$  for Case 4.



Table 5.9d (cont'd.)

--EIGENVALUES--		13	14	15	16	17	18	19
--EIGENVECTORS--		13	14	15	16	17	18	19
1		61.48.	80.48.	125.86.	138.00.	188.07.	146.88.	001
2		001	001	001	001	001	001	001
3		001	001	001	001	001	001	001
4		001	001	001	001	001	001	001
5		001	001	001	001	001	001	001
6		001	001	001	001	001	001	001
7		001	001	001	001	001	001	001
8		001	001	001	001	001	001	001
9		001	001	001	001	001	001	001
10		001	001	001	001	001	001	001
11		001	001	001	001	001	001	001
12		001	001	001	001	001	001	001
13		001	001	001	001	001	001	001
14		001	001	001	001	001	001	001
15		001	001	001	001	001	001	001
16		001	001	001	001	001	001	001
17		001	001	001	001	001	001	001
18		001	001	001	001	001	001	001
19		001	001	001	001	001	001	001
20		001	001	001	001	001	001	001
21		001	001	001	001	001	001	001
22		001	001	001	001	001	001	001

--EIGENVALUES--		20	21	22	23	24	25	26
--EIGENVECTORS--		20	21	22	23	24	25	26
1		83.72.	153.87.	88.84.	1	001	001	001
2		001	001	001	001	001	001	001
3		001	001	001	001	001	001	001
4		001	001	001	001	001	001	001
5		001	001	001	001	001	001	001
6		001	001	001	001	001	001	001
7		001	001	001	001	001	001	001
8		001	001	001	001	001	001	001
9		001	001	001	001	001	001	001
10		001	001	001	001	001	001	001
11		001	001	001	001	001	001	001
12		001	001	001	001	001	001	001
13		001	001	001	001	001	001	001
14		001	001	001	001	001	001	001
15		001	001	001	001	001	001	001
16		001	001	001	001	001	001	001
17		001	001	001	001	001	001	001
18		001	001	001	001	001	001	001
19		001	001	001	001	001	001	001
20		001	001	001	001	001	001	001
21		001	001	001	001	001	001	001
22		001	001	001	001	001	001	001

Table 5.10a. Sensitivity matrix  $S_{Q_G^E}$  for Case 5.

Table 5.10b. Eigenvalues and eigenvectors of  $S_{Q_G^E}$  for Case 5.

Table 5.10a.

1	272.62	101.48	2	-2.30	15.75	4	5.85	5	-2.71	7	-2.71	8
2	15.18	88.28	3	-2.25	15.75	4	-1.72	5	1.88	7	1.88	8
3	15.24	5.88	4	20.28	13.07	5	-1.82	6	1.88	7	1.88	8
4	14.84	5.88	5	-20.42	-1.30	6	115.28	7	14.00	8	8.88	8
5	-28.42	-1.30	6	-2.15	15.75	7	15.00	8	14.00	8	8.88	8
6	-28.42	-1.30	7	15.00	15.75	8	14.51	8	14.00	8	8.88	8
7	15.43	84	8	1.87	15.75	8	14.51	8	14.00	8	8.88	8
8	15.06	71	8	1.87	15.75	8	14.51	8	14.00	8	8.88	8

\*\*\*\* MATRIX SSB \*\*\*\*\*

Table 5.10b.

1	282.48	121.77	2	88.82	55.52	3	21.30	4	21.30	5	21.30	6	21.30	7	21.30	8	21.30
2	88.82	121.77	3	21.30	55.52	4	21.30	5	21.30	6	21.30	7	21.30	8	21.30	9	21.30
3	21.30	55.52	4	21.30	55.52	5	21.30	6	21.30	7	21.30	8	21.30	9	21.30	10	21.30
4	21.30	55.52	5	21.30	55.52	6	21.30	7	21.30	8	21.30	9	21.30	10	21.30	11	21.30
5	21.30	55.52	6	21.30	55.52	7	21.30	8	21.30	9	21.30	10	21.30	11	21.30	12	21.30
6	21.30	55.52	7	21.30	55.52	8	21.30	9	21.30	10	21.30	11	21.30	12	21.30	13	21.30
7	21.30	55.52	8	21.30	55.52	9	21.30	10	21.30	11	21.30	12	21.30	13	21.30	14	21.30
8	21.30	55.52	9	21.30	55.52	10	21.30	11	21.30	12	21.30	13	21.30	14	21.30	15	21.30

1	12.28	15.05	2	15.05	15.05	3	15.05	4	15.05	5	15.05	6	15.05	7	15.05	8	15.05
2	15.05	15.05	3	15.05	15.05	4	15.05	5	15.05	6	15.05	7	15.05	8	15.05	9	15.05
3	15.05	15.05	4	15.05	15.05	5	15.05	6	15.05	7	15.05	8	15.05	9	15.05	10	15.05
4	15.05	15.05	5	15.05	15.05	6	15.05	7	15.05	8	15.05	9	15.05	10	15.05	11	15.05
5	15.05	15.05	6	15.05	15.05	7	15.05	8	15.05	9	15.05	10	15.05	11	15.05	12	15.05
6	15.05	15.05	7	15.05	15.05	8	15.05	9	15.05	10	15.05	11	15.05	12	15.05	13	15.05
7	15.05	15.05	8	15.05	15.05	9	15.05	10	15.05	11	15.05	12	15.05	13	15.05	14	15.05
8	15.05	15.05	9	15.05	15.05	10	15.05	11	15.05	12	15.05	13	15.05	14	15.05	15	15.05

Table 5.10c. Sensitivity matrix  $S_{Q_L V}$  for Case 5.

[illegible]

1	15	17	18	19	20	21	22
2	00	00	00	00	00	23	23
3	14	00	08	08	00	24	24
4	10	00	07	08	01	25	25
5	00	00	00	00	00	26	26
6	00	00	12	00	01	27	27
7	00	00	28	28	07	28	28
8	22	00	28	28	06	29	29
9	00	00	48	48	06	30	30
10	00	00	14	02	01	31	31
11	02	00	28	03	03	32	32
12	55	00	50	25	08	33	33
13	77	00	78	53	08	34	34
14	28	01	48	53	47	35	35
15	23	16	85	82	00	36	36
16	21	41	22	18	78	37	37
17	22	41	22	22	02	38	38
18	27	22	22	192	14	39	39
19	15	00	150	102	14	40	40
20	00	00	15	14	74	41	41
21	03	00	12	89	44	42	42
22	50	22	34	28	49	43	43
23	00	00	00	00	00	44	44
24	00	00	00	00	00	45	45
25	00	00	00	00	00	46	46
26	00	00	00	00	00	47	47
27	00	00	00	00	00	48	48
28	00	00	00	00	00	49	49
29	00	00	00	00	00	50	50
30	00	00	00	00	00	51	51
31	00	00	00	00	00	52	52
32	00	00	00	00	00	53	53
33	00	00	00	00	00	54	54
34	00	00	00	00	00	55	55
35	00	00	00	00	00	56	56
36	00	00	00	00	00	57	57
37	00	00	00	00	00	58	58
38	00	00	00	00	00	59	59
39	00	00	00	00	00	60	60
40	00	00	00	00	00	61	61
41	00	00	00	00	00	62	62
42	00	00	00	00	00	63	63
43	00	00	00	00	00	64	64
44	00	00	00	00	00	65	65
45	00	00	00	00	00	66	66
46	00	00	00	00	00	67	67
47	00	00	00	00	00	68	68
48	00	00	00	00	00	69	69
49	00	00	00	00	00	70	70
50	00	00	00	00	00	71	71
51	00	00	00	00	00	72	72
52	00	00	00	00	00	73	73
53	00	00	00	00	00	74	74
54	00	00	00	00	00	75	75
55	00	00	00	00	00	76	76
56	00	00	00	00	00	77	77
57	00	00	00	00	00	78	78
58	00	00	00	00	00	79	79
59	00	00	00	00	00	80	80
60	00	00	00	00	00	81	81
61	00	00	00	00	00	82	82
62	00	00	00	00	00	83	83
63	00	00	00	00	00	84	84
64	00	00	00	00	00	85	85
65	00	00	00	00	00	86	86
66	00	00	00	00	00	87	87
67	00	00	00	00	00	88	88
68	00	00	00	00	00	89	89
69	00	00	00	00	00	90	90
70	00	00	00	00	00	91	91
71	00	00	00	00	00	92	92
72	00	00	00	00	00	93	93
73	00	00	00	00	00	94	94
74	00	00	00	00	00	95	95
75	00	00	00	00	00	96	96
76	00	00	00	00	00	97	97
77	00	00	00	00	00	98	98
78	00	00	00	00	00	99	99
79	00	00	00	00	00	100	100
80	00	00	00	00	00	101	101
81	00	00	00	00	00	102	102
82	00	00	00	00	00	103	103
83	00	00	00	00	00	104	104
84	00	00	00	00	00	105	105
85	00	00	00	00	00	106	106
86	00	00	00	00	00	107	107
87	00	00	00	00	00	108	108
88	00	00	00	00	00	109	109
89	00	00	00	00	00	110	110
90	00	00	00	00	00	111	111
91	00	00	00	00	00	112	112
92	00	00	00	00	00	113	113
93	00	00	00	00	00	114	114
94	00	00	00	00	00	115	115
95	00	00	00	00	00	116	116
96	00	00	00	00	00	117	117
97	00	00	00	00	00	118	118
98	00	00	00	00	00	119	119
99	00	00	00	00	00	120	120
100	00	00	00	00	00	121	121
101	00	00	00	00	00	122	122
102	00	00	00	00	00	123	123
103	00	00	00	00	00	124	124
104	00	00	00	00	00	125	125
105	00	00	00	00	00	126	126
106	00	00	00	00	00	127	127
107	00	00	00	00	00	128	128
108	00	00	00	00	00	129	129
109	00	00	00	00	00	130	130
110	00	00	00	00	00	131	131
111	00	00	00	00	00	132	132
112	00	00	00	00	00	133	133
113	00	00	00	00	00	134	134
114	00	00	00	00	00	135	135
115	00	00	00	00	00	136	136
116	00	00	00	00	00	137	137
117	00	00	00	00	00	138	138
118	00	00	00	00	00	139	139
119	00	00	00	00	00	140	140
120	00	00	00	00	00	141	141
121	00	00	00	00	00	142	142
122	00	00	00	00	00	143	143
123	00	00	00	00	00	144	144
124	00	00	00	00	00	145	145
125	00	00	00	00	00	146	146
126	00	00	00	00	00	147	147
127	00	00	00	00	00	148	148
128	00	00	00	00	00	149	149
129	00	00	00	00	00	150	150
130	00	00	00	00	00	151	151
131	00	00	00	00	00	152	152
132	00	00	00	00	00	153	153
133	00	00	00	00	00	154	154
134	00	00	00	00	00	155	155
135	00	00	00	00	00	156	156
136	00	00	00	00	00	157	157
137	00	00	00	00	00	158	158
138	00	00	00	00	00	159	159
139	00	00	00	00	00	160	160
140	00	00	00	00	00	161	161
141	00	00	00	00	00	162	162
142	00	00	00	00	00	163	163
143	00	00	00	00	00	164	164
144	00	00	00	00	00	165	165
145	00	00	00	00	00	166	166
146	00	00	00	00	00	167	167
147	00	00	00	00	00	168	168
148	00	00	00	00	00	169	169
149	00	00	00	00	00	170	170
150	00	00	00	00	00	171	171
151	00	00	00	00	00	172	172
152	00	00	00	00	00	173	173
153	00	00	00	00	00	174	174
154	00	00	00	00	00	175	175
155	00	00	00	00	00	176	176
156	00	00	00	00	00	177	177
157	00	00	00	00	00	178	178
158	00	00	00	00	00	179	179
159	00	00	00	00	00	180	180
160	00	00	00	00	00	181	181
161	00	00	00	00	00	182	182
162	00	00	00	00	00	183	183
163	00	00	00	00	00	184	184
164	00	00	00	00	00	185	185
165	00	00	00	00	00	186	186
166	00	00	00	00	00	187	187
167	00	00	00	00	00	188	188
168	00	00	00	00	00	189	189
169	00	00	00	00	00	190	190
170	00	00	00	00	00	191	191
171	00	00	00	00	00	192	192
172	00	00	00	00	00	193	193
173	00	00	00	00	00	194	194
174	00	00	00	00	00	195	195
175	00	00	00	00	00	196	196
176	00	00	00	00	00	197	197
177	00	00	00	00	00	198	198
178	00	00	00	00	00	199	199
179	00	00	00	00	00	200	200
180	00	00	00	00	00	201	201
181	00	00	00	00	00	202	202
182	00	00	00	00	00	203	203
183	00	00	00	00	00	204	204
184	00	00	00	00	00	205	205
185	00	00	00	00	00	206	206
186	00	00	00	00	00	207	207
187	00	00	00	00	00	208	208
188	00	00	00	00	00	209	209
189	00	00	00	00	00	210	210
190	00	00	00	00	00	211	211
191	00	00	00	00	00	212	212
192	00	00	00	00	00	213	213
193	00	00	00	00	00	214	214
194	00	00	00	00	00	215	215
195	00	00	00	00	00	216	216
196	00	00	00	00	00	217	217
197	00	00	00	00	00	218	218
198	00	00	00	00	00	219	219
199	00	00	00	00	00	220	220
200	00	00	00	00	00	221	221
201	00	00	00	00	00</		

[illegible][illegible]



Table 5.10d (continued).

--EIGENVALUES--		14		15		16		17		18	
	12	13	14	15	16	17	18	19	20	21	22
--EIGENVECTORS--											
1	55.09	0.01	189.67	0.01	138.24	0.01	184.03	0.01	188.32	0.01	103.55
2	14	0.01	0.0	0.01	0.0	0.01	0.0	0.01	0.0	0.01	0.0
3	10	0.01	0.7	0.01	0.8	0.01	22	0.01	0.8	0.01	2
4	26	0.01	0.1	0.01	0.4	0.01	57	0.01	27	0.01	3
5	47	0.01	0.2	0.01	0.8	0.01	1	0.01	38	0.01	1
6	0.3	0.01	0.0	0.01	0.2	0.01	24	0.01	1	0.01	1
7	18	0.01	37	0.01	32	0.01	55	0.01	24	0.01	2
8	11	0.01	10	0.01	14	0.01	11	0.01	26	0.01	4
9	24	0.01	0.6	0.01	0.1	0.01	0.4	0.01	0.2	0.01	2
10	32	0.01	0.1	0.01	17	0.01	0.6	0.01	21	0.01	1
11	25	0.01	10	0.01	11	0.01	0.3	0.01	1	0.01	2
12	15	0.01	16	0.01	61	0.01	18	0.01	13	0.01	4
13	18	0.01	42	0.01	24	0.01	0.7	0.01	0.2	0.01	0.6
14	14	0.01	14	0.01	14	0.01	0.8	0.01	0.1	0.01	10
15	0.2	0.01	46	0.01	28	0.01	0.8	0.01	0.1	0.01	0.3
16	12	0.01	18	0.01	10	0.01	0.3	0.01	0.8	0.01	0.1
17	0.6	0.01	0.3	0.01	0.2	0.01	0.1	0.01	0.2	0.01	0.2
18	23	0.01	29	0.01	0.0	0.01	0.7	0.01	0.2	0.01	1.6
19	25	0.01	22	0.01	33	0.01	11	0.01	10	0.01	3.0
20	48	0.01	0.6	0.01	0.0	0.01	0.7	0.01	0.7	0.01	0.1
21	0.2	0.01	15	0.01	28	0.01	0.2	0.01	13	0.01	1.1
22	16	0.01	0.7	0.01	0.0	0.01	0.0	0.01	0.8	0.01	2.0

...EIGENVALUES...		19		20		21		22	
EIGENVECTORS...		86.22		86.88		88.63		89.27	
1	0	0.01	0.00	0.01	0.00	0.01	0.00	0.01	0.00
2	0	0.01	0.00	0.01	0.00	0.01	0.00	0.01	0.00
3	0	0.01	0.00	0.01	0.00	0.01	0.00	0.01	0.00
4	0	0.01	0.00	0.01	0.00	0.01	0.00	0.01	0.00
5	0	0.01	0.00	0.01	0.00	0.01	0.00	0.01	0.00
6	0	0.01	0.00	0.01	0.00	0.01	0.00	0.01	0.00
7	0	0.01	0.00	0.01	0.00	0.01	0.00	0.01	0.00
8	0	0.01	0.00	0.01	0.00	0.01	0.00	0.01	0.00
9	0	0.01	0.00	0.01	0.00	0.01	0.00	0.01	0.00
10	0	0.01	0.00	0.01	0.00	0.01	0.00	0.01	0.00
11	0	0.01	0.00	0.01	0.00	0.01	0.00	0.01	0.00
12	0	0.01	0.00	0.01	0.00	0.01	0.00	0.01	0.00
13	0	0.01	0.00	0.01	0.00	0.01	0.00	0.01	0.00
14	0	0.01	0.00	0.01	0.00	0.01	0.00	0.01	0.00
15	0	0.01	0.00	0.01	0.00	0.01	0.00	0.01	0.00
16	0	0.01	0.00	0.01	0.00	0.01	0.00	0.01	0.00
17	0	0.01	0.00	0.01	0.00	0.01	0.00	0.01	0.00
18	0	0.01	0.00	0.01	0.00	0.01	0.00	0.01	0.00
19	0	0.01	0.00	0.01	0.00	0.01	0.00	0.01	0.00
20	0	0.01	0.00	0.01	0.00	0.01	0.00	0.01	0.00
21	0	0.01	0.00	0.01	0.00	0.01	0.00	0.01	0.00
22	0	0.01	0.00	0.01	0.00	0.01	0.00	0.01	0.00

Table 5.11a. Sensitivity matrix  $S_{Q_G^E}$  for Case 6.

Table 5.11b. Eigenvalues and eigenvectors of  $S_{Q_G^E}$  for Case 6.

Table 5.11a.

1	1365.08	124.47	2	19.91	19.17	5	16.17	6	00	-2.00	7	00	28
2	-80.88	97.01	3	00	-3.17	6	-3.17	7	00	1.10	8	00	28
3	106.38	10.88	4	13.48	00	13.48	00	00	00	1.00	9	00	28
4	13.53	00	5	00	115.08	115.08	115.08	14.23	14.23	00	10	00	28
5	-180.12	-4.27	6	00	18.03	18.03	18.03	15.13	15.13	00	144.23	-120.83	133.51
6	00	00	7	86.70	2.84	-6.2	00	00	00	00	00	00	00
7	47.06	1.41	8	00	00	00	00	00	00	00	00	00	00
8	00	00	9	00	00	00	00	00	00	00	00	00	00
***** MATRIX SQR *****													

Table 5.11b.

--EIGENVALUES--																			
{ 1352.42																			
--EIGENVECTORS--																			
1	88	0011	280.38	2	0011	121.67	3	0011	106.85	4	0011	96.51	5	0011	20.88	6	0011	0011	0011
2	06	0011	00	00	0011	00	00	0011	00	00	0011	00	00	0011	00	00	0011	0011	0011
3	04	0011	00	00	0011	00	00	0011	00	00	0011	00	00	0011	00	00	0011	0011	0011
4	01	0011	00	00	0011	00	00	0011	00	00	0011	00	00	0011	00	00	0011	0011	0011
5	12	0011	00	00	0011	00	00	0011	00	00	0011	00	00	0011	00	00	0011	0011	0011
6	00	0011	00	00	0011	00	00	0011	00	00	0011	00	00	0011	00	00	0011	0011	0011
7	07	0011	72	00	0011	00	00	0011	00	00	0011	00	00	0011	00	00	0011	0011	0011
8	03	0011	89	00	0011	13	00	0011	15	0011	00	00	0011	00	00	0011	0011	0011	0011

1	15.18	7	0011	13.40	8	0011	0011	0011
2	00	0011	00	00	0011	00	0011	0011
3	00	0011	00	00	0011	00	0011	0011
4	00	0011	00	00	0011	00	0011	0011
5	00	0011	00	00	0011	00	0011	0011
6	00	0011	00	00	0011	00	0011	0011
7	00	0011	00	00	0011	00	0011	0011
8	00	0011	00	00	0011	00	0011	0011

Table 5.11c. Sensitivity matrix  $S_{Q_L V}$  for Case 6.

[illegible]

1	16	00	00	17	16	18	20	21	22
2	75	00	00	00	71	-4	00	00	106
3	00	00	00	00	02	01	00	00	08
4	00	00	00	00	07	-04	01	00	21
5	00	00	00	00	00	00	00	00	01
6	00	00	00	00	13	08	01	00	27
7	08	00	00	00	151	84	00	00	40
8	08	00	00	00	238	37	00	00	148
9	01	00	00	00	07	00	00	00	85
10	01	00	00	00	00	00	00	00	52
11	01	00	00	00	23	08	02	104	71
12	57	00	00	00	57	18	58	20	37
13	78	00	00	00	57	18	08	358	77
14	24	00	00	00	00	00	00	00	00
15	24	00	01	01	87	5	475	272	15
16	18	23	00	00	00	52	04	30	7
17	23	25	-23	37	14	-11	00	01	45
18	23	25	23	37	14	-11	00	01	30
19	80	00	00	00	245	48	00	00	00
20	80	00	00	00	188	47	14	17	37
21	-75	00	00	00	153	00	18	03	35
22	00	00	00	00	117	18	28	84	24
23	00	00	00	00	117	18	28	84	24
24	00	00	00	00	13	00	12	03	87
25	00	00	00	00	13	00	12	03	87
26	00	00	00	00	13	00	12	03	87
27	00	00	00	00	13	00	12	03	87
28	00	00	00	00	13	00	12	03	87
29	00	00	00	00	13	00	12	03	87
30	00	00	00	00	13	00	12	03	87
31	00	00	00	00	13	00	12	03	87
32	00	00	00	00	13	00	12	03	87
33	00	00	00	00	13	00	12	03	87
34	00	00	00	00	13	00	12	03	87
35	00	00	00	00	13	00	12	03	87
36	00	00	00	00	13	00	12	03	87
37	00	00	00	00	13	00	12	03	87
38	00	00	00	00	13	00	12	03	87
39	00	00	00	00	13	00	12	03	87
40	00	00	00	00	13	00	12	03	87
41	00	00	00	00	13	00	12	03	87
42	00	00	00	00	13	00	12	03	87
43	00	00	00	00	13	00	12	03	87
44	00	00	00	00	13	00	12	03	87
45	00	00	00	00	13	00	12	03	87
46	00	00	00	00	13	00	12	03	87
47	00	00	00	00	13	00	12	03	87
48	00	00	00	00	13	00	12	03	87
49	00	00	00	00	13	00	12	03	87
50	00	00	00	00	13	00	12	03	87
51	00	00	00	00	13	00	12	03	87
52	00	00	00	00	13	00	12	03	87
53	00	00	00	00	13	00	12	03	87
54	00	00	00	00	13	00	12	03	87
55	00	00	00	00	13	00	12	03	87
56	00	00	00	00	13	00	12	03	87
57	00	00	00	00	13	00	12	03	87
58	00	00	00	00	13	00	12	03	87
59	00	00	00	00	13	00	12	03	87
60	00	00	00	00	13	00	12	03	87
61	00	00	00	00	13	00	12	03	87
62	00	00	00	00	13	00	12	03	87
63	00	00	00	00	13	00	12	03	87
64	00	00	00	00	13	00	12	03	87
65	00	00	00	00	13	00	12	03	87
66	00	00	00	00	13	00	12	03	87
67	00	00	00	00	13	00	12	03	87
68	00	00	00	00	13	00	12	03	87
69	00	00	00	00	13	00	12	03	87
70	00	00	00	00	13	00	12	03	87
71	00	00	00	00	13	00	12	03	87
72	00	00	00	00	13	00	12	03	87
73	00	00	00	00	13	00	12	03	87
74	00	00	00	00	13	00	12	03	87
75	00	00	00	00	13	00	12	03	87
76	00	00	00	00	13	00	12	03	87
77	00	00	00	00	13	00	12	03	87
78	00	00	00	00	13	00	12	03	87
79	00	00	00	00	13	00	12	03	87
80	00	00	00	00	13	00	12	03	87
81	00	00	00	00	13	00	12	03	87
82	00	00	00	00	13	00	12	03	87
83	00	00	00	00	13	00	12	03	87
84	00	00	00	00	13	00	12	03	87
85	00	00	00	00	13	00	12	03	87
86	00	00	00	00	13	00	12	03	87
87	00	00	00	00	13	00	12	03	87
88	00	00	00	00	13	00	12	03	87
89	00	00	00	00	13	00	12	03	87
90	00	00	00	00	13	00	12	03	87
91	00	00	00	00	13	00	12	03	87
92	00	00	00	00	13	00	12	03	87
93	00	00	00	00	13	00	12	03	87
94	00	00	00	00	13	00	12	03	87
95	00	00	00	00	13	00	12	03	87
96	00	00	00	00	13	00	12	03	87
97	00	00	00	00	13	00	12	03	87
98	00	00	00	00	13	00	12	03	87
99	00	00	00	00	13	00	12	03	87
100	00	00	00	00	13	00	12	03	87

Table 5.11d. Eigenvalues and eigenvectors of  $S_{Q_L} v$  for Case 6.

EIGENVALUES		EIGENVECTORS		EIGENVALUES		EIGENVECTORS		EIGENVALUES		EIGENVECTORS		EIGENVALUES		EIGENVECTORS	
1	789.78	1	0011	2	532.07	1	0011	3	484.83	1	0011	4	378.10	1	0011
2	00	2	0011	2	00	2	0011	3	00	2	0011	4	00	2	0011
3	01	3	0011	3	01	3	0011	4	01	3	0011	5	01	3	0011
4	00	4	0011	4	00	4	0011	5	00	4	0011	6	00	4	0011
5	00	5	0011	5	00	5	0011	6	00	5	0011	7	00	5	0011
6	00	6	0011	6	00	6	0011	7	00	6	0011	8	00	6	0011
7	00	7	0011	7	00	7	0011	8	00	7	0011	9	00	7	0011
8	00	8	0011	8	00	8	0011	9	00	8	0011	10	00	8	0011
9	00	9	0011	9	00	9	0011	10	00	9	0011	11	00	9	0011
10	00	10	0011	10	00	10	0011	11	00	10	0011	12	00	10	0011
11	00	11	0011	11	00	11	0011	12	00	11	0011	13	00	11	0011
12	00	12	0011	12	00	12	0011	13	00	12	0011	14	00	12	0011
13	00	13	0011	13	00	13	0011	14	00	13	0011	15	00	13	0011
14	00	14	0011	14	00	14	0011	15	00	14	0011	16	00	14	0011
15	00	15	0011	15	00	15	0011	16	00	15	0011	17	00	15	0011
16	00	16	0011	16	00	16	0011	17	00	16	0011	18	00	16	0011
17	00	17	0011	17	00	17	0011	18	00	17	0011	19	00	17	0011
18	00	18	0011	18	00	18	0011	19	00	18	0011	20	00	18	0011
19	00	19	0011	19	00	19	0011	20	00	19	0011	21	00	19	0011
20	00	20	0011	20	00	20	0011	21	00	20	0011	22	00	20	0011
21	00	21	0011	21	00	21	0011	22	00	21	0011	23	00	21	0011
22	00	22	0011	22	00	22	0011	23	00	22	0011	24	00	22	0011

Table 5.11d (continued).

**EIGENVALUES**		13	14	15	16	17	18	
EIGENVECTORS**		183 55	108 85	137 22	158 04	83 12	85 81	
1		00	00	00	00	00	00	00
2		00	00	00	00	00	00	00
3		00	00	00	00	00	00	00
4		00	00	00	00	00	00	00
5		00	00	00	00	00	00	00
6		00	00	00	00	00	00	00
7		00	00	00	00	00	00	00
8		00	00	00	00	00	00	00
9		00	00	00	00	00	00	00
10		00	00	00	00	00	00	00
11		00	00	00	00	00	00	00
12		00	00	00	00	00	00	00
13		00	00	00	00	00	00	00
14		00	00	00	00	00	00	00
15		00	00	00	00	00	00	00
16		00	00	00	00	00	00	00
17		00	00	00	00	00	00	00
18		00	00	00	00	00	00	00
19		00	00	00	00	00	00	00
20		00	00	00	00	00	00	00
21		00	00	00	00	00	00	00
22		00	00	00	00	00	00	00

**EIGENVALUES**		19	20	21	22	
EIGENVECTORS**		184 18	149 60	93 08	88 41	
1		00	00	00	00	00
2		00	00	00	00	00
3		00	00	00	00	00
4		00	00	00	00	00
5		00	00	00	00	00
6		00	00	00	00	00
7		00	00	00	00	00
8		00	00	00	00	00
9		00	00	00	00	00
10		00	00	00	00	00
11		00	00	00	00	00
12		00	00	00	00	00
13		00	00	00	00	00
14		00	00	00	00	00
15		00	00	00	00	00
16		00	00	00	00	00
17		00	00	00	00	00
18		00	00	00	00	00
19		00	00	00	00	00
20		00	00	00	00	00
21		00	00	00	00	00
22		00	00	00	00	00

group IV which has the voltage collapse. In Case 4 with 500 MVAR capacitance, the eigenvalue 6 has value of only 2.20 and the eigenvector 6 no longer has a large element value (.88) at only bus 4 at group 4, but now has moderately large values 11-40 at all buses in group 4 except bus 11. In Case 5 with 400 MVAR of capacitance, the eigenvalue 6 drops further and the magnitude of the elements for the eigenvector increases at all buses in group 4 except at bus 4, which originally had the large dominant value in these eigenvectors. The value of the eigenvector element for bus 11 is still small. In Case 6, with the 1250 MVAR capacitance and 750 reactive load, the eigenvalue decreases to 0.13 but the eigenvector for eigenvalue 6 is similar to the values in Case 5. It is evident that reducing the capacitive reactive support in Cases 3-5 causes reliance on the weak transmission boundary and thus causes a weakening of this boundary as evidenced by:

- (1) A large reduction in the magnitude of eigenvalue 6.
- (2) A significant increase in the magnitude of the elements of the eigenvector for eigenvalue 6 at all buses in group 4 except buses 4 and 11. Bus 11 with the capacitance is no longer part of the group since its voltage is maintained by the capacitance. The increase in eigenvalue elements at all other buses in group 4 except bus 11 indicates eigenvalue 6 becomes a group against group eigenvalue rather than a local bus 4 eigenvalue. The evolution of group eigenvalues reflects the fact that the reactive flows so weaken the boundary of the group that it effectively acts as an equivalent bus.

(3) The sign of elements in eigenvector 6 in group 4 changes sign, indicating that eigenvalue 6 is destabilizing the network as the boundary is weakened.

In Cases 3-5 the addition of capacitance and reactive load injection confirms that adding capacitance in the group and retaining the reliance on reactive support across the boundary reduces eigenvalue from approximately 2.2 to 0.13 from results in Cases 4 and 6. Moreover, adding this capacitance and load simultaneously also increases the magnitude of elements in group 4. Both of these results indicate the addition of capacitance in a group with a weak boundary significantly weakens the boundary and causes the group to act as a single equivalent bus. Further additions of capacitance in this group would appear to cause the eigenvalue 6 to go negative and the elements of eigenvector 6 in group IV to further increase. These results were not obtained because the PE loadflow did not converge for the cases run with additional capacitance and load at bus 11.

The  $S_{QGE}$  eigenvalues 4, 5, and 8 experience major changes as capacitance is added in Cases 3-6 in Tables 5.3-5.8. The eigenvalue 4 decreases initially as the capacitance is decreased from 600 MVAR to 500 MVAR in Cases 3 and 4. However, all three eigenvalues increase rapidly for Cases 5 and 6, where the boundary is weakened due to additional flows across the boundary or additional capacitive reactive support, respectively. Eigenvector 4 has large values at generators 25 and 19. Eigenvector 5 has a large element at 19, and eigenvector 8 has a large element at 22, all of which



experience high voltages in Cases 5 and 6. Thus, the effect of capacitance at bus 11 in group 4 has an effect on the  $S_{QGE}$  even when there are no generators in group 4 because the weakened boundaries raise voltages at generators in other groups. This raise in voltage at generator buses in other groups is effected by increases in the eigenvalues that have eigenvectors with large components at these generator buses.

A loss of observability and stability is thus evidenced by the increases in eigenvalues in  $S_{QGE}$  and the increases in elements of the associated eigenvectors at generator buses that experience high voltage problem.

## CHAPTER 6

### CONCLUSIONS AND RECOMMENDATIONS FOR FUTURE RESEARCH

#### 6.1. Review

The existence and location of weak transmission boundaries is well known to utility system planners and operators based on their years of experience with a particular system. Formal methods for determining the location of weak transmission boundaries, ranking the relative vulnerability of the boundary, and determining the transmission elements that belong to the weak transmission boundaries did not exist.

A method for determining and ranking weak phase transmission boundaries was recently developed in [1]. These weak phase transmission boundaries were shown to cause phase oscillations and thermal and steady state stability problems for either inertial loadflow simulated loss of generation contingencies or line outage contingencies. A computer package was developed that allowed ranking of the network branches in terms of their impact on either thermal security or based on steady state stability. Contingencies that most severely affect each of the most vulnerable network branches are also determined as part of this package [1].

This thesis extends these previous results by defining weak transmission boundaries for voltage and for current variations. The

groups of buses within a stiffly interconnected group surrounded by a weak voltage transmission boundary will be a voltage control area. The weak voltage and weak current transmission boundaries should be those boundaries across which large voltage variations occur and large current changes that lead to thermal overload occur. The weak phase transmission boundaries defined in [1] should determine the network branches and boundaries where steady state stability problems should occur.

A phase, voltage, and current coherency measure is proposed and theoretically shown to detect the weak phase, voltage, and current transmission boundaries. A method for determining and ranking weak phase, voltage, and current transmission boundaries was developed and was applied to the 30 bus New England System model. Weak phase, voltage, and current transmission boundaries were determined and ranked. The current and phase boundaries are similar but the ranking of the boundaries is different. The weak voltage boundaries are quite different from either the phase or current boundaries and separate buses into local voltage control areas as would be expected from engineering judgment.

Voltage controllability, observability, and stability are defined in section 4. Necessary conditions on the properties of sensitivity matrices  $S_{VE}$ ,  $S_{QLV}$ ,  $S_{QGE}$ , and  $S_{QGQL}$  were found that assure voltage controllability, observability, and stability. Finally, it was shown that lack of PV (reactive sources) buses in any stiffly interconnected group is a sufficient condition for a loss of voltage

controllability or observability. A sufficient condition for loss of stability for light load conditions is that the shunt capacitive admittance at all buses in a stiffly interconnected group exceed the admittance of all branches in the weak transmission boundary that surrounds the group. These results suggest that sufficient reactive reserve must be maintained in each control area since relying on reactive support across weak transmission boundaries can cause a loss of voltage controllability and observability that may lead to voltage collapse. Moreover, the percentage of reactive support and reactive reserve in any control area made up of switchable shunt capacitance should be limited depending on the weakness or possible contingency induced weakness of the voltage transmission boundary. Thus the more expensive synchronous condensers may have to be used rather than switchable capacitors as is the present practice when insufficient generation reactive support is available in a stiffly connected group. Long transmission lines with large shunt capacitance may also need to be switched out under light load conditions to avoid having total shunt capacitance in a stiffly connected group exceed the admittance of the weak boundaries for that group. A further sufficient condition requires the network to be nonuniform since if all buses in a group are connected together by nearly identical branch elements, a loss of stability can occur. This could occur on a power system distribution network where all buses are often interconnected by nearly identical transmission elements.

The simulation of multiple loss of generation and line outage contingencies confirms that buses in a stiffly connected group behave similarly and that large voltage variations occur across weak boundaries. These results confirm that weak transmission boundaries cause voltage security problems due to loss of voltage controllability and observability. A loss of voltage stability is then shown to occur for a network where a group has weak transmission boundaries. The greater the reliance on the boundary for reactive support the greater and more widespread the low voltage problem is within the group. This reduction in the magnitude of eigenvalues, the increase in magnitude of elements of the associated eigenvectors within the group experiencing low voltage problems, and the sign change of elements of eigenvectors for buses in the group all indicate that requiring additional reactive power flow across weak boundaries will lead to loss of voltage stability and thus voltage collapse. Addition of capacitance in the stiffly connected group in a like manner caused dramatic reduction of positive eigenvalues, an increase in the magnitude of elements for buses in the group, and finally a decrease of voltage at buses in the group. The loadflow would not converge if too much capacitive admittance was inserted. The results clearly confirm that reactive flows across weak transmission boundaries and capacitive support within the stiffly interconnected group can both cause loss of voltage controllability and loss of observability, voltage security problems, and ultimately voltage collapse.

## 6.2. Recommendations for Future Research

Future research on voltage stability and security problems could:

(1) Determine whether the constraints on the shunt capacitive admittance in stiffly interconnected group developed for light load conditions can be applied or modified for non light load conditions.

(2) Define phase controllability, observability, and stability in a similar manner as performed for voltage and determine necessary conditions for phase controllability, observability, and stability.

(3) Determine sufficient conditions that assure phase and voltage controllability, observability, and stability.

(4) Relate how phase and voltage stability affect the asymptotic stability of the non classical transient stability model.

(5) Determine a fast computational method for determining and ranking the voltage security of elements based on a voltage network element security measure. The method for determining and ranking the contingencies that most severely affect the most insecure elements would also be desired. This security assessment methodology could be based on the work performed for phase stability or thermal overload security problems [1].

(6) Determine a pattern recognition procedure that could identify voltage security and stability problems based on steady state estimation data or for a simulated contingency. The problems would be identified without the checking of voltage constraints,

reactive reserve constraints, or capacitive support constraints in each voltage control area [14].

(7) Development of robust operating constraints that can assure voltage security and stability in each stiffly interconnected group.

## APPENDIX 1

### BASE CASE LOADFLOW DATA IN COMMON FORMAT



## APPENDIX 1

## BASE CASE LOADFLOW DATA IN COMMON FORMAT

11/14/80 CONSUMERS POWER CO. 100.0 1980 TEST		DAY 317 OF 1980		30 ITEMS		37 ITEMS	
BUS DATA FOLLOWS							
1	01ALPHA	1	1	0	1.0476	-9.46	0.0
2	01KAPPA	1	1	2	1.0490	-6.84	0.0
25	01GAMMA	1	1	2	1.0580	-5.50	224.00
26	01DELTA	1	1	0	1.0529	-6.75	139.00
28	01EPSILON	1	1	0	1.0511	-6.25	206.00
29	01ZETA	1	1	2	1.0300	-0.49	283.50
30	01THETA	1	1	2	1.0300	-10.94	1104.00
4	02THETA	2	2	0	1.0045	-10.49	500.00
3	03ETA	3	3	0	1.0309	-9.69	322.00
5	03IOTA	3	3	0	1.0056	-9.30	0.0
21	03ALPHA	3	3	0	1.0331	-5.22	274.00
9	05HU	4	4	0	1.0283	-11.13	0.0
10	05XI	4	4	2	1.0180	-6.22	0.0
19	05PSI	4	4	2	1.0510	-3.00	0.0
20	05OMEGA	4	4	2	0.9910	-4.41	680.00
27	05EPSILON	4	4	0	1.0387	-8.76	281.00
11	06MICRON	5	5	0	1.0134	-7.03	0.0
7	07LAMBDA	6	6	0	0.9973	-10.80	233.80
12	07PI	6	6	0	1.0008	-7.05	8.50
16	07UPSILON	6	6	0	1.0332	-7.62	329.40
17	07PHI	6	6	0	1.0347	-8.61	0.0
22	07BETA	6	6	2	1.0510	-0.78	0.0
24	07DELTA	6	6	0	1.0387	-7.50	308.60
6	08GAMMA	7	7	3	1.0080	-8.60	9.20
8	08MU	7	7	0	0.9963	-11.31	522.00
13	08RHO	7	7	0	1.0151	-6.93	0.0
14	08SIGMA	7	7	0	1.0126	-8.60	0.0
15	08TAU	7	7	0	1.0167	-9.02	320.00
18	08CHI	7	7	0	1.0319	-9.45	158.00
23	08BETA	7	7	2	1.0460	-0.98	247.50
-999							
BRANCH DATA FOLLOWS				37 ITEMS			
2	1	1	1	0	0.003500	0.041100	0.69860
30	1	1	1	0	0.001000	0.025000	0.75000
25	2	1	1	0	0.007000	0.008600	0.14600
3	2	1	1	0	0.001300	0.015100	0.25720
26	25	1	1	0	0.003200	0.032300	0.51300
28	26	1	1	0	0.004300	0.047400	0.78020
29	26	1	1	0	0.005700	0.062500	1.02900
27	26	1	1	0	0.001400	0.014700	0.23960
29	28	1	1	0	0.001400	0.015100	0.24900
5	4	1	2	1	0.000800	0.012800	0.13420
14	4	1	2	1	0.000800	0.012900	0.13820
4	3	1	3	1	0.001300	0.021300	0.22160
18	3	1	3	1	0.001100	0.013300	0.21380
6	5	1	3	1	0.000200	0.002600	0.04340
8	5	1	3	1	0.000800	0.011200	0.14760
22	21	1	3	1	0.000800	0.014000	0.25660
30	21	1	3	1	0.001000	0.025000	1.20000
11	10	1	4	1	0.000400	0.004300	0.07280
13	10	1	4	1	0.000400	0.004300	0.07280
19	20	1	4	1	0.000700	0.013800	0.0
12	11	1	5	1	0.001600	0.043500	0.0
8	1	1	6	1	0.000400	0.004600	0.07800
-999							
1	2	0.0	0.0	0.0	0.0	0.0	0.0
2	3	0.0	0.0	0.0	0.0	0.0	0.0
3	4	0.0	0.0	0.0	0.0	0.0	0.0
4	5	0.0	0.0	0.0	0.0	0.0	0.0
5	6	0.0	0.0	0.0	0.0	0.0	0.0
6	7	0.0	0.0	0.0	0.0	0.0	0.0
7	8	0.0	0.0	0.0	0.0	0.0	0.0
8	9	0.0	0.0	0.0	0.0	0.0	0.0
9	10	0.0	0.0	0.0	0.0	0.0	0.0
10	11	0.0	0.0	0.0	0.0	0.0	0.0
11	12	0.0	0.0	0.0	0.0	0.0	0.0
12	13	0.0	0.0	0.0	0.0	0.0	0.0
13	14	0.0	0.0	0.0	0.0	0.0	0.0
14	15	0.0	0.0	0.0	0.0	0.0	0.0
15	16	0.0	0.0	0.0	0.0	0.0	0.0
16	17	0.0	0.0	0.0	0.0	0.0	0.0
17	18	0.0	0.0	0.0	0.0	0.0	0.0
18	19	0.0	0.0	0.0	0.0	0.0	0.0
19	20	0.0	0.0	0.0	0.0	0.0	0.0
20	21	0.0	0.0	0.0	0.0	0.0	0.0
21	22	0.0	0.0	0.0	0.0	0.0	0.0
22	23	0.0	0.0	0.0	0.0	0.0	0.0
23	24	0.0	0.0	0.0	0.0	0.0	0.0
24	25	0.0	0.0	0.0	0.0	0.0	0.0
25	26	0.0	0.0	0.0	0.0	0.0	0.0
26	27	0.0	0.0	0.0	0.0	0.0	0.0
27	28	0.0	0.0	0.0	0.0	0.0	0.0
28	29	0.0	0.0	0.0	0.0	0.0	0.0
29	30	0.0	0.0	0.0	0.0	0.0	0.0
30	31	0.0	0.0	0.0	0.0	0.0	0.0
31	32	0.0	0.0	0.0	0.0	0.0	0.0
32	33	0.0	0.0	0.0	0.0	0.0	0.0
33	34	0.0	0.0	0.0	0.0	0.0	0.0
34	35	0.0	0.0	0.0	0.0	0.0	0.0
35	36	0.0	0.0	0.0	0.0	0.0	0.0
36	37	0.0	0.0	0.0	0.0	0.0	0.0
37	38	0.0	0.0	0.0	0.0	0.0	0.0
38	39	0.0	0.0	0.0	0.0	0.0	0.0
39	40	0.0	0.0	0.0	0.0	0.0	0.0
40	41	0.0	0.0	0.0	0.0	0.0	0.0
41	42	0.0	0.0	0.0	0.0	0.0	0.0
42	43	0.0	0.0	0.0	0.0	0.0	0.0
43	44	0.0	0.0	0.0	0.0	0.0	0.0
44	45	0.0	0.0	0.0	0.0	0.0	0.0
45	46	0.0	0.0	0.0	0.0	0.0	0.0
46	47	0.0	0.0	0.0	0.0	0.0	0.0
47	48	0.0	0.0	0.0	0.0	0.0	0.0
48	49	0.0	0.0	0.0	0.0	0.0	0.0
49	50	0.0	0.0	0.0	0.0	0.0	0.0
50	51	0.0	0.0	0.0	0.0	0.0	0.0
51	52	0.0	0.0	0.0	0.0	0.0	0.0
52	53	0.0	0.0	0.0	0.0	0.0	0.0
53	54	0.0	0.0	0.0	0.0	0.0	0.0
54	55	0.0	0.0	0.0	0.0	0.0	0.0
55	56	0.0	0.0	0.0	0.0	0.0	0.0
56	57	0.0	0.0	0.0	0.0	0.0	0.0
57	58	0.0	0.0	0.0	0.0	0.0	0.0
58	59	0.0	0.0	0.0	0.0	0.0	0.0
59	60	0.0	0.0	0.0	0.0	0.0	0.0
60	61	0.0	0.0	0.0	0.0	0.0	0.0
61	62	0.0	0.0	0.0	0.0	0.0	0.0
62	63	0.0	0.0	0.0	0.0	0.0	0.0
63	64	0.0	0.0	0.0	0.0	0.0	0.0
64	65	0.0	0.0	0.0	0.0	0.0	0.0
65	66	0.0	0.0	0.0	0.0	0.0	0.0
66	67	0.0	0.0	0.0	0.0	0.0	0.0
67	68	0.0	0.0	0.0	0.0	0.0	0.0
68	69	0.0	0.0	0.0	0.0	0.0	0.0
69	70	0.0	0.0	0.0	0.0	0.0	0.0
70	71	0.0	0.0	0.0	0.0	0.0	0.0
71	72	0.0	0.0	0.0	0.0	0.0	0.0
72	73	0.0	0.0	0.0	0.0	0.0	0.0
73	74	0.0	0.0	0.0	0.0	0.0	0.0
74	75	0.0	0.0	0.0	0.0	0.0	0.0
75	76	0.0	0.0	0.0	0.0	0.0	0.0
76	77	0.0	0.0	0.0	0.0	0.0	0.0
77	78	0.0	0.0	0.0	0.0	0.0	0.0
78	79	0.0	0.0	0.0	0.0	0.0	0.0
79	80	0.0	0.0	0.0	0.0	0.0	0.0
80	81	0.0	0.0	0.0	0.0	0.0	0.0
81	82	0.0	0.0	0.0	0.0	0.0	0.0
82	83	0.0	0.0	0.0	0.0	0.0	0.0
83	84	0.0	0.0	0.0	0.0	0.0	0.0
84	85	0.0	0.0	0.0	0.0	0.0	0.0
85	86	0.0	0.0	0.0	0.0	0.0	0.0
86	87	0.0	0.0	0.0	0.0	0.0	0.0
87	88	0.0	0.0	0.0	0.0	0.0	0.0
88	89	0.0	0.0	0.0	0.0	0.0	0.0
89	90	0.0	0.0	0.0	0.0	0.0	0.0
90	91	0.0	0.0	0.0	0.0	0.0	0.0
91	92	0.0	0.0	0.0	0.0	0.0	0.0
92	93	0.0	0.0	0.0	0.0	0.0	0.0
93	94	0.0	0.0	0.0	0.0	0.0	0.0
94	95	0.0	0.0	0.0	0.0	0.0	0.0
95	96	0.0	0.0	0.0	0.0	0.0	0.0
96	97	0.0	0.0	0.0	0.0	0.0	0.0
97	98	0.0	0.0	0.0	0.0	0.0	0.0
98	99	0.0	0.0	0.0	0.0	0.0	0.0
99	100	0.0	0.0	0.0	0.0	0.0	0.0



## BIBLIOGRAPHY

## BIBLIOGRAPHY

- [1] R.A. Schlueter, P. Rusche, M. Lotfalian, L. Shu, A. Yazdankhah, S. Tedeschi, R. Rhodes, D. Idzior, D. Whiting, and J. Sekerke, "Method of Analysis of Generation's Governor Response and System Security," Final Report for the Electric Power Research Institute, January 1984.
- [2] J. Lawler and R.A. Schlueter, "An Algorithm for Computing Modal Coherent Equivalents," IEEE Trans. on Power Apparatus and Systems," Vol. PAS-101, No. 5, pp. 1071-1080, May 1982.
- [3] J. Dorsey and R.A. Schlueter, "Local and Global Dynamic Equivalents Based on Structural Archetypes for Coherency," IEEE Trans. on Power Apparatus and Systems, Vol. PAS-102, No. 6, pp. 1793-1802, June 1983.
- [4] V.A. Venikov and M. Rozonov, "Izc. Akad. Nauk SSSR (Energetika i Automatica), Vol. 6, pp. 121-125, 1961.
- [5] S. Abe and A. Isono, "Determination of Power System Voltage Stability, Parts I and II," IEEE of Japan, Vol. 96-B, No. 4, pp. 171-186, 1976.
- [6] S. Abe, Y. Fukunaga, A. Isono, and B. Kondo, "Power System Voltage Stability," IEEE Trans. on Power Apparatus and Systems, Vol. PAS-101, No. 10, pp. 3830-3840.
- [7] I. Hano, Y. Tamura, S. Narita, and K. Matsumoto, "Real Time Control of System Voltage and Reactive Power," IEEE Trans. on Power Apparatus and Systems, Vol. PAS-88, pp. 1544-1559, October 1969.
- [8] Y. Yamura, H. Mori, and S. Iwamoto, "Relationship Between Voltage Instability and Multiple Load Flow Solutions in Electric Power Systems," Vol. PAS-102, No. 5, pp. 1115-1125, May 1983.
- [9] R. Rischl, T. Halpin, and A. Guvenis, "The Application of Decision Theory to Contingency Selection," CAS 29, No. 11, pp. 712-723, November 1982.
- [10] M. Calovic, "Applications of Automatically Regulated Under Load Tap Changing Transformers in Voltage and Reactive Flow Control," submitted to Electric Machines and Electromagnetics.

- [11] F. Wu and S. Kumagai, "Steady-State Security Regions of Power Systems," IEEE Trans. on Circuits and Systems, Vol. CAS-29, No. 11, November 1982.
- [12] Mohamed E. El-Hawary, "Electrical Power Systems: Design and Analysis," Reston Publishing Company, 1983.
- [13] Richard S. Varga, "Matrix Iterative Analysis," Englewood Cliffs, NJ: Prentice-Hall, Inc., 1962.
- [14] O. Saito, K. Koizumi, M. Udo, M. Sato, H. Mukae, and T. Tsuji, "Security Monitoring Systems Including Fast Transient Stability Studies," IEEE Trans. on Power Apparatus and Systems, Vol. PAS-94, No. 5, September/October 1975.
- [15] J. Zaborszky, G. Huang, and S.Y. Lin, "Control of Reactive Power and Voltage in Emergencies," International Conference on Large High Voltage Electric Systems, Electra, No. 92, January 1984.